SYNTHESIS AND CHARACTERIZATION OF SURFMERS FOR THE SYNTHESIS OF POLYSTYRENE-CLAY NANOCOMPOSITES

By

Austin Samakande

Thesis presented in partial fulfillment of the requirements for the degree of Master of Science in Polymer Science

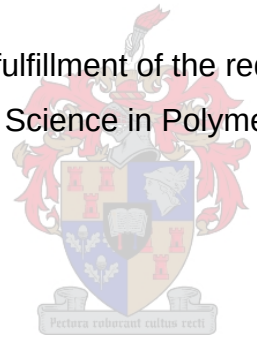

At the

University of Stellenbosch

Study leader: Prof. R.D. Sanderson

Co-study leader: Dr. P.C. Hartmann

December 2005

Declaration

I, the undersigned, hereby declare that the work contained in this thesis is my own original work and that I have not previously in its entirety or in part submitted it at any university for a degree.

Signature: _____ Date: _____

Austin Samakande

Abstract.

Two cationic polymerizable surfactants (surfmers), (11-acryloyloxyundecyl)dimethyl-(2-hydroxyethyl)ammonium bromide (Ethanol surfmer) and (11-acryloyloxyundecyl)-dimethylethylammonium bromide (Ethyl surfmer) were synthesized and characterized. Characterization was done using, conductivity, Fourier transform infra-red spectroscopy (FT-IR), electrospray mass spectrometry (ESMS), differential scanning calorimetry (DSC), thermogravimetric analysis (TGA), small angle X-ray scattering (SAXS) and polarized light microscopy with a heating stage. These surfmers and the commercial surfactant cetyltrimethylammonium bromide (CTAB) were used for functionalization of sodium montmorillonite (Na^+-MMT), thereby forming organophilic MMT. The functionalization of MMT dispersions was carried out by ion exchange of the sodium ions in Na^+-MMT by surfactants in aqueous media. Organophilic MMT clays were then dispersed in styrene and subsequently polymerized by a free radical reaction to yield polystyrene-clay nanocomposites. This *in-situ* intercalative polymerization process resulted in an exfoliated structure for Ethyl surfmer modified clay, a partially exfoliated structure for Ethanol surfmer modified clay and an intercalated structure for CTAB modified clay. These nanocomposite structures were confirmed by SAXS and transmission electron microscopy (TEM). The nanocomposites exhibited enhanced thermal stability. All the nanocomposites exhibited an inferior storage modulus (G^I) at low clay contents relative to polystyrene. At higher clay loadings there was an increase in G^I which was dependent on the level of clay dispersion and the clay content. All the nanocomposites showed an increase in glass transition temperature (T_g), regardless of the amount of clay and the level of clay dispersion. There was a shift towards higher temperatures and broadening of the tan δ peak, which was in turn dependent on the amount of clay and level of clay dispersion. Molecular masses of polystyrene-clay nanocomposites were in the range 10^5 g/mol for bulk polymerization relative to 10^3 g/mol for solution polymerization as revealed by gel permeation chromatography (GPC).

Opsomming.

Twee kationiese polimeriseerbare sepe (Eng. surfmers), (11-akrieloksi-undekiel)dimetiel-(2-hidroksi-etiel)ammoniumbromied (‘Etanol’-seep) en (11-akrieloksi-undekiel)dimetielammoniumbromied (‘Etiel’-seep) is gesintetiseer en gekarakteriseer. Hierdie verbindings is gekarakteriseer d.m.v. die volgende analitiese tegnieke: Fourier-transformasie-infrarooispektroskopie (FT-IR), elektrosproei-massaspektrometrie (ESMS), differensieëlskandeerkalorometrie (DSC), termogravimetriese analise (TGA), kleinhoek-X-straaldiffraksie (SAXS) en gepolariseerde-ligmikroskopie met ‘n verhittingsintervlak.

Hierdie sepe, asook die kommersiële seep setieltrimetielammoniumbromied (CTAB), is gebruik om natrium-montmorilloniet (Na^+MMT) te funksionaliseer, om sodoende die organofiliese MMT te vorm. Die funksionalisering van die MMT-dispersies is in ‘n waterige medium d.m.v. ioonuitruiling van die natriumione van die Na^+MMT bewerkstellig. Daarna is die organofiliese kleie in stireen gedispergeer en toe gepolimeriseer d.m.v. ‘n vryradikaalpolimerisasiereaksie, om sodoende polistireen-nanosamestellings te lewer. Hierdie *in-situ* interkalerende polimerisasieproses het die volgende strukture opgelewer: ‘n verskilferde struktuur vir die ‘Etiel’-seep-gemodifiseerde klei; ‘n gedeeltelike verskilferde struktuur vir die ‘Etanol’-seep-gemodifiseerde klei, en ‘n geinterkaleerde struktuur vir die CTAB-gemodifiseerde klei.

Hierdie nanosamestellingstrukture is d.m.v. van SAXS en transmissie-elektronmikroskopie (TEM) bevestig. Die nanosamestellings het verhoogde termiese stabiliteit en ‘n laer stoormodulus (G^I), relatief tot polistireen, vertoon by lae klei-inhoud. By hoër kleiladings was daar ‘n toename in G^I, wat afhanklik was van die graad van kleidispersie en klei-inhoud. Alle nanosamestellings het ‘n toename in glasoorgang (T_g) getoon, onafhanklik van die hoeveelheid klei en die vlak van kleidispersie. Daar was ‘n verskuiwing na hoër temperature en ‘n verbreding van die tan-δ-piek, wat op sy beurt afhanklik was van die hoeveelheid klei en graad van kleidispersie. Die molekulêre massas van die polistireen-nanosamestellings was van die orde 10^5 g/mol vir massapolimerisasie, in vergelyking met 10^3 g/mol vir oplossingpolimerisasie, soos bepaal deur gelpermeasiechromatografie (GPC).

Pectora roborant cultus recti

Table of contents

List of figures.

Appendix 1.

Appendix 2.

List of tables.

List of abbreviations.

ABS	Acrylonitrile-butadiene-styrene
AFM	Atomic force microscope
AIBN	Azobisisobutyronitrile
AUTMAB	11-acryloyloxyundecyltrimethylammonium bromide
BUA	11-bromoundecyl acrylate
$CDCl_3$	Deuterated chloroform
CEC	Cation exchange capacity
CMC	Critical micelle concentration
CTAB	Cetyltrimethylammonium bromide
CTAB-MMT	CTAB surfmer modified MMT
d	Interlayer distance
DMA	Dynamic mechanical analysis
DMAc	Dimethyl acetamide
DHA	Dimethylethyl amine
DOA	Dimethylethanol amine
DSC	Differential scanning calorimetry
Ethanol surfmer	(11-acryloyloxyundecyl)dimethyl(2-hydroxyethyl) ammonium bromide
Ethanol-MMT	Ethanol surfmer modified MMT
Ethyl surfmer	(11-acryloyloxyundecyl)dimethylethylammonium bromide
Ethyl-MMT	Ethyl surfmer modified MMT
ESMS	Electrospray mass spectroscopy
FT-IR	Fourier-transform infrared

G^I	Storage modulus
G^{II}	Loss modulus
GPC	Gel permeation chromatography
LLC	Lyotropic liquid crystalline
MMT	Montmorillonite clay
M_n	Number average molecular mass
M_W	Weight average molecular mass
M_W/M_n	Polydispersity index
m/z	mass per unit charge ratio
Na^+-MMT	Montmorillonite clay containing predominantly sodium ions
NMR	Nuclear magnetic resonance
PCNs	Polymer-clay nanocomposites
PEO	Poly (ethylene oxide)
PP	Polypropylene
PVA	Poly (vinyl alcohol)
SAXS	Small angle X-ray scattering
SBR	Styrene butadiene rubber
SDS	Sodium dodecyl sulphate
sPS	Syndiotactic polystyrene
TEM	Transmission electron microscopy
TGA	Thermogravimetric analysis
T_g	Glass transition temperature
THF	Tetrahydrofuran

UV	Ultraviolet
WAXD	Wide angle X-ray diffraction
wt	Weight
XRD	X-ray diffraction

Acknowledgements.

Firstly, I would like to thank the Department of Chemistry and Polymer Science, the UNESCO centre for Macromolecules, NRF and THRIP for funding this very exciting project.

Secondly, I would like to thank my supervisor Professor Sanderson for giving me an opportunity to study under his guidance at one of the leading polymer science research institutions in the world. I also want to thank him for his unwavering support and advice during the entire study period.

To Dr Hartmann, my co supervisor, I say thank you for all your input, from the first day I entered the laboratory until the day I finally handed in my thesis. You were there whenever I needed you, even when you were on holiday you had time for me.

The paper coatings group at Polymer Science is also thanked for their help and support, especially Valeska Cloete for her time, advice and encouragement. You guys were my second family; I really enjoyed your company and will never forget you for the time we spent together. Once again I thank you for accepting me into your family.

I thank my family for their patience, and support for my wish to realize my dreams, I really thank them. I also thank my friends at Stellenbosch.

Lastly, I would like to thank Dr Margie Hurndall for helping me with editing this document. Mum, thank you for your time and energy.

Over and above all, I would like to give praise and worship to God, for with Him nothing is impossible. With faith we can move mountains …Mark 11 vs 24.

Chapter 1: Introduction and objectives.

1.1 Background.

The ever increasing use of thermoplastic raw materials as well as the sometimes insufficient physical and mechanical properties exhibited by some of the unmodified thermoplastics have led to the search for inexpensive ways of producing materials with enhanced properties. Several methods have been introduced that have not only been successful in producing inexpensive materials but also materials with improved physical and mechanical properties [1-2]. There are two basic types of thermoplastic materials, i.e. those that at ambient conditions are below the glass transition temperature (T_g) and those that are above the T_g.

The amorphous polymers below T_g (glassy polymers) are generally hard and brittle, and most suffer brittle failure under impact conditions. To improve their properties, two main methods of reinforcing them have been introduced.

- The inclusion of incompatible, nanophase rubber materials. This involves grafting a rubber phase onto a glassy matrix or blending with a grafted thermoplastic elastomer terpolymer having compatible glassy phases. The properties of the resultant composite are governed by the rubber (content, particle size, distribution and T_g) and the interfacial adhesion between the glassy polymer and the rubber [2-3]. This group of materials has mainly improved impact strength and toughness.
- The inclusion of inorganic fillers. Such fillers have specific uses, e.g. calcium carbonate for low cost materials, aluminum trihydrate or magnesium hydroxide for improved flame retardancy [4]. Lately there is the move towards the use of clay fillers due to the abundance of clay, its low cost and dispersability at a nanometer level, that often results in improvements in both physical and thermo mechanical properties of the resultant materials [1].

Polystyrene is an example of an inexpensive glassy thermoplastic. It is clear, rigid and brittle and, although it has high tensile strength, which depends on the molecular mass, it possess low impact strength. Of the many methods by which its properties can be improved, the use of nanoclays is one of the newest [1].

1.2 Polystyrene.

Polystyrene itself has poor mechanical properties, such as poor impact strength, and is therefore limited in its applications [5]. Ways of improving its thermal and mechanical properties have therefore been introduced. One of the ways is to copolymerize styrene with other monomers, to yield copolymers [5]. Copolymerization of styrene and butadiene gives rise to styrene butadiene rubber (SBR), which has found many applications in the rubber industry. Styrene, acrylonitrile and butadiene, used in an interpenetrating polymer network with a styrene matrix, to yield acrylonitrile-butadiene-styrene (ABS), is one of the most widely used copolymers today, from household appliances to automobile applications. Most polystyrene copolymers and block-copolymers, when included into the polystyrene matrix, impart improved impact strength and toughness, as in the case of ABS. There is continuing research to expand the market possibilities of polystyrene.

1.3 Clay fillers.

Another method by which to improve the thermal and mechanical properties of polystyrene is the incorporation of filler particles. Fillers generally range from organic based to inorganic based. Inorganic fillers, in the form of clay, have been extensively used. Clay is one of the most abundant natural and inexpensive filler materials [6]. Clays have a layered structure in their natural state. There are two basic types of clays available: the non-swelling clays e.g. kaolinite, and the swelling clays e.g. pyrophyllite. The swelling clays have the ability to expand or contract their interlayer structure without loosing their two-dimensional crystallographic integrity. In recent years the swelling clays have attracted wide attention, from both the academic and engineering fields, as their use provides a route to the preparation of polymer-clay nanocomposites [1,7-9]. This is mainly due to the clay's intrinsic anisotropic character as well as its swelling capabilities. Because of the layered structure and the swelling capability, these clays can be dispersed in a polymer matrix as nanometer-size platelets. The ability of clay platelets to be exfoliated or delaminated in a polymer matrix, giving rise to a high aspect ratio (ratio of the length to thickness of an individual clay platelet) and improved thermal and mechanical properties, has resulted in clay becoming a most attractive filler. The commonly used swelling clays are montmorillonite (MMT), hectorite and saponite [1].

Clay is an attractive filler for polystyrene; it offers many inherent advantages. These include toughness, improved resistance to chemicals, fire and ignition, and, as clay is inexpensive, it can offer a route to the production of less expensive polystyrene materials [1,7-10].

1.4 Montmorillonite.

The most studied clay for the preparation of polystyrene-clay nanocomposites is MMT [1,7-10]. In its natural state it contains small cations, normally Na^+ or K^+, in between its layers (interlayer space or gallery space), and these small cations can be exchanged for other cations in aqueous solution. This ability to undergo ion exchange provides a route for organic cations (surfactants) that are compatible with styrene to be introduced into the interlayer space of the clay. After the introduction of these cationic surfactants, styrene can penetrate and swell the interlayer space. Polymerization then leads to polystyrene-clay nanocomposites. This process can lead to three types of composites:

(i) Phase-separated composites, which have poor thermal and mechanical properties, because of a poor dispersion of clay particles in the polymer matrix, resulting in regions rich in clay particles which then act as defect points,

(ii) Intercalated nanocomposites, which have improved properties,

(iii) Exfoliated nanocomposites, which have excellent properties relative to the above two types of composites [1].

BASF has a commercial exfoliated polystyrene-clay nanocomposite (Styrolox) that is obtained by using an amino-terminated polystyrene to exfoliate clay [11].

1.5 Polystyrene-clay nanocomposites.

In recent years clays have been used for the preparation of polystyrene-clay nanocomposites, taking advantage of clay's ability to have its layers swollen and dispersed in the polymer matrix on a nanoscale [1]. Na^+-MMT was chosen as the clay for the synthesis of polystyrene-clay nanocomposites in this study. Na^+-MMT implies that this clay contains only hydrated sodium ions (Na^+) in its gallery space, making

the gallery space hydrophilic. Styrene monomer and polystyrene are hydrophobic and thus will be immiscible with Na^+-MMT. The Na^+ can be exchanged for other cations in aqueous solution. This ability to undergo ion exchange provides a route for organic cations (surfactants) that are compatible with styrene to be introduced into the interlayer space of clay. Successive layers of MMT are held by electrostatic and weak van der Waal forces. Consequently, MMT has the ability to undergo extensive interlayer expansion or swelling in a direction perpendicular to the layers. After the ion exchange of Na^+ by surfactants, styrene can be used to swell the clay, followed by polymerization to give rise to polystyrene-clay nanocomposites.

Extensive studies have been carried out on the synthesis and characterization of polystyrene-clay nanocomposites [7]. It has been found that exfoliated nanocomposites have several improved properties when compared with other composite systems, due to the better dispersion of clay particles in the polymer matrix. Thus, efforts have mainly been directed towards the synthesis and characterization of exfoliated nanocomposites, with the intention of obtaining a better understanding of the attributes which result in their improved properties. In an attempt to synthesize exfoliated polystyrene-clay nanocomposites, many already modified, commercially available (ion exchanged) clays have been used, but unfortunately mainly intercalated nanocomposites have been obtained [7].

1.6 Surfmers for polystyrene-clay nanocomposites.

A successful and novel approach in the synthesis of exfoliated polystyrene-clay nanocomposites was achieved when surfactants containing polymerizable groups (surfmers) were used to ion exchange clay [12]. This success was attributed to the fact that the reactive groups on the surfmers take part in the polymerization of styrene and thus provide the exfoliation driving force for the formation of an exfoliated structure. It is to be remembered that the properties of polystyrene can be altered by copolymerization and introduction of fillers. When surfmers are used to modify clay, and subsequently for the preparation of the nanocomposites, the properties of polystyrene are altered in two ways, i.e. by copolymerization, and by introduction of filler. Thus the chemical structure of the surfmer may also play a significant role in the properties of the resulting nanocomposites.

The most commonly used surfmers to date are those containing the vinyl benzyl polymerizable group [12-13], probably because of the ease of copolymerization of styrenics. Other reactive groups such as meth(acrylates) have been used to a lesser extent [14-15].

1.7 Motivation and objectives.

Benzene-ring-containing surfmers have been extensively used to modify Na^+-MMT clay and the modified clay subsequently used to synthesize exfoliated polystyrene–clay nanocomposites. This however provides little scope for varying the properties of the resultant polystyrene matrix because these types of surfmers and the styrene monomer are structurally similar. Thus, the use of other surfmers (non-benzene-ring-containing surfmers) to modify clay and subsequently synthesize exfoliated polystyrene–clay nanocomposites could provide a way to vary the properties of the final polystyrene matrix.

Thus, the overall objective of this research was to synthesize exfoliated polystyrene–clay nanocomposites by making use of selected surfmers, other than benzene-ring-containing surfmers.

Hence, the first objective was to synthesize and characterize new acrylate-based polymerizable quaternary ammonium surfmers (for reasons explained later) with different head group polarities. The structure–property relationships of these surfmers in water were also to be determined. This was motivated by the fact that in recent years there has been increasing interest in synthesizing new surfactants for specific applications. The behavior of surfactants above their critical micelle concentration where higher-order associations are found have resulted in their finding applications ranging from their use as lyotropic liquid crystals (LLC) to their use as templates for the synthesis of nanometer-size tailored architectures.

The second objective was to use the synthesized surfmers to modify Na^+-MMT clay and then to compare the extent of ion exchange (clay modification) reaction with that of a commercially available non-polymerizable surfactant i.e. cetyltrimethylammonium bromide (CTAB) that has a carbon backbone that is similar to that of the synthesized surfmers (in terms of chain length and head group). Factors

that might affect the ion exchange reaction (i.e. temperature and shear rate) were also to be investigated.

The third objective was to actually synthesize exfoliated polystyrene–clay nanocomposites using the modified clays. The effects of the surfmer/surfactant structure on the resultant nanocomposites were to be investigated. Acrylate-based surfmers were selected because the acrylate group contains a carbonyl group which can interact with the polar clay surface by hydrogen bonding. This increases the favorable interactions that can lead to an exfoliated structure. The acrylate groups are highly reactive, thus enabling easy copolymerization with styrene. The nanocomposite structure–property relationships were also to be investigated and compared to those of nanocomposites synthesized from CTAB modified clay, which only form intercalated polystyrene-clay nanocomposites.

The fourth objective was to use physical blends of surfmer modified clays and CTAB modified clays to synthesize polystyrene–clay nanocomposites and investigate the structure and properties of the nanocomposites, and then compare the results to those obtained when only one modified clay was used to synthesize the nanocomposites.

Results of these investigations could help in the preparation of cheaper exfoliated polystyrene–clay nanocomposites, given that surfmers are expensive to make; thus if blends of surfmer modified clay and a classical surfactant modified clay can be used to attain an exfoliated structure then the synthesis of exfoliated nanocomposites could become more economically viable.

The following tasks were to be carried out to achieve the above objectives:

- Synthesize and characterize selected acrylate-based surfmers.
- Use the synthesized surfmers to modify (ion exchange) Na^+-MMT clay.
- Characterize the modified clay using TGA, FT-IR and SAXS.
- Disperse the modified clay in styrene monomer (for bulk polymerization) and styrene monomer solution (styrene monomer in toluene) (for solution polymerization), followed by polymerization to form polystyrene–clay nanocomposites.

- Characterize the synthesized polystyrene–clay nanocomposites using FT-IR, SAXS, TEM, atomic force microscopy (AFM), TGA, DMA and GPC.

- Modify the Na^+-MMT clay using cetyltrimethylammonium bromide (CTAB), a classical surfactant (non-polymerizable surfactant).

- Characterize the modified clay using TGA, FT-IR, and SAXS and compare it to the surfmer modified clays.

- Disperse the classical surfactant modified clay in styrene monomer, and polymerize to form polystyrene–clay nanocomposites.

- Characterize the synthesized polystyrene–clay nanocomposites obtained from the classical surfactant modified clay using FT-IR, SAXS, TEM, TGA, DMA and GPC, and compare the results to those obtained for surfmer modified clays.

- Disperse physical mixtures (blends) of surfmer modified clay and classical surfactant-modified clay in styrene monomer, and polymerize to form polystyrene–clay nanocomposites.

- Characterize the synthesized polystyrene–clay nanocomposites obtained using blends of modified clays using SAXS, TGA and GPC.

References.

1. M. Alexandre, P. Dubois; Materials Science and Engineering, 28 (2000) 1-63.

2. D. Klempner, K. C. Frisch; Polymer Science and Technology, Plenum Press. New York and London, 10 (1977) 20-22, 327-328.

3. R. D. Deamin, A. M. Crugnola; Advances in Chemistry Series 154, American Chemical Society, (1976) 263-266.

4. www.specialchem4polymers.com, Accessed (March, 2005).

5. H. F. Mark, N. M. Bikales, C. G. Overberger, G. Menger; Encyclopedia of Polymer Science and Engineering; John Wiley and Sons Inc. New York, 16 (1989) 1-246.

6. R. Tantatherdtam; PhD Thesis, The Pennsylvania State University (2003).

7. M. Rosorff; Nano Surface Chemistry. Marcel Dekker Inc. New York-Basel, (2002) 653-673.

8. M. Biswas, S. S. Ray; Adv. Polym. Sci, 155 (2001) 170-221.

9. M. Okamoto; Encyclopedia of Nanoscience and Nanotechnology. American Scientific Publishers, California, 8 (2004) 791-843.

10. S. S Ray, M. Okamoto; Prog. Polym. Sci., 28 (2003) 1539-1641.

11. Dr Walburg; Oral presentation, Nanotechnology in Science, Economy, and Society. Conference in Marburg, Germany, 13-15 January (2005).

12. X. A. Fu, S. Qutubuddin; Abstact from the AIChE Annual Meeting, Miami, Florida, USA, 15-20 November (1998).

13. J. Zhu, A. B Morgan, F. J. Lamelas, C. A. Wilkie; Chem. Mater., 13 (2001) 3774-3780.

14. W. A. Zhang, D. Z. Chen, H. Y. Xu, X. F. Shen, Y. E. Fang; European Polymer Journal, 39 (2003) 2323-2328.

15. C. Zeng, L. J. Lee; Macromolecules, 34 (2001) 4098-4103.

Chapter 2: Theoretical background.

2.1 Overview of nanocomposites.

One of the many ways by which to improve the stiffness, toughness, chemical resistance, fire and ignition of polymeric materials is by the addition of particle fillers. Fillers can also offer a route to the production of inexpensive materials. The efficiency of reinforcement is dependent on the aspect ratio (i.e. length to thickness of a clay platelet), filler mechanical properties and the adhesion between the matrix and the filler [1-2].

The most abundant natural and inexpensive filler materials are the clays. They possess a layered structure, which can be exfoliated, giving rise to a high aspect ratio onto which polymers can adsorb. The dispersion of clay particles in a monomer or polymer matrix can give rise to the formation of three types of composite materials [1-5].

- The first type is the conventional composites that contain clay tactoids (aggregated clay platelets), in which clay layers are aggregated in an unintercalated face-to-face form. This type of composite possesses poor mechanical and physical properties.

- The second type is intercalated polymer-clay nanocomposites, which are formed by insertion of one or more molecular layers of polymer into the clay host galleries.

- The third type is the exfoliated polymer-clay nanocomposites, characterized by a low clay content, a monolithic structure, and an average distance between the clay nanolayers that depends on the clay content of the composites.

Exfoliated nanocomposites show exceptional physical, chemical and mechanical properties relative to conventional composites and intercalated polymer-clay nanocomposites (PCNs). PCNs are a new class of materials that have received much attention from engineers and scientists in recent years because of their outstanding properties, such as enhanced mechanical properties, reduced gas permeability, optical clarity, flame retardancy, gas barrier performance, high heat deflection temperature and high dimensional stability (ability to resist change in volume and shape with

changes in the surrounding environment e.g. temperature) relative to pristine polymers and conventional composites (micro and macro composites) [1-5]. The term nanocomposite describes a two-phase material in which one of the phases is dispersed in the second one on a nanometer scale (10^{-9}m) [6]. Thus the dispersed clay in nanocomposites possesses one dimension in the nanometer range. PCNs differ from the conventional composites because of their exceptionally large interfacial area per unit volume or weight of the dispersed phase (e.g. 750 m^2/g). Dispersion of exfoliated clay monolayers into polymers is hindered by the intrinsic incompatibility of hydrophilic layered silicates with hydrophobic polymers and the inherent tendency to form face-to-face stacks in agglomerated tactoids due to high interlayer cohesive energy. However, as was first demonstrated by the Toyota research group [7], the replacement of the inorganic exchangeable cations in the galleries of the native clay by alkylammonium surfactants can compatibilize the surface chemistry of the clay and the hydrophobic polymer matrix. The first successful nanocomposite, reported by the Toyota research group [7-9], was in the form of a Nylon 6/clay nanocomposite obtained by *in-situ* polymerization, a method viable for production on industrial scale. The use of organoclays as a route to nanocomposite formation has been extended to other polymer systems, including epoxies, polyurethanes, polyimides, nitrile rubber, polyesters, polypropylene, polystyrene and polysiloxanes [3]. There is growing interest in the surface chemistry of clays in pursuit of nanocomposites synthesized using specific monomers, prepolymers, and polymer melts [2].

Many studies have been devoted to PCNs since their intrinsically excellent polymer properties have attractive potential for continuous expansion of application versatility.

2.2 Structure of clay and its dispersion in a polymer.

Clay consists of small size crystalline particles made up of aluminosilicates of various compositions, with possible iron and magnesium substitutions by alkaline earth elements [2]. The basic unit is a silicon atom surrounded by four oxygen atoms forming a tetrahedron. The tetrahedra are then linked in two dimensions to form a sheet of hexagonal rings. There is also an octahedron of aluminium surrounded by oxygen atoms, and the octahedra link to form a more closely packed two dimensional sheet. There are two basic types of clays structures, i.e. 1:1 and 2:1. The 1:1 is the non-swelling dioctahedral clay e.g. kaolinite, which is composed of an alumina

octahedra sitting on top of a sheet of silica tetrahedra. The apical oxygen atoms from silica are shared with the aluminium atoms of the upper layer. The other basic type of clay is of the 2:1 type, which consists of two sheets of silica to one alumina (parent compound is the pyrophyllite) or two sheets of silica to one of magnesium oxide (parent compound is talc) (see Fig. 2.1 below).

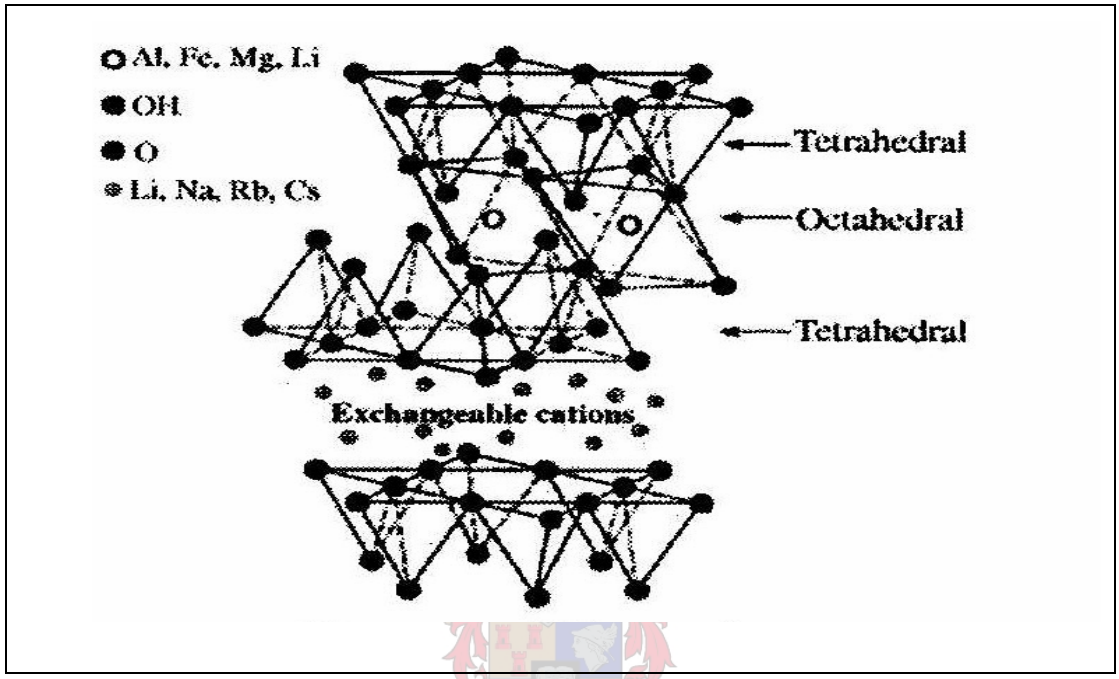

Fig. 2.1 Structure of 2:1 layered silicate [5].

Clays used in the preparation of PCNs belong to the 2:1 family. The layer thickness is around 1 nm and the lateral dimensions may vary from 30 nm to several micrometers and even larger, depending on the particular layered silicate. Stacking of the layers then leads to a regular gap between the layers, called the interlayer distance. Isomorphic substitution within the layers (e.g. Al^{3+} replaced by Mg^{2+} or by Fe^{2+}, or Mg^{2+} replaced by Li^{+}) generates negative charges that are counterbalanced by hydrated alkali and alkaline earth cations situated inside the galleries. The commonly used layered silicates are MMT, hectorite and saponite, having different chemical formulae (see Table 2.1). The type of clay is characterized by a moderate charge called the cation exchange capacity (CEC), which ranges between 80-120 meq/100 g.

Table 2.1 Chemical structure of commonly used 2:1 layered phyllosilicates [1]

2:1 phyllosilicate	General formula
Montmorillonite	$M_x (Al_{4-x} Mg_x) Si_8O_{20} (OH)_4$
Hectorite	$M_x (Mg_{6-x} Li_x) Si_8O_{20} (OH)_4$
Saponite	$M_x [Mg_x] (Si_{8-x} Al_x) O_{20} (OH)_4$

M is the counterbalancing ion, and x is the degree of isomorphous substitution (between 0.5 and 1.3).

One of the most interesting and widely investigated clays for PCNs is MMT. The structure of MMT consists of layers made up of one octahedral alumina sheet sandwiched between two tetrahedral silica sheets. About one in six of the aluminum ions in the octahedral layers of MMT is isomorphously substituted by magnesium or other divalent ions, resulting in negative charges that are counter-balanced by cations (e.g. Na^+, K^+, or Ca^{2+}) residing in the interlayer.

The forces that hold the stacks together are relatively weak, resulting in easy intercalation of small hydrophilic molecules between the layers [1]. At this point the clay is only miscible with hydrophilic polymers such as poly (ethylene oxide) (PEO) and poly(vinyl alcohol) (PVA) [4-5]. To improve miscibility with other hydrophobic polymer matrices, it is necessary to convert the hydrophilic silicate surfaces to organophilic surfaces. This can be achieved by ion exchange reactions between the small hydrated inorganic cations in the gallery space and cationic surfactants, which include primary, secondary, tertiary and quaternary alkyl ammonium or alkyl phosphonium cations [4-5]. There are three processes that may lead to complete dispersion or exfoliation of clay tactoids in a monomer or polymer matrix [2]. The first is wetting of the clay surface by monomer or polymer, the second is intercalation of a monomer or polymer into the clay galleries and the last step is exfoliation of the clay layers. The first and second steps are thermodynamically controlled while the last step is controlled by mechanical and reaction driving forces. Driving forces may be in the form of copolymerization of the base monomer with surfmers to give a copolymer. This is common with polystyrene based-clay nanocomposites [10]. In the case of Nylon 6 and epoxy-clay nanocomposites, protonated alkyl amines can

catalyze the reaction in-between the layers relative to the bulk polymer, thus providing the driving force for exfoliation of the clay.

2.3 Surfactants.

The word surfactant comes from two words i.e. “surface” and “active”, meaning that surfactants can be described as surface-active agents. The surface activity of surfactants arises from their amphiphilic nature. The word amphiphilic means that surfactants contain hydrophilic (water loving) and hydrophobic (water hating) groups in their structures. A general structure of a surfactant is shown below.

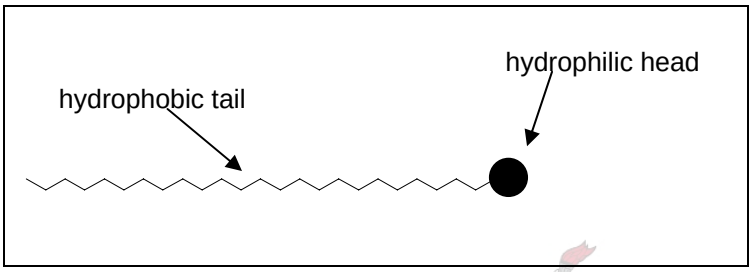

Fig. 2.2 General structure of surfactants.

Thus, surfactants can interact with both hydrophilic and hydrophobic species, hence their surface activity. In general, surfactants are characterized by their critical micelle concentration (CMC) values, which are characteristic for every surfactant.

Above the CMC value, the hydrophobic moieties aggregate together because they are not soluble in water, whereas the hydrophilic parts dissolve in the water. Due to the chemical link between the hydrophobic and hydrophilic components, phase separation does not take place. This leads to the formation of micelles. For more concentrated solutions, structures with characteristic dimensions in the nanometer range [11] i.e., lyotropic liquid crystalline (LLC) mesophases are formed. LLC mesophases include lamellar, hexagonally packed coil-like micelles, sponge-like bicontinuous phases etc (see Fig. 2.3 below). The driving force for the self-organization comes from thermodynamic and surfactant packing parameter considerations where the reduction of the hydrocarbon-water interface is energetically favored.

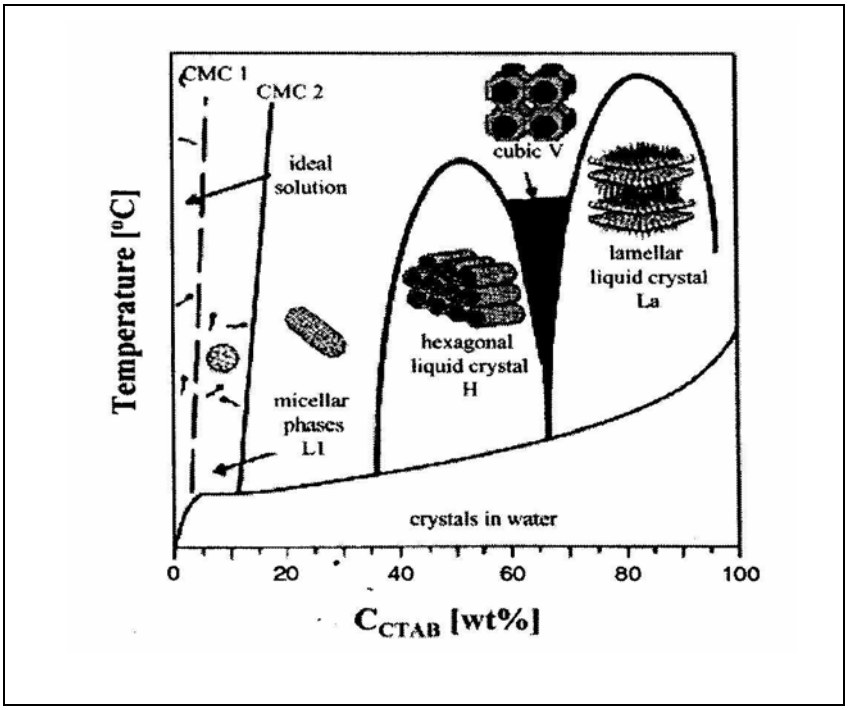

Fig. 2.3 Schematic representation of the behavior of cetyltrimethylammonium bromide (CTAB) surfactant in water. The diagram shows a phase diagram depicting the dependence of lyotropic liquid crystalline phases on the concentration of the amphiphile and temperature [12].

Surfactants can be divided into two groups: non-reactive surfactants and reactive surfactants.

Non-reactive surfactants are the conventional surfactants which have found many applications: from household use, as soaps and detergents, to academic and industrial use, as stabilizers/compatibilizers. Stabilizers for reactions such as polymerization, e.g. emulsion, miniemulsion, suspension, etc., are used to control particle size, particle size distribution as well as to ensure the stability of the dispersion during the polymerization process. The most remarkable aspect about them is that they do not take part in the reaction process itself, apart from acting as stabilizers. The major drawback associated with this group of surfactants is that they can be desorbed from the particle surface, for they are not bound to the polymer particles. A common example of this group of surfactants is sodium dodecyl sulphate (SDS).

Reactive surfactants, on the contrary, can play a role in one of the reactions involved in the free radical polymerization process. Free radical polymerization involves initiation (formation of radicals), propagation (growing of the polymer chain), or a transfer reaction (a radical that moves from a growing chain to a dormant species) and termination (destruction of radicals). Depending on their behaviour during a free

radical polymerization, reactive surfactants can further be divided into three subgroups: transurf (surfactant which also acts as a transfer agent), inisurf (combining initiator and surfactant properties) and surfmer (a monomer as well as a surfactant). Upon taking part in the polymerization reaction, these surfactants become covalently attached to the polymer particles and thus cannot be desorbed. These surfactants replace non-reactive surfactants in requirements where desorption of surfactants from particles was formerly a problem. They also find use in other novel applications where thermal, chemical or mechanical properties are required, because they chemically bond to the base polymer and thus change the base polymer properties.

The most widely studied group of the reactive surfactants is the surfmers. This is because of their ability to homopolymerize as well as copolymerize with a variety of conventional monomers. Their unique capabilities have led to their use in the synthesis of unique nano materials, such as open-cell polymer networks, ultra-fine polymer latexes and inorganic/organic nanocomposites [13].

The hydrophilic part (head group) of both the non-reactive and the reactive surfactants can either be positively or negatively charged. The nitrogen containing, positively charged surfactants are the ones widely used for the modification of clay for the synthesis of PCNs. This is due to the fact that clay structures possess negative surface charges that can interact with positively charged species by electrostatic interaction.

2.4 Modification of clay by surfactants.

In pristine clay, small inorganic cations can be replaced by any positively charged species. These positively charged species can be simple inorganic cations, such as Cd^{2+}, which can be precipitated by SH^- to give CdS nanoparticles in-between the clay layers, thereby creating nanoreactors [8]. The ion exchange reaction can also be effected by surfactants which can be simple surfactants, surfmers, inisurfs or transurfs, positively charged oligomers, etc. The total number of replaceable small inorganic cations is governed by the moderate negative surface charge called the cation exchange capacity (CEC) i.e. the maximum number of exchangeable sites. The CEC values are different for different types of clays and they range from 80-120 meq/100 g of clay [1]. For the preparation of polymer-clay nanocomposites organic cations are normally used for ion exchanging the small inorganic cations in pristine

clay. The organic cations lower the surface energy and decrease the cohesive energy by expanding the interlayer distance, thus facilitating the wetting and intercalation of monomer or polymer. In addition, the organic cations may contain various functional groups (e.g. polymerizable surfactants, i.e. surfmers) that can react with monomer or polymer resin. In some cases, these functional groups can initiate polymerization of monomers and thus improve interfacial adhesion between the individual clay nanolayers and the polymer matrix.

The ion exchange of cationic surfactants onto a homo-ionic MMT dispersed in water was found to be independent of the size of the hydrophilic head group of cationic surfactants at its natural pH [2]. The cationic exchange capacity is approximately equal to the total amount of surfactant that can be adsorbed as a monolayer. The surfactant's chemical structure and the charge density of the clay determine the orientation of the surfactant in the galleries. Increasing the chain length or the clay charge density leads to a larger d-spacing and interlayer volume.

There are many possible orientations of the surfactants in gallery spacing. These orientations vary from solid-like to liquid-like, where the liquid-like dominates with an increase in temperature, or as the surfactant chain length decreases, or as the interlayer density decreases [2,4-5]. Other factors that might influence the orientations of the surfactants in the galleries include surfactant's number of tails and branching.

After the ion exchange of inorganic cations by surfactants, the clay surface becomes compatible with the monomer or polymer matrix. The surfactant used for the ion exchange of small inorganic cations in pristine clay, to give rise to organically modified clay, plays a critical role in the formation of a particular type of composite. The chemical structure of the surfactant should be compatible with both the clay and the polymer matrix, thus providing the interactions (ionic, hydrogen or van der Waals) between surfactant-clay and surfactant-polymer. If interactions are very favourable, then an exfoliated structure can be obtained. On the other hand, if poor interactions exist then a conventional composite is generally obtained [14-16].

Surfactants used for the synthesis of polystyrene clay nanocomposites range from alkyl and aromatic-containing ammonium surfactants [6-7,10,14-24], to alkyl phosphonium surfactants [25] and polymerizable surfactants (surfmers) [7,10,26-31].

Fig. 2.4 below shows examples of surfactants that have been used in the synthesis of polystyrene clay nanocomposites.

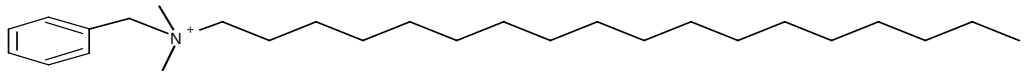

Dimethylbenzyloctadecylammonium cation [32]

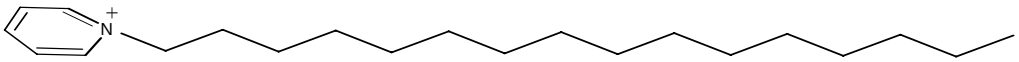

Cetylpyridinium cation [28]

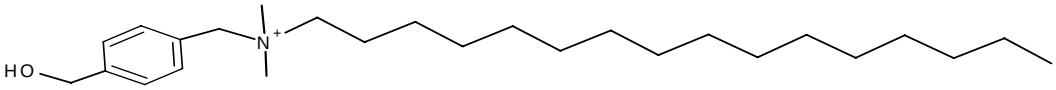

Hexadecylhydroxybenzyldimethylammonium cation [25]

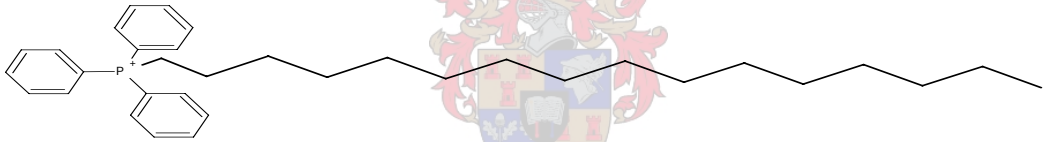

Hexadecyltriphenylphosphonium cation [25]

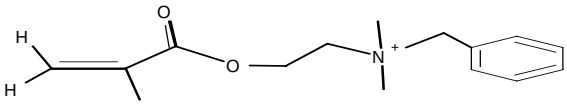

2-Methacryloyloxyethylbenzyldimethylammonium cation [10]

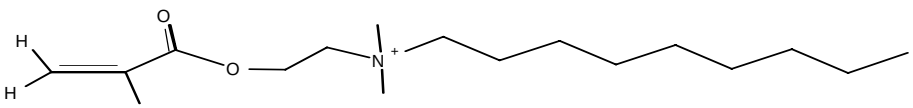

2-Methacryloyloxyethylhexadecyldimethylammonium cation [10]

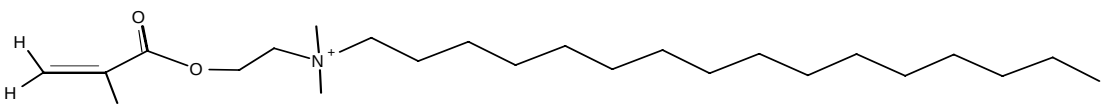

2-Methacryloyloxyethyloctyldimethylammonium cation [10]

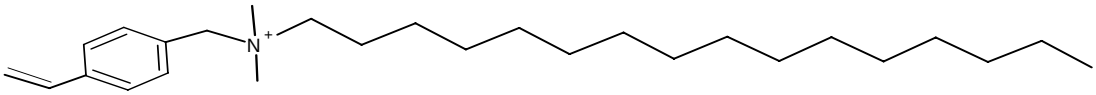

Hexadecylvinylbenzyldimethylammonium cation [25]

Fig. 2.4 Surfactants used for the modification of clay for the synthesis of polystyrene-clay nanocomposites.

The use of surfactants affects especially the physical, mechanical and chemical properties of the prepared nanocomposites. The polymerizable group in the surfmer takes part in the polymerization reaction, resulting in a copolymer rather than a homopolymer. Classic surfactants have been extensively used for the modification of clay, for the synthesis of PCNs. However most efforts have mainly resulted in intercalated nanocomposites [7,14-18,20-21]. The use of surfmers for the modification of clay and subsequently the synthesis of exfoliated polystyrene-clay nanocomposites has been successful [10,26,29-31]. It is believed that the polymerization of the surfmer and styrene in-between the clay galleries provides the driving force for the clay exfoliation. Many researchers used benzene ring-containing surfactants and vinyl benzyl-containing surfmers for the modification of clay, mainly because the benzene ring of the surfmers interacts by van der Waals forces with the benzene rings of styrene and polystyrene [22,26]. Other surfactants have also been used for the modification of clay for the preparation of polystyrene-clay nanocomposites [10,19,28-29].

In this research, acrylate containing surfmers were used to modify clay for the synthesis of polystyrene-clay nanocomposites. It is believed that the high polarity of the acrylate group will result in greater interaction with the clay surface [15]. In addition, the copolymerization of the acrylate group with styrene will provide the reaction driving force for the formation of exfoliated polystyrene-clay nanocomposites [2]. Whereas most previous studies used reactive-head surfmers, this study uses reactive-tail surfmers.

2.5 Polymer-clay nanocomposite structure.

There are three main types of composites that can be obtained (Fig. 2.5 a-c), depending on the compatibility of the components used i.e. organic cation, layered silicate and polymer matrix. The differences in these three composites only arise from

the different morphology (exfoliation) levels of clay particles in relation to the polymer matrix.

Phase separated micro composite: This conventional composite contains clay tactoids of stacked layers in a coplanar orientation. The clay tactoids are associated in aggregates and agglomerates dispersed as a segregated phase with no inserted polymer matrix between their layers. Properties of this composite are similar to those of traditional microcomposites.

Intercalated nanocomposite: In this nanocomposite, polymer chains are intercalated between the clay layers in a crystallographically regular fashion [33]. Only a few molecular layers of polymer interlay the nanocomposite and the properties of the particle are of the same order as those of the ceramic host.

Exfoliated nanocomposite: In this nanocomposite the clay layers are separated from each other giving rise to individual silicate layers which are uniformly dispersed in a continuous polymer matrix, with average distances between layers depending on clay concentration. The properties of the nanocomposite are governed by the matrix and in general exhibit better properties than intercalated ones with the same number of particles. It is the most interesting of the composites, because of the greater clay-polymer interaction, which makes the entire surface of the clay available to a polymer, leading to maximum mechanical and physical property enhancement [6]. At moderate loadings the entire matrix assumes the properties of a surface-bound polymer rather than free polymer. This added mobility restriction makes this system a true nanocomposite where a new material is created.

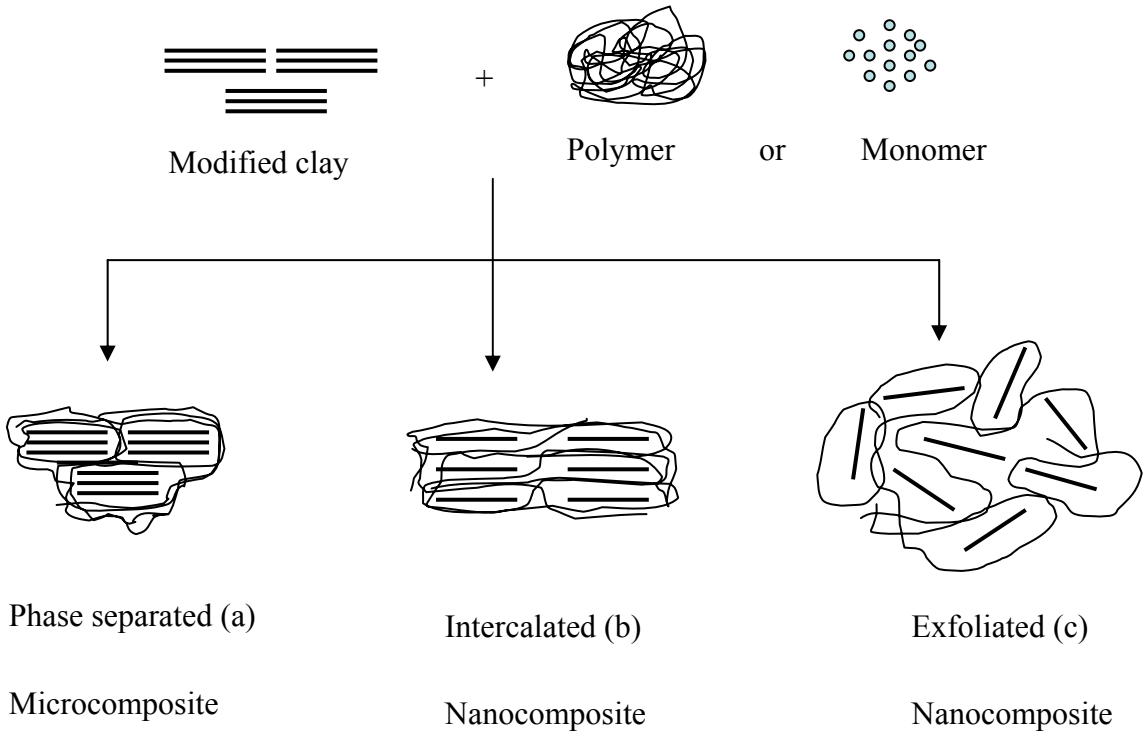

Fig. 2.5 Schematic illustration of the three main types of polymer-clay composites.

2.6 Characterization of nanocomposites.

There are traditionally two main complementary techniques that are used for the characterization of nanocomposites, namely X-ray diffraction (XRD) and transmission electron microscopy (TEM).

2.6.1 X-ray diffraction.

Clays are layered compounds that have a defined interlayer distance (d spacing) in their natural state and this interlayer distance can be determined by the use of XRD. The diffraction angle and interlayer distance are related through the Bragg's relation (see Equation 2.1 below):

$$n\lambda = 2d \sin \theta \qquad (2.1)$$

where n is the order of interference, λ corresponds to the wavelength of the X-ray radiation used in the diffraction experiment, d is the spacing between diffractional lattice planes and θ is the measured diffraction angle or glancing angle. When

surfactants and polymers are introduced into the gallery spacing there is an increase in the interlayer distance and the diffraction peak shifts towards smaller angles i.e. larger interlayer distance. This can be followed by the use of XRD. When it comes to exfoliated nanocomposites the diffraction peaks disappear in the XRD diffractograms, either because of a much too large spacing between the layers, i.e. exceeding 8 nm in the case of ordered exfoliated structure, or there is no more order in the nanocomposite (see Fig. 2.6 below).

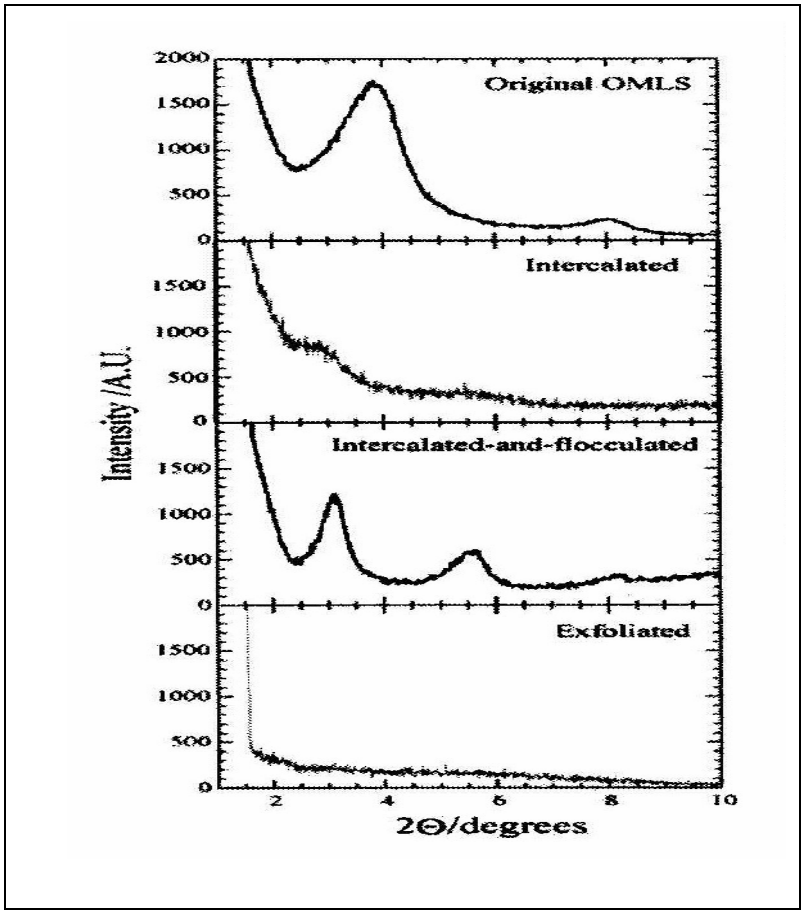

Fig. 2.6 WAXD patterns of three layered silicates structures. Original OMLS is an organically modified layered silicate for reference [5].

Although XRD, commonly used in the form of wide-angle X-ray diffraction (WAXD) and to a lesser extent small angle X-ray scattering (SAXS), is a convenient method for the determination of the interlayer spacing in the intercalated nanocomposites (within 1-4 nm) [4], it gives very little information on the spatial arrangement of the silicate layers or any structural inhomogeneity in PCNs. On the other hand, some (probably mixed structure) nanocomposites show a very ill-defined interlayer spacing. Thus, a broadening and/or a decrease in the intensity of diffraction peaks in XRD makes it

difficult to make plausible conclusions. This means that results from XRD should not be treated as complete, without supporting TEM images.

2.6.2 Transmission electron microscopy.

Nanocomposite morphology can be characterized by TEM. TEM allows a qualitative understanding of the internal structure and spatial distribution of the various phases, and also defect structure through direct visualization. It should be noted here that it is necessary to analyze a sample that is representative of the bulk composite.

2.6.3 Other characterization techniques.

2.6.3.1 Hyphenated techniques.

Hyphenated techniques have also been exploited for the quantitative characterization of polymer-clay nanocomposites, although not extensively. Simultaneous SAXS and WAXD measurements have been used to quantitatively characterize the nanostructure and crystalline structure of Nylon 6 nanocomposites [5]. 2D SAXS and 2D WAXS have also been used for the quantitative determination and determination of the three-dimensional orientations of various organic and inorganic structures in polymer-clay nanocomposites. Solid-state nuclear magnetic resonance spectroscopy (NMR) (^{1}H and ^{13}C) has also been used by some researchers to develop an understanding of the morphology, surface structure chemistry and, to a lesser extent, the dynamics of nanocomposites [5].

2.6.3.2 Infrared spectroscopy.

The majority of polymers are composed of organic molecules that absorb electromagnetic radiation in the infrared region. This is caused by the molecules undergoing transitions between vibrational states of different energies, causing both the absorption and emission of radiation. The correlation between the infrared absorption frequencies and particular vibration modes can be used to analyze the microstructure of polymer molecules. Thus infrared can be used for structural characterization as well as identification.

In PCNs, infrared has numerous uses for identification purposes. Clay in its natural state is composed of infrared-active species, hence when organic surfactants are

introduced into its layers infrared can be a very useful, simple and fast method of identifying the introduced species [28-29].

2.6.3.3 Thermal stability.

The thermal stability of polymeric materials is usually studied by thermogravimetric analysis (TGA). TGA measures the weight loss of a material (in this case polymeric) due to the formation of organic volatile species (products of the degradation) as a function of a temperature programme. TGA experiments can be carried out in an inert environment, normally nitrogen, where degradation takes place in the absence of oxygen. When carried out in the presence of oxygen, oxidative degradation takes place. PCNs in general show improved thermal stability relative to the pristine polymers, regardless of the experimental environment. The first report on the thermal stability of PCNs was for PMMA-clay nanocomposites [34]. The thermal stability is due to the formation of char by clay, which acts as a mass transport barrier and as an insulator between the polymer and the superficial zone where the combustion of the polymer is taking place. Wang *et al*. [24] used X-ray photoelectron spectroscopy to study the mechanism of thermal stability of polystyrene-clay nanocomposites. They discovered that there was accumulation of clay at the surface of the nanocomposites as degradation proceeded, and the clay then acted as an insulator and a barrier to mass transport, thus making the nanocomposites more thermally stable relative to pristine polystyrene.

Very small amounts of clay are required for an improvement in thermal stability relative to pristine polymers. Doh and Cho [32] observed that maximum thermal stability of their intercalated polystyrene-clay nanocomposites was attained when only 0.3 wt % of clay was used. They used dimethybenzyloctadecylammonium modified MMT clay. The environment under which the TGA experiment was carried out had a significant effect on the extent of thermal stability of the polymer-clay nanocomposites. Poly(ethylene-*co*-vinyl acetate) synthesized by melt intercalation showed better thermal stability in a nitrogen environment relative to air, and the thermal stability increased with an increasing amount of clay [35].

The chemical structure of surfactants used for the modification of clay has a significant effect on the extent of thermal stability of the polystyrene-clay nanocomposites. In general, surfmer modified clays give rise to enhanced thermal

stability relative to non-reactive modified clays [10,29]. Zhang *et al*. [10] used three surfmer-modified clays and a non-reactive surfactant-modified clay to prepare polystyrene-clay nanocomposites and discovered that surfmer-based nanocomposites had superior thermal stability relative to non-reactive surfactant-based nanocomposites.

Exfoliated polystyrene nanocomposites have been found to possess better properties relative to the other types of composites [1-5]. Thermal stability is one such property. This enhanced stability has been attributed to the high thermal stability of clay and its excellent barrier properties, which prevents heat from being transmitted quickly, thereby limiting the continuous decomposition of the nanocomposites [10]. Many researchers [10,19,26-29] have observed that exfoliated polystyrene-clay nanocomposites show exceptional thermal stability. The exfoliated nanocomposites were prepared using reactive modified clays, save Yei *et al*, who used a very bulky aminopropylisobutyl polyhedral oligomeric silsesquioxane (POSS) cation to modify clay [19].

The enhanced thermal stability of polymer-clay nanocomposites is one of the driving factors that has led to the efforts by researchers to synthesize exfoliated polymer-clay nanocomposites. This drive has been necessitated by the fact that many polymers fail at high temperatures of operation. To overcome this drawback, high temperature stabilizers are chemically added, but this addition often results in the loss of other vital properties of polymers e.g. impact strength, toughness, etc.

2.6.3.4 Dynamic mechanical analysis.

Dynamic mechanical analysis (DMA) measures the response of a material to cyclic deformation as a function of temperature. There are three main parameters that are used to express DMA results: (i) the storage modulus (G^I) which is a measure of elastic response to the deformation; (ii) the loss modulus (G^{II}) which is a measure of the plastic response, and (iii) tan δ, i.e. the ratio of G^{II}/G^I. Tan δ is used for the determination of molecular mobility such as the glass transition temperature (T_g).

The interaction between polymer and silicate layers at the interface of layers and polymer matrix can suppress the mobility in the polymer segments near the interface, leading to improved mechanical properties. In general, higher G^I values for

nanocomposites below the T_g (i.e. glassy state) and in the rubbery region, relative to pristine polymers and conventional composites, are obtained. This can be attributed to the large aspect ratio of the structural hierarchy on the nanoscale level. The incorporation of small quantities of polar comonomers during the synthesis of PCNs not only affects the resultant nanocomposite structure, but the mechanical properties as well. Okamoto *et al*. [36] synthesized poly (methyl methacrylate)-clay nanocomposites as well as nanocomposites of poly (methyl methacrylate) containing small amounts of polar comonomers. The comonomers were N,N-dimethyl aminopropyl acrylamide; N,N-dimethyl aminoacrylate and acrylamide. They discovered that blends of PMMA-clay and PMMA-quartenary ammonium compounds had very small differences between their G^I and tan δ values against temperature curves. Incorporation of small amounts of comonomers led to a significant enhancement of G^I in the glassy region i.e. below T_g. The G^I values of copolymer-clay nanocomposites were enhanced by 200-400% compared to those of the corresponding clay-free blends. The explanation for these enhancements is the high aspect ratio of the dispersed clay and the interaction of the copolymer chains and clay layers resulting in the suppression of the mobility of the copolymer segments near the interface. The structure of the surfactant used to modify the clay, the amount of clay and the level of dispersion of clay in the polymer matrix have been shown to have an effect on the mechanical properties. An increase in the amount of clay results in an improvement in the storage modulus of the nanocomposites. Fang *et al*. [35] discovered that an increase in the amount of clay resulted in an increase in the storage modulus of poly (ethylene-*co*-vinyl acetate)-clay nanocomposites. They also used three different types of organic modifiers from which they obtained nanocomposites with different levels of clay dispersion. The differences in clay dispersion of the nanocomposites manifested themselves in the mechanical properties, with partially exfoliated nanocomposites showing significant enhancement in the storage modulus relative to the intercalated nanocomposites. The variation of tan δ against temperature was not significantly affected by the amount of clay. The increase in storage modulus of polymer-clay nanocomposites was also observed for polyimide-clay nanocomposites [37] and polypropylene-clay nanocomposites [38].

Intercalated polystyrene-clay nanocomposites containing 17.2 wt % of Na^+-MMT, synthesized by emulsion polymerization, did not show any improvement in the

storage modulus but rather a shift towards high temperatures and broadening of the tan δ peak relative to the pristine polystyrene [39]. This implies that the clay only restricted the segmental motion of the polystyrene matrix, resulting in the increase of the glass transition temperature [39]. However, enhanced storage modulus was obtained by Chung *et al*. [29] who used the reactive surfactant 2-acrylamido-2-methyl-1-propane (AMPS) to modify Na^+-MMT, followed by synthesis of poly(styrene-*co*-methyl methacrylate)/clay nanocomposites by emulsion polymeri zation. The storage modulus increased with an increase in the clay level.

Fu and Qutubuddin [26] also found an increase in modulus after they had synthesized exfoliated polystyrene-clay nanocomposites using a reactive modified clay (vinylbenzyldimethyldodecyl ammonium modified MMT) by bulk polymerization. The storage modulus increased slightly with the amount of clay. On the other hand, the T_g decreased from 100 ^{0}C in pure polystyrene to 94 ^{0}C for a polystyrene-clay nanocomposite containing 7.6% clay. They attributed the decrease in the T_g to the reduced molecular weight resulting from hindered diffusion of the polymerization initiator (hindered by the high viscosity of the styrene swelled clay) giving faster termination, as well as the restricted propagation of styrene chains by the impervious clay platelets.

2.6.3.5 Gel permeation chromatography.

In gel permeation chromatography (GPC) a dilute polymeric solution is passed through a tubular column packed with polymeric gel beads. The solution moves, under pressure, and some polymer chains pass through the pores of the gel beads while others pass by the gel beads. The time that a polymer chain spends in the column depends on the path it takes through the gel. High molecular mass polymer chains cannot fit into the pores of the beads due to their large hydrodynamic volume and thus take a short time to elute. On the other hand, low molecular mass polymer chains have a smaller hydrodynamic volume and thus can easily fit into the pores, hence they take a longer time to elute. Thus, GPC separates polymers on the basis of their hydrodynamic volumes. The time that a particular polymer chain takes to elute from the column is proportional to its molecular mass. The detection of the analytes is carried out using either a refractive index or ultra violet detector and evaporative light

scattering. Molecular mass distribution and polydispersity of polymers are thus obtained.

GPC has found application for the determination of molecular mass, molecular mass distribution and polydispersity of polymer-clay nanocomposites [29,40]. It has also been used for the determination of the difference in molecular masses of the polymer bound to the clay particles relative to the unbound polymer. Here the unbound polymer is extracted from the clay particles and analysed, leaving behind the bound polymer. The bound polymer is then desorbed from the clay particles by a reverse ion exchange reaction, normally using lithium chloride, and the bound polymer is also analyzed [29]. This analysis gives some idea of the degrees of polymerization inside the clay galley space relative to the bulk polymer; and this in turn can provide an insight into the kinetics of polymerization and hence the exfoliation process.

References.

1. M. Alexandre, P. Dubois; Materials Science and Engineering, 28 (2000) 1-63.

2. M. Rosorff; Nano Surface Chemistry. Marcel Dekker Inc. New York-Basel, (2002) 653-673.

3. M. Biswas, S. S. Ray; Adv. Polym. Sci., 155 (2001) 170-221.

4. M. Okamoto; Encyclopedia of Nanoscience and Nanotechnology. American Scientific Publishers, California, 8 (2004) 791-843.

5. S. S Ray, M. Okamoto; Prog. Polym. Sci., 28 (2003) 1539-1641.

6. S. Sadhu, A. K. Bhowmick; J. App. Polym. Sci., 92 (2004) 698-709.

7. P. Pinnavaia; Applied Clay Science, 15 (1999) 11-29.

8. F. Bergaya, G. Lagaly; Applied Clay Science, 19 (2001) 1-3.

9. N. Sheng, M. C. Boyce, D. M. Parks, G. C. Rutledge, J. I. Abes, R. E. Cohen; Polymer, 45 (2004) 487-506.

10. W. A. Zhang, D. Z. Chen, H. Y. Xu, X. F. Shen, Y. E. Fang; European Polymer Journal, 39 (2003) 2323-2328.

11. R. G. Laughlin; The aqueous phase behavior of surfactants, Academic Press Inc, London, 1994.

12. S. Svenson; Journal of Dispersion Science and Technology, 25 (2004) 101-118.

13. M. Summers, J. Eastoe; Advances in Colloid and Interface Science, 100-102 (2003) 137-152.

14. R. A. Vaia, E. P. Giannelis; Macromolecules, 30 (1997) 7990-7999.

15. R. A. Vaia, K. D. Jandt, E. J. Kramer, E. P. Giannelis; Macromolecules, 28 (1995) 8080-8085.

16. R. A. Vaia, E. P. Giannelis; Macromolecules, 30 (1997) 8000-8009.

17. C. I. Park, O. O. Park, J.G. Lim, H. J. Kim; Polymer, 42 (2001) 7465-7475.

18. C. Tseng, J. Wu, H. Lee, F. Chang; Polymer, 42 (2001) 10063-10070.

19. D. Yei, S. Kuo, Y. Su, F. Chang; Polymer, 45 (2004) 2633-2640.

20. D. B. Zax, D. K. Santos, H. Hegemann, E. P. Giannelis, E. Manias; J. Chem. Phys., 112 (2000) 2945-2951.

21. J. G. Ryu, S. W. Park, H. Kim, J. W. Lee; Materials Science and Engineering, 24(2004) 285-288.

22. D. R. Robello, N. Yamaguchi, T. Blanton, C. Barnes; J. Am. Chem. Soc., 126 (2004) 8118-8119.

23. G. Chigwanda, C. A. Wilkie; Polymer Degradation and Stability, 80 (2003) 551-557.

24. J. Wang, J. Du, J. Zhu, C.A Wilkie; Polymer Degradation and Stability, 77 (2002) 249-252.

25. J. Zhu, A. B Morgan, F. J. Lamelas, C. A. Wilkie; Chem. Mater., 13 (2001) 3774-3780.

26. S. Qutubuddin, X. Fu; Polymer, 42 (2001) 807-813.

27. C. A. Wilkie, J. Zhang; Polymer Degradation and Stability, 83 (2004) 301-307.

28. C. Tseng, J. Wu, H. Lee, F. Chang; J. App. Polym. Sci., 85 (2002) 1370-1377.

29. M. Xu, Y. S. Choi, Y. K. Kim, K. H. Wang, I. J. Chung; Polymer, 44 (2003) 6387-6395.

30. C. I. Park, H. Kim, O. O. Park; Polymer, 45 (2004) 1267-1273.

31. C. Zeng, L. J. Lee; Macromolecules, 34 (2001) 4098-4103.

32. J. H. Doh, I. Cho; Polym. Bull., 41 (1998) 511.

33. I. M. Daniel, J. Luo; Composites Science and Technology, 63 (2003) 1607-1616.

34. A. Bluimstein; J. Polym. Sci A., 3 (1965) 2665-2673.

35. W. Zhang, D. Chen, Q. Zhao, Y. Fang; Polymer, 44 (2003) 7953-7691.

36. P. H. Nam, P. Maiti, M. Okamoto, T. Kotaka, N. Hasegawa, A. Usuki; Polymer, 42 (2001) 1201-1206.

37. H. Tyan, K. Wei, T. Hseh; J. Polym. Sci. Part B: Polym. Phys., 38 (2000) 2873-2878.

38. M. Kawasumi, N. Hasegawa, M. Kato, A. Usuki, A. Okada; Macromolecules, 30 (1997) 6333-6338.

39. M. W. Noh, D. C. Lee; Polym. Bull., 42 (1999) 619-626.

40. L. Biasci, M. Aglietto, G. Ruggeri, F. Ciardelli; Polymer, 35 (1994) 3296-3304.

Chapter 3: Survey of the methods of synthesis of polymer-clay nanocomposites.

3.1 Introduction.

A literature survey was carried out to determine the best method for the synthesis of polystyrene-clay nanocomposites using surfmer modified clay. Many techniques mentioned in secton 3.1.1 below have been used for the synthesis of polystyrene based nanocomposites. A review of these methods, with special emphasis on the parameters that govern each synthesis technique, is given in Section 3.2.

3.1.1 Techniques of synthesizing polymer-clay nanocomposites.

There are four main techniques for the preparation of polymer-layered silicate nanocomposites, using various combinations of organoclays and polymer matrixes [1-3].

(i) *In-situ* intercalative polymerization: Monomer, or a monomer solution, is used to swell the organically modified clay, followed by polymerization. Thus polymer formation can also occur in-between the intercalated sheets. Polymerization can be initiated by heat or radiation; the initiator either diffuses into the intercalated layers or the organic initiator or catalyst is prefixed in the interlayer through cation exchange prior to the swelling by the monomer. A schematic presentation of the *in-situ* intercalative process is given below.

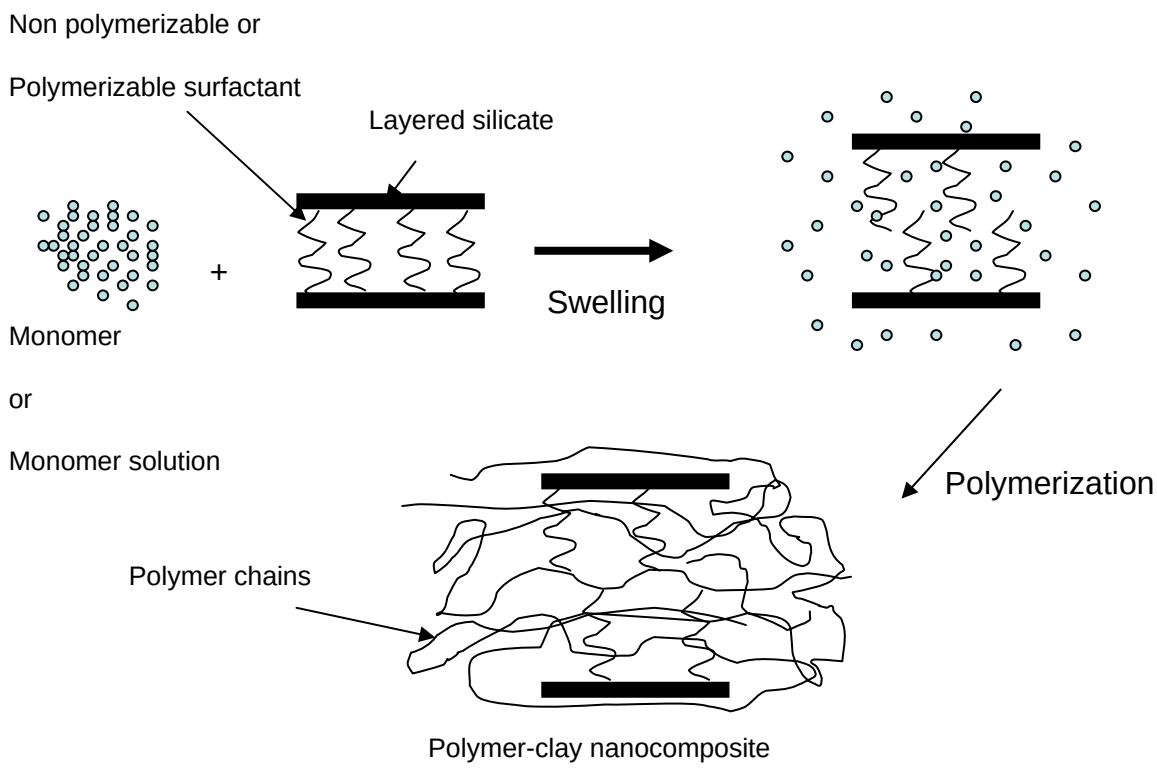

Fig. 3.1 Schematic representation of the synthesis of polymer-clay nanocomposites by *in-situ* intercalative polymerization.

(ii) Melt intercalation: This is a relatively new approach, where the polymers and organoclays are mixed statically or under shear above the glass transition temperature or melting temperature. The polymer can then penetrate the interlayer space [3].

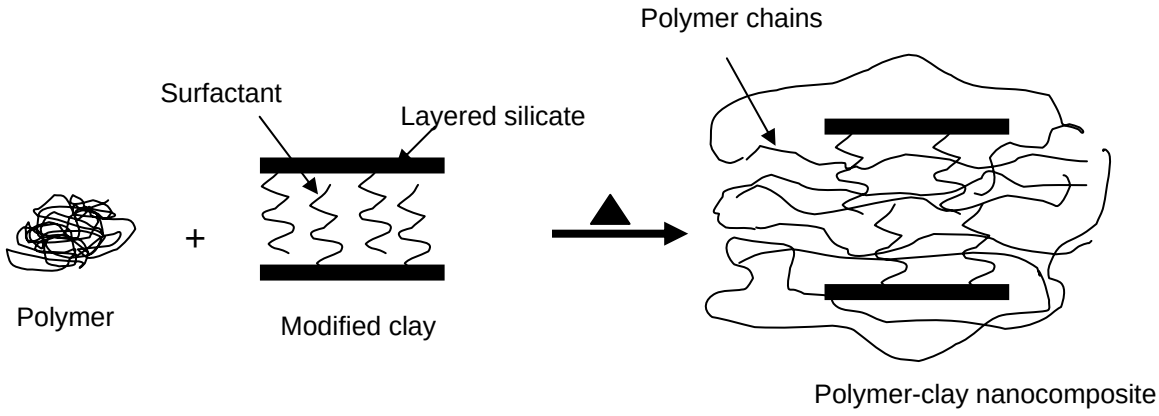

Fig. 3.2 Schematic illustration of the synthesis of polymer-clay nanocomposites using melt intercalation.

(iii) Exfoliation-adsorption: A solvent in which a polymer or prepolymer is soluble is used to exfoliate the layered silicate into single layers. This

method takes advantage of the fact that the weak forces that stack the layers together in layered silicates can easily be dispersed in an appropriate solvent. The polymer then adsorbs onto the delaminated clay layers. When the solvent is removed or the mixture precipitated there is reassembly of sheets with the polymer in-between, giving rise to an ordered multilayer structure [1].

(iv) Template synthesis: An aqueous solution containing the silicate building blocks is used to form the silicate layers in-situ. This method has been widely used for the synthesis of layered, double hydroxide based nanocomposites [1]. The polymer in aqueous solution aids the nucleation and growth of the inorganic host crystals and gets trapped within the layers as they grow. This method is far less developed for layered silicates and thus is of no significance here.

3.2 Review of the methods of the synthesis of polystyrene-clay nanocomposites.

3.2.1 Exfoliation adsorption technique.

The success of this method lies in the most suitable choice of solvent, organic modifier and type of clay for a specific polymer. The solvent facilitates the intercalation of the polymer into the clay interlayer spacing. The polarity of the solvent plays a critical role as the solvent should be able to homogeneously disperse the clay. Thermodynamics play a critical role in this technique, as there is need for the negative variation of the Gibbs free energy for polymer chains to be exchanged with a previously intercalated solvent. The driving force of polymer intercalation is the gain in entropy by desorption of solvent molecules; this entropy gain compensates for the decrease in conformational entropy of the confined polymer chains [3]. This technique is, however, not ideal for commercial purposes because of the use of organic solvents that are environmentally unfriendly. Exfoliation adsorption is also economically prohibitive [3-4].

The method has nonetheless been successfully used for the synthesis of intercalated nanocomposites of some water soluble polymers, including poly (ethylene oxide) [5],

polyvinyl alcohol [6], poly (vinyl pyrrolidone) [7] and poly (ethylene vinyl alcohol) [8].

The importance of the choice of the organic modifier for the preparation of PCNs by the exfoliation adsorption technique has been clearly demonstrated by Yano *et al*. [9]. They used various organic modifiers for the synthesis of polyimide-MMT nanocomposites. The nanocomposites were prepared from a solution of polyamic acid and organoclays dispersed in dimethyl acetamide (DMAc). The clay was modified by dodecyl ammonium cations (12 carbon backbone) terminated by an acidic substituent to yield 12C-COOH-MMT organoclay and a methyl group to yield 12C-CH_3-MMT organoclay, whereas 10A-MMT is a commercial organoclay. They obtained different levels of clay dispersion in the nanocomposites. 12C-CH_3-MMT clay gave a intercalated/exfoliated structure followed by 12C-COOH-MMT, while 10A-MMT resulted in only an intercalated structure. The type of clay used can also affect the resulting nanocomposite. This is a result of the differences in the aspect ratios of different clays. The Toyota Research group demonstrated the importance of the clay type when they prepared exfoliated polyimide-clay nanocomposites by mixing dimethyl acetamide and a modified-MMT with polyamic acid, followed by thermal imidization to obtain the final polyimide-clay nanocomposites [9]. When they extended their findings to other clays (i.e. hectorite, saponite and synthetic mica having different aspect ratios), the prepared nanocomposites showed different levels of exfoliation. MMT and synthetic mica, having high aspect ratios and high CEC values, resulted in an exfoliated structure whereas a partially exfoliated structure was obtained for hectorite and saponite [10].

To date, the exfoliation adsorption method has not been widely used for the synthesis of polystyrene-clay nanocomposites. An attempt to intercalate polystyrene in the organically modified clay from toluene solution only resulted in the intercalation of toluene instead of the polymer [4]. Recently intercalated syndiotactic polystyrene (sPS)-clay nanocomposites were prepared by the exfoliation adsorption technique; here cetyl pyridinium chloride (partially compatible with sPS) was used to modify clay [4]. These nanocomposites were prepared using hot dichlorobenzene as the solvent. The interlayer distance was dependent on the amount of sPS in the

nanocomposites. Biswas *et al*. [4] concluded that miscibility between the surfactant and sPS was crucial for dispersing clay in sPS.

This method has however been shown to be very successful for the preparation of nanocomposites of polystyrene containing rubber-clay [11].

The exfoliation adsorption technique has not been widely used for polystyrene based nanocomposites, probably because of the disadvantages associated with this method. The disadvantages include:

(i) Competition for the clay gallery space between the solvent and the polymer [12]. This implies that there is no assurance that polymer will intercalate into the clay interlayer space.

(ii) Notwithstanding conducting experiments under similar experimental conditions, the exfoliation adsorption technique can produce quite different results, much depending upon the solvent, polymer and modified clay.

(iii) Many solvent molecules need to be desorbed from the host to accommodate the incoming polymer chain. From a thermodynamic point of view, the entropy gain of solvents should be very large to offset the conformational entropy of the confined polymer. This of course is a big price to pay sometimes. To circumvent this constraint there is a need to establish numerous segment-clay contacts to offset the large decrease in conformational energy that opposes intercalation, which is sometimes not possible.

3.2.2 Melt intercalation.

Melt intercalation is a very recent technique, promoted by Vaia *et al*. [19] for the preparation of PCNs and is fast becoming the standard approach. Its versatility makes it compatible with current polymer processing techniques such as extrusion and blow moulding. It is an environmentally friendly process as no solvents are involved, and it could thus be economically viable [13]. The obtained hybrids range from intercalated to exfoliated nanocomposites, depending on the extent of favorable interactions between polymer and modified clay system. The intercalation of polymer into the clay

galleries is dependent on clay functionalization and constituent interactions [3]. Vaia *et al*. [12-14] established the kinetics, thermodynamics and model predictions for the preparation of polystyrene-clay nanocomposites by melt intercalation in organically modified clay.

Kinetics were monitored by the change in intensity of the intercalated versus pristine clay's diffraction peaks in XRD patterns with time as this reflects the kinetics of the polymer intercalation process as a function of time, temperature and molecular weight. The limiting step to hybrid formation is mass transport into the clay particles and the degree of mixing is critical for rapid hybrid formation [13]. Vaia and Giannelis [12] developed a mean-field, lattice-based model of polymer melt intercalation in organically-modified clay, where they proposed that there is an interplay of entropic and energetic factors that determine the outcome of polymer intercalation. Maximization of the magnitude and number of favorable polymer surface interactions is critical so as to overcome the penalty of polymer confinement if complete exfoliation is to occur. By considering energy and entropic factors, three types of composites can be proposed from Vaia and Giannelis's mean-field, lattice-based model i.e. immiscible polymer-clay composite, intercalated and exfoliated polymer-clay nanocomposites. The same authors [14] also investigated the effects of annealing temperature, polymer molecular weight, modification of clay and interactions on polymer melt intercalation. They deduced that there is a need for optimum interlayer interactions favouring nanocomposite formation if exfoliation or intercalation is to occur. Polar type (hydrogen bonding or electrostatic) and van der Waals interactions are critical for nanocomposite formation.

The importance of polar type interactions are clearly seen in the preparation of polypropylene (PP) based nanocomposites. The synthesis of PP nanocomposites using non polar PP was not successful until functionalized polar PP was used for the preparation of PP-clay nanocomposites [15-18].

Polystyrene nanocomposites have been prepared extensively by melt intercalation. Vaia *et al*. [19] reported the first ever PCNs based on polystyrene, prepared using the melt intercalation method. Vaia and Giannelis [14] investigated the influence of clay functionalization, the intercalation temperature, the molecular mass of the polymer and the interactions of the polymer and the modified clay. They made the modified

clays by ion exchanging Li^+-fluorohectorite and Na^+-MMT with excess alkylammonium ions. The alkylammonium ions included dioctadecyl dimethyl ammonium bromide, octadecyl trimethyl ammonium bromide and a series of primary alkyl ammonium chlorides with different numbers of carbon atoms ($C_nH_{2n+1}NH_3^+Cl^-$, where n = 6, 9-16, and 18), prepared by acidifying the corresponding amines. The nanocomposites were prepared by mechanically mixing the organosilicate and the polymer powder, followed by making pellets under pressure. The pellets were then annealed statically at temperatures above the T_g of the polymers to obtain intercalated nanocomposites for some modified clays and phase separated composites for others. The final gallery height of the intercalated nanocomposites was dependent on the chain length of the surfactants. They discovered that the molecular mass of PS did not affect the final structure. Furthermore, existence of polar interactions between the modified clay and the polymer were crucial if intercalation is to occur.

The importance of favorable interactions between the clay and the polymer was clearly demonstrated when blends of sPS and styrene copolymers (i.e. styrene-maleic anhydride random copolymer, and maleic anhydride grafted styrene-ethylene-butylene-styrene block copolymer) were prepared by melt intercalation. Park *et al*. [20] used a dimethyl dehydrogenated tallow alkyl ammonium modified MMT clay to prepare the nanocomposites by two methods: (a) a stepwise mixing method and (b) a simultaneous mixing method. They discovered that direct mixing of sPS and the modified clay resulted in the formation of conventional microcomposites. This was attributed to rupture of bonds or thermal desorption of the organic modifier, followed by a decrease in the wettability between polymer and clay. Exfoliated nanocomposites were obtained for the maleic anhydride grafted styrene-ethylene-butylene-styrene copolymers, possibly because of the polar nature of maleic anhydride interacting with the hydroxide group on the clay surface.

The effects of the compatibility between the organic modifier (i.e. surfactant) and the polymer have been widely investigated. It is generally agreed that if there is a high degree of compatibility between the surfactant and polymer then an exfoliated structure can be obtained. Park *et al*. [21] synthesized a blend of poly (styrene-*co*-vinyloxazolin) and sPS-clay nanocomposites. They investigated the influence of different surfactants and their packing density during the synthesis of

nanocomposites. The organic surfactants were dimethyl dehydrogenated tallow ammonium, dimethyl benzyl hydrogenated tallow ammonium and trimethyl octadecyl ammonium cations. They discovered that exfoliated nanocomposites at relatively low melt intercalation temperature were obtained only for the clay modified with dimethyl benzyl hydrogenated tallow ammonium ions, the other surfactants resulted in intercalated structures. They attributed their findings partly to the affinity between poly (styrene-*co*-vinyloxazolin) and the benzene group in the dimethyl benzyl hydrogenated tallow ammonium modifier as well as its lower packing density, which in turn allows a high quantity of poly (styrene-*co*-vinyloxazolin) to intercalate and interact with clay surface, leading to exfoliation.

The structure of the polymer itself can result in different nanocomposites. Robello *et al*. [22] investigated the effect of using a five-armed polystyrene polymer relative to linear polystyrene. The five-armed polystyrene resulted in an exfoliated polystyrene-clay nanocomposite whilst an intercalated structure was obtained for the latter.

Although melt intercalation looks like a very attractive way of synthesizing nanocomposites, it has some associated drawbacks which cannot be overlooked at this point. These drawbacks include:

(i) Thermal stability of the surfactant during high-temperature melt processing [15]. Park *et al*. [20] discovered that with an increase in temperature from 200 to 280 ^{0}C the interlayer spacing decreased due to the degradation and desorption of the surfactants from the gallery at high temperature. This hinders the intercalation of polymer into the gallery space.

(ii) This method relies on the efficiency of the shearing rate since, under static conditions, i.e. simple annealing without mixing or shearing, the method is kinetically limited.

(iii) Amorphous polystyrene intercalates into the clay layer via weak Lewis acid/base interaction between phenyl groups in polystyrene and the clay surface. Heat treatment weakens this interaction, resulting in part of the polystyrene being excluded from the clay galleries, leading to a decrease in interlayer spacing [20].

(iv) The method is dependent on the annealing temperature, possibly because the polymer needs to flow to enter the interlayer spacing and therefore it must be melted and the viscosity must allow easy flow.

3.2.3 *In-situ* intercalative polymerization.

Although polymerization inside the gallery space of clays was already reported in the 1960s and 1970s, it was a report by the Toyota Research group in 1993 that revived interest in the synthesis of polymer clay nanocomposites [3,23-24]. The Toyota Research group reported the synthesis of exfoliated Nylon 6 nanocomposites by *in-situ* intercalative polymerization.

In-situ intercalative polymerization, like other synthesis methods, relies on the compatibility between the monomer and the organically modified clay. Incorporation of polar groups was found to be important for the exfoliation of clay [25].

A novel way of synthesizing exfoliated polystyrene based nanocomposites with controlled molecular masses was reported by Weimer *et al*. [26]. This entailed the preparation of modified MMT clay by anchoring an ammonium cation bearing a nitroxide moiety inside the clay gallery space. Nitroxide mediated polymerization is well known for the control of free radical polymerization of styrene in bulk. Styrene is intercalated *in-situ* into the modified clay, followed by polymerization, giving rise to exfoliated polystyrene-clay nanocomposites.

The compatibility between the modified clay and the monomer plays a critical role in the resultant nanocomposite structure. Doh and Cho [27] compared the ability of MMT modified by three tetraalkylammonium cations of the general formula: $(CH_3)_2N^+$(hydrogenated tallow alkyl)R, where R is a hydrogenated tallow alkyl, a 2-ethyl hexyl or a benzyl group, to intercalate polystyrene through polymerization of styrene initiated by AIBN. XRD results showed that best intercalation occured for the surfactant containing the benzyl R group, probably because of the better compatibility between styrene and the benzyl groups. 2-ethyl hexyl containing surfactant also showed intercalation of polystyrene whereas very little intercalation occurred for the surfactant which had a hydrogenated tallow alkyl as its R group. Their results further showed the importance of the compatibility between the organically modified clay and styrene for the *in-situ* intercalative polymerization.

If a monomer solution is used, the polarity of the solvent greatly affects the obtained nanocomposites. The solvent's ability to interact with the polar surfaces of clay to a greater extent could result in a high concentration of monomer inside the gallery space. Akelah and Moet [28] used (vinyl benzyl)trimethyl ammonium chloride to modify Na^{+}-MMT and Ca^{2+}-MMT clays, and the modified clays were then dispersed in acetonitrile, acetonitrile/toluene and acetonitrile/THF. Styrene was added to the dispersed clay and polymerized using AIBN initiator. They obtained intercalated nanocomposites with interlayer distances ranging from 17.2 to 24.5 Å, depending on the nature of solvent used; acetonitrile was found to be the best solvent.

Efforts to prepare exfoliated polystyrene nanocomposites were greatly rewarded by the application of *in-situ* intercalative polymerization, mostly in the presence of polymerizable surfactant (surfmer) modified clays [29].

The effect of using a polymerizable surfactant modified clay, as opposed to the use of non-polymerizable surfactant modified clay, for the synthesis of polystyrene based nanocomposites, has been investigated by many researchers. It is believed that the copolymerization of the surfmer and styrene in-between the clay galleries could provide the driving force for the clay exfoliation [2,30-31], whereas no such driving force is present in non-polymerizable systems, which often results in intercalated nanocomposites.

Lee and Zeng [30] synthesized polystyrene-clay nanocomposites using the polymerizable surfactant 2-methacryloyloxyethylhexadecyldimethylammonium bromide. The surfmer was then used to modify Na^{+}-MMT by an ion exchange reaction, giving rise to modified clay. The nanocomposites were prepared by dispersing the modified clay in styrene monomer by sonication, adding a free radical initiator, further sonication, followed by polymerization, to obtain the nanocomposites. For comparison they prepared polystyrene nanocomposites using a non-polymerizable surfactant modified clay. PS nanocomposites prepared from non-polymerizable surfactant modified clay resulted in an intercalated structure whereas polymerizable surfactant modified clay resulted in an exfoliated structure. They also investigated the effect of using different initiators, e.g. AIBN and benzoyl peroxide, from which they concluded that the polarity and hydrophilicity of initiators were

critical since the combined use of more polar, less hydrophobic monomer and initiator leads to a better dispersion of clay in the nanocomposites.

Other researchers using surfmer modified clays had a similar approach for the synthesis of exfoliated polystyrene-clay nanocomposites [31-32]. This technique also relies on the proper choice of the organic modifier and the type of clay, like other techniques, but it offers certain advantages with respect to those techniques.

(i) With *in-situ* intercalative polymerization there is no need to worry about high temperature as is the case with melt intercalation. In *in-situ* intercalative polymerization mild temperatures are used as opposed to the high temperatures used for melt intercalation. Thus no decomposition of surfactants takes place.

(ii) Minimal quantities of solvents are used (in cases where monomer solutions are used) as opposed to very dilute solutions used for the exfoliation adsorption technique [11].

(iii) It is currently the only method that is compatible with the use of surfmers as the organic modifiers and thus it is ideal for our requirements.

(iv) The low viscosity of monomers results in their easy diffusion into the layered silicate aggregates, thus separating the clay layers as promoted by shear stress during their polymerization.

Although *in-situ* intercalative polymerization using surfmer-modified clays does not ensure complete exfoliation [28,32], at this point it appears to be the best method for the requirements of this investigation, i.e. the use of polymerizable surfactants for the preparation of polystyrene-clay nanocomposite structures. Polymerization takes place with the monomer inside the clay gallery space, thus ensuring the formation of a random copolymer, with the surfmer giving rise to, at least, an intercalated nanocomposite. Another reason for the choice of this technique is that most of the exfoliated polystyrene-clay nanocomposites described in the literature to date have been synthesized by this method.

References.

1. M. Alexandre, P. Dubois; Materials Science and Engineering, 28 (2000) 1-63.
2. M. Rosorff; Nano Surface Chemistry. Marcel Dekker Inc. New York-Basel (2002) 653-673.
3. S. S. Ray, M. Okamoto; Prog. Polym. Sci., 28 (2003) 1539-1641
4. M. Biswas, S. S. Ray; Adv. Polym. Sci., 155 (2001) 170-221.
5. P. Aranda, E. Ruiz-Hitzky; Chem. Mater., 4 (1992) 1395-1403.
6. D. J. Greenland; J. Colloid. Sci., 18 (1963) 647-664.
7. C. W. Francis; Soil Sci., 115 (1973) 40-54.
8. X. Zhao, K. Urano, S. Ogasawara; Colloid. Polym. Sci., 267 (1989) 899-906.
9. K. Yano, A. Usuki, A. Okada, T. Kurauchi, O. Kamigaito; J. Polym. Sci., Part A: Polym. Chem., 31 (1993) 2493-2498.
10. K. Yano, A. Usuki, A. Okada; J. Polym. Sci., Part A: Polym. Chem, 35 (1997) 2289-2294.
11. S. Sadhu, A. K. Bhowmick; J. Appl. Polym. Sci., 92 (2004) 698-709.
12. R. A. Vaia, E. P. Giannelis; Macromolecules, 30 (1997) 7990-7999.
13. R. A. Vaia, K. D. Jandt, E. J. Kramer, E. P. Giannelis; Macromolecules, 28 (1995) 8080-8085.
14. R. A. Vaia, E. P. Giannelis; Macromolecules, 30 (1997) 8000-8009.
15. P. H. Nam, P. Maiti, M. Okamoto, T. Kotaka, N. Hasegawa, A. Usuki; Polymer, 42 (2001) 9633-9646.
16. A. Usuki, M. Kato, A. Okada; J. Appl. Polym. Sci., 63(1997) 137-138.

17. N. Hasegawa, M. Kawasumi, M. Kato, A Usuki, A, Okada; J. Appl. Polym. Sci., 67 (1998) 87-92.

18. H. Tyan, K. Wei, T. Hsieh; J. Polym. Sci., Part B: Polym. Phys., 38 (2000) 2873-2878.

19. R. A. Vaia, H. Ishii, E. P. Giannelis; Chem. Mater., 5 (1993) 1694-1695.

20. C. I Park, O. O. Park, J.G. Lim, H. J. Kim; Polymer, 42 (2001) 7465-7475.

21. C. I. Park, H. Kim, O. O. Park; Polymer, 45 (2004) 1267-1273.

22. D. R. Robello, N. Yamaguchi, T. Blanton, C. Barnes; J. Am. Chem. Soc., 126 (2004) 8118-8119.

23. M. Okamoto; Encyclopedia of Nanoscience and Nanotechnology. American Scientific Publishers, California, (2004) 791-843.

24. N. Sheng, M. C. Boyce, D, M Parks, G. C. Rutledge, J. I. Abes, R. E. Cohen; Polymer, 45 (2004) 487-506.

25. M. Okamoto, S. Morita, H. Y. Kim, T. Kotaka, H. Tateyama; Polymer, 42 (2001) 1201-1206.

26. S. A. Zerda, C. T. Caskey, J. A. Lesser; Macromolecules, 36 (2003) 1603-1608.

27. J. H. Doh, I. Cho; Polym. Bull., 41 (1998) 511.

28. A. Akelah, A. Moet; J. Mater. Sci., 31 (1996) 3589-3596.

29. S. Qutubuddin, X. Fu; Polymer, 42 (2001) 807-813.

30. C. Zeng, L. J. Lee; Macromolecules, 34 (2001) 4098-4103.

31. W. A. Zhang, D. Z. Chen, H. Y. Xu, X. F. Shen, Y. E. Fang; European Polymer Journal, 39 (2003) 2323-2328.

32. C. Tseng, J. Wu, H. Lee, F. Chang; J. Appl. Polym. Sci., 85 (2002) 1370-1377.

Chapter 4: Synthesis, characterization and polymerization of polymerizable surfactants (surfmers).

4.1 Introduction.

This Section details the synthesis and characterization of the surfmers. In this project one of the major aims was to synthesize two novel similar surfmers, i.e. surfmers with the same polymerizable group but with different polar head groups. The polymerizable group was chosen to be on the tail of the surfmers.

This allowed us to study the influence of the presence of the polymerizable group as well as the effect of the polarity of the head group on exfoliation of clay in polystyrene-clay nanocomposites. This implied that surfmers of high purity had to be synthesized.

Properties of surfactants greatly depend on their purity levels. These properties include behaviour in water below and above the CMC values, surface properties [1-2] and also their ability to homopolymerize and copolymerize.

The chemical structures of the synthesized surfmers were confirmed by ^{1}H NMR, FT-IR and ESMS (see below). Their thermal properties were analysed by DSC and TGA. A conductivity meter, an optical microscope using crossed polarizers with a heating stage and SAXS were used for the determination of surfmer behaviour in water. Homopolymers were characterized by ^{1}H NMR and thermal analysis.

The synthesis and characterization of (11-acryloyloxyundecyl)dimethyl(2-hydroxy ethyl)ammonium bromide (Ethyl surfmer) and (11-acryloyloxyundecyl)dimethyl-ethylammonium bromide (Ethanol surfmer) and their homopolymers is now reported. To the author's knowledge, there is no available literature on the synthesis and characterization of these surfmers. However, (11-acryloyloxyundecyl)dimethyl(2-hydroxyethyl)ammonium bromide is registered in SciFinder Scholar (registration number 244626-86-6) but there are no references associated with it.

4.2 Experimental procedures.

The materials and the procedures used in the synthesis of surfmers and their homopolymers are outlined here.

4.2.1 Materials.

11-Bromoundecan-1-ol (98%, Aldrich); acryloyl chloride (98% Acros); sodium hydrogen carbonate (99%, Aldrich); sodium carbonate decahydrate (99%, Merck); anhydrous magnesium sulphate (62%, Merck); N, N-dimethylethanol amine (99% Acros); N, N-dimethylethylamine (99% Acros); hydroquinone (99%, Merck); dry dichloromethane, diethyl ether, ethyl acetate, and acetone were common laboratory reagents. Distilled and deionized water was obtained from a "Milli-Q" water purification system (Millipore Corp.); azobisisobutyronitrile (AIBN) was obtained from Aldrich and re-crystallised from hot methanol before use. Unless stated otherwise all the other reagents were used without further purification.

4.2.2 Synthesis of 11-bromoundecylacrylate.

11-bromoundecan-1-ol (2.017 g, 0.008 mol) was dissolved in 15 ml of previously dried dichloromethane in a 2-necked round bottomed flask; one neck was fitted with a $CaCl_2$ tube. The flask was immersed in an ice bath and stirred for 15 min. Sodium hydrogen carbonate (1.344 g, 0.016 mol) and hydroquinone (0.003 g, a radical polymerization inhibitor) were added to the stirring solution, followed by the dropwise addition of acryloyl chloride (1.448 g, 0.016 mol) over a period of 15 min. The mixture was continuously stirred for 4 days at room temperature, after which it was filtered. The organic layer was subsequently washed with 4 x 50 ml of 4% sodium carbonate decahydrate solution. The product was then dried over anhydrous magnesium sulphate and filtered. The solvent (dichloromethane) was removed under high vacuum at 45 ^{0}C. A brownish-yellowish oil of 11-bromoundecylacrylate was obtained in 94% yield. The product was analyzed by ^{1}H NMR.

4.2.3 Synthesis of (11-acryloyloxyundecyl)dimethyl(2-hydroxy-ethyl)ammonium bromide.

11-bromoundecylacrylate (0.200 g, 6.55 x 10^{-4} mol), dimethylethanolamine (0.100 g, 1.02 x 10^{-3} mol) and hydroquinone (0.003 g) were placed in a round bottom flask fitted

with a condenser. The set up was immersed in an oil bath and vigorously stirred at 50 ^{0}C for 150 min, giving rise to a brownish solid. Thereafter the solid was washed several times with diethyl ether, yielding an off-white product. The product (surfmer) was then vacuum dried overnight to yield an off-white powder. The surfmer was then recrystallised from hot ethyl acetate (10 ml), filtered and dried under vacuum overnight to yield 75% of an off-white crystalline powder (11-acryloyloxyundecyl)-dimethyl(2-hydroxyethyl)ammonium bromide. Characterization of the surfmer was carried out using ^{1}H NMR, FT-IR, TGA, DSC, ESMS, conductivity, polarised optical microscopy with a heating stage, and SAXS.

4.2.4 Synthesis of (11-acryloyloxyundecyl)dimethylethyl-ammonium bromide.

11-bromoundecylacrylate (0.200 g, 6.55 x 10^{-4} mol), dimethylethylamine (0.240 g, 3.26 x 10^{-3} mol) and hydroquinone (0.003 g) were placed in a round bottom flask fitted with a condenser. The set up was immersed in an oil bath and vigorously stirred at 50 ^{0}C for 6 h. To this whitish suspension 15 ml of diethyl ether was added and the reaction was carried out for a total of 72 h, yielding a white suspension. The product (surfmer) was filtered and washed several times with diethyl ether. The surfmer was then vacuum dried overnight to yield a dry white powder. The surfmer was then recrystallised from hot ethyl acetate (10 ml), filtered and dried under vacuum overnight to yield 46% of white crystalline (11-acryloyloxyundecyl)dimethyl-ethylammonium bromide. Characterization of the surfmer was carried out using ^{1}H NMR, FT-IR, TGA, DSC, ESMS, conductivity, polarised optical microscopy with a heating stage, and SAXS.

4.2.5 Homopolymerization of surfmers.

(11-acryloyloxyundecyl)dimethyl(2-hydroxyethyl)ammonium bromide (0.504 g, 0.001 mol), 4 ml of deionised water and AIBN (0.006 g) were placed in a Schlenk tube. The Schlenk tube was immersed in liquid nitrogen and the contents frozen. Vacuum suction was then applied to the frozen mixture for 5 mins, to remove any oxygen from the tube. The frozen mixture was then brought to ambient temperature. This process was repeated twice. While continuing stirring, the Schlenk tube was placed in an oil bath and polymerization was then carried out at 70 ^{0}C for 48 h. After cooling the polysurfmer was freeze dried to remove water, followed by washing with acetone several times to remove residual initiator and monomer. The homopolymers obtained

were then dried in a vacuum drier at 50 ^{0}C overnight. Analysis of the product was carried out using ^{1}H NMR, TGA, ESMS and DSC.

The homopolymerization of (11-acryloyloxyundecyl)dimethylethylammonium bromide was carried out using the same procedure.

4.3 Analytical methods.

4.3.1 ^{1}H NMR spectrometry.

The technique was used to elucidate the chemical structures of products. It was also used to prove the occurrence of the polymerization of surfmers by monitoring the disappearance of the ethylenic protons of the acrylate group.

^{1}H NMR was perfomed at 20 ^{0}C using Varian VXR-Unity 300 MHz and Varian Unity Inova 600 MHz NMR spectrometers.

4.3.2 FT-IR spectroscopy.

The technique was used for the identification of functional groups present on the surfmers. Prior to analysis samples were mixed in a ratio of 1 part sample to 300 parts of KBr then ground into a very fine powder. The powders were then pressed into KBr discs which were then analysed using a Nexus FT-IR instrument, by averaging 32 scans with a wavenumber resolution of 4 cm^{-1}.

4.3.3 Electrospray mass spectroscopy.

This technique was used to prove the deductions made from ^{1}H NMR and FT-IR by showing the molecular mass of the surfmers and their abundances relative to impurities. A Waters-Micromass QTOF Ultima API instrument was used for the analysis.

4.3.4 Thermogravimetric analysis.

The thermal stabilities of the surfmers and homopolymers were analysed on a Perkin Elmer TGA 7 instrument. Samples of less than 20 mg were used for all analyses. Samples were analyzed from ambient temperature to 600 ^{0}C at 20 ^{0}C/min heating rate.

4.3.5 Differential scanning calorimetry.

This technique was used for the measurement of temperatures and heat flows associated with the phase transitions of the surfmers. Measurements were carried out on a TA Instruments DSC Q 100 instrument. Samples of less than 5 mg were analyzed from -10 ^{0}C to 180 ^{0}C then cooled followed by a second heating process. DSC was also used for the analysis of the polysurfmers. Measurements were carried out on a Mettler Toledo DSC 25 with a Mettler TC 11 TA processor. Samples of less than 10 mg were analyzed from room temperature to 200 ^{0}C then cooled followed by a second heating process.

4.3.6 Conductivity.

Conductivity measurements were done using a Eurotech cell combined with a Cyberscan 500 device. All measurements were carried out at 295 K.

4.3.7 Polarized optical microscope with a heating stage.

Samples were prepared by weighing the components into glass vials with screw caps. The samples were then flushed with nitrogen, mixed and heated in a vacuum oven at 40 ^{0}C for 24 h. The samples were removed from the heater and allowed to equilibrate at ambient temperature for a further week. The textures of the liquid crystalline phases were then determined by an optical microscope using crossed polarizers. Phase transition temperatures were determined using a heating stage. Analyses were carried out on a microscope equipped with a Leitz 350 heating stage.

4.3.8 Small angle X-ray scattering.

SAXS measurements were performed at 298 K. SAXS diffraction measurements were carried out in a transmission configuration. A copper rotating anode X-ray source (functioning at 4 kW) with a multilayer focusing "Osmic" monochromator giving high flux (10^8 photons/sec) and punctual collimation was used. An "image plate" 2D detector was used. Diffraction curves were obtained, giving diffracted intensity as a function of the wave vector *q*.

For crystalline compounds, the d spacing d_{hkl} between reticular planes *hkl* can be determined from the position of corresponding Bragg peaks observed on the diffraction curve. d_{hkl} was calculated from the Bragg's law:

$$2d_{hkl}\sin\theta = \lambda \qquad (4.1)$$

where 2θ is the diffraction angle and λ_{Cu} = 1.54 Å.

The wave vector q is related to θ by the relation:

$$q = \frac{4\pi \sin\theta}{\lambda} \qquad (4.2)$$

From relations (4.1) and (4.2), the following can be deduced:

$$d_{hkl} = \frac{2\pi}{q_{hkl}} \qquad (4.3)$$

were q_{hkl} is the q value corresponding to the associated Bragg peak position.

4.4 Results and discussion.

4.4.1 Synthesis of surfmers.

The synthesis of surfmers can be hampered by two major problems i.e. difficulties in the isolation and purification of intermediate products due to the surface-active nature of such products and secondly polymerization of the acrylic group [1-2]. Introduction of the hydrophilic head group or polymerizable group at the very end of the synthesis process, working at mild temperatures, and the use of polymerization inhibitors to prevent the polymerization at the double bonds during synthesis, can circumvent these problems. Introducing the polymerizable group at the end avoids the requirement for polymerization inhibitors and reduces temperature restrictions associated with polymerizable groups. Thus, a suitable selection of a synthetic procedure is critical to ensure pure products and high yields.

In this synthesis, it was decided to introduce the head group at the end of the synthesis strategy and to use mild temperatures and polymerization inhibitors. It is easier to control reaction conditions than to be faced with difficulties associated with isolation of a surface-active product. Thus, a two-step synthetic pathway was used for the synthesis of the surfmers.

The first step was the introduction of the acryloyl polymerizable group to a long alkyl chain i.e. 11-bromoundecan-1-ol. Below is an outline of this synthetic pathway.

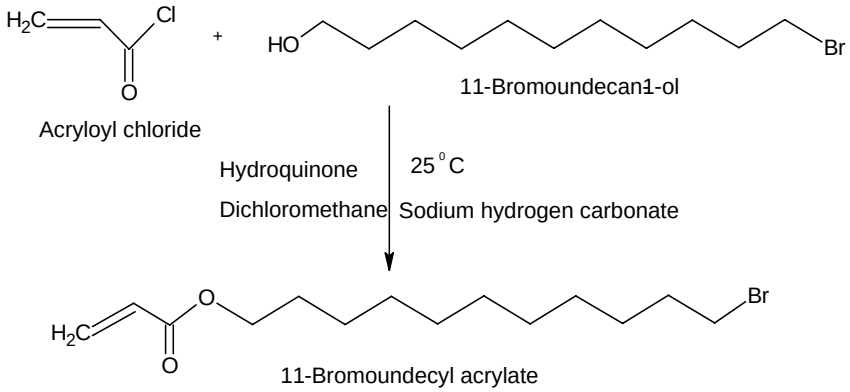

Fig. 4.1 Synthesis of 11-bromoundecyl acrylate.

The above exothermic esterification reaction generates heat, thus acryloyl chloride (a very reactive reagent) was added to 11-bromoundecan-1-ol dropwise at 0 ^{0}C (contents were placed in ice during this addition) to avoid heat build up which could lead to polymerization at the double bonds. After the addition of acryloyl chloride the reaction was carried out at room temperature in the presence of hydroquinone (i.e. a radical inhibitor). The reaction by-product i.e. hydrogen chloride was quickly neutralized with sodium hydrogen carbonate.

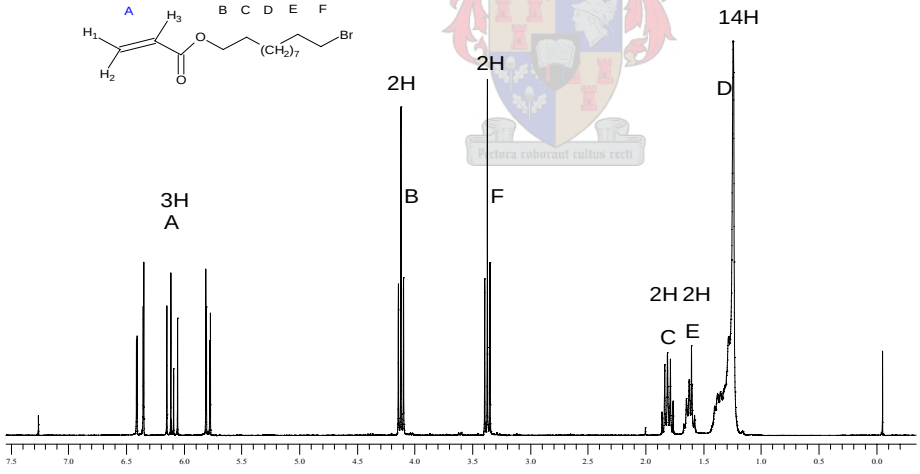

Fig. 4.2 ^{1}H NMR spectrum of 11-bromoundecyl acrylate (in $CDCl_3$).

The intermediate compound 11-bromoundecyl acrylate was characterised by ^{1}H NMR. The major change was associated with the formation of the ester bond that resulted in the methylene protons at ~ 3.6 ppm in 11-bromoundecan-1-ol [3] to shift to ~ 4.2 ppm in 11-bromoundecyl acrylate. The chemical shifts of the protons in 11-bromoundecyl acrylate are in close agreement with those found by Sherrington and Joynes [1].

The second step was the introduction of the surfactant head group according to the following general pathway.

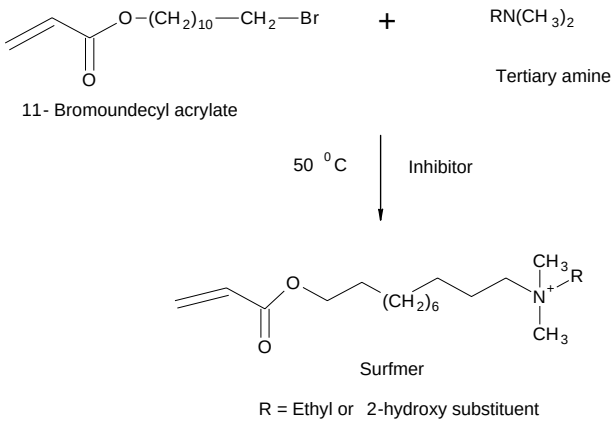

Fig. 4.3 General method for the synthesis of the surfmers.

The reactions were carried out at mild temperatures in the presence of a free radical inhibitor to ensure inhibition of spurious polymerization from taking place.

4.4.1.1 (11-acryloyloxyundecyl)dimethyl(2-hydroxyethyl)ammonium bromide.

The ^{1}H NMR spectrum of (11-acryloyloxyundecyl)dimethyl(2-hydroxyethyl) ammonium bromide is shown in Fig. 4.4 and the spectral data of the reactants are shown in Table 4.1. Compared to 11-bromoundecyl acrylate (BUA), the methylene protons (H^{E1}, H^{E2} and H^{F}) in (11-acryloyloxyundecyl)dimethyl(2-hydroxyethyl)-ammonium bromide (ethanol surfmer) are shifted downfield. This can also be said for the methylene protons (H^{G}, H^{H} and H^{I}) in dimethylethanol amine (DOA) which are shifted downfield in the ethanol surfmer. All these protons are close to the quaternary nitrogen atom which is known for causing such shifts [4]. Surprisingly, the effect of the nitrogen atom is also felt by the hydroxyl proton H^{J} which has shifted from 3.95 ppm in DOA to 5.00 ppm in the ethanol surfmer. Chemical shift predictions were carried out using ACD/ChemSketch and there is very good agreement of these values with those obtained experimentally.

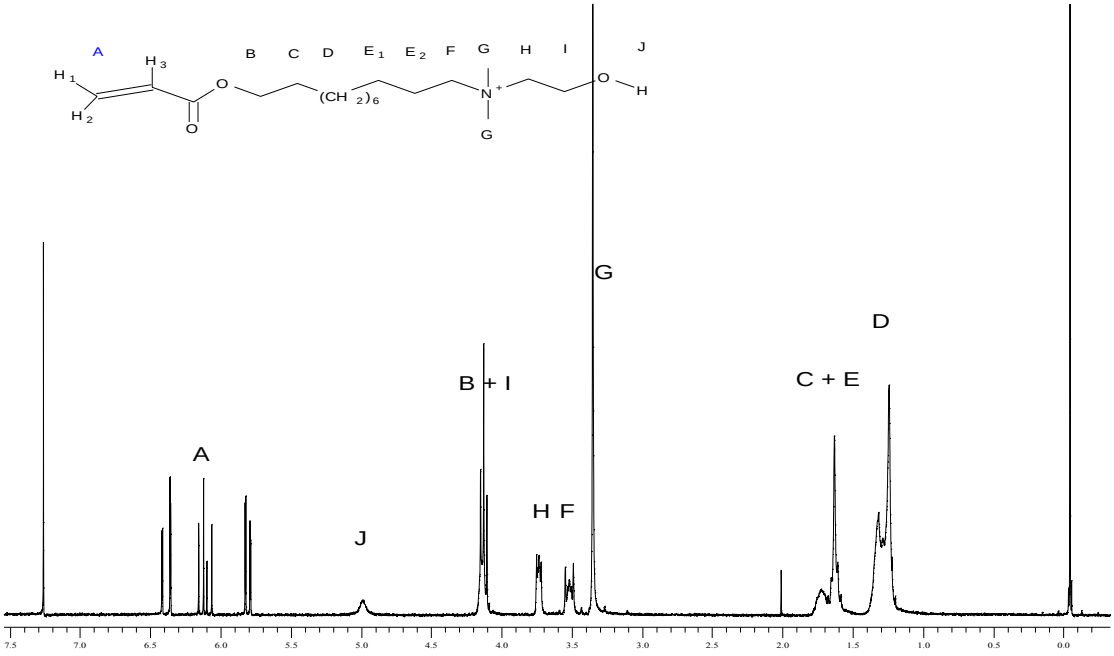

Fig. 4.4 ^{1}H NMR spectrum of (11-acryloyloxyundecyl)dimethyl(2-hydroxyethyl)ammonium bromide (in $CDCl_3$)

Table 4.1 ^{1}H NMR chemical shift data of (11-acryloyloxyundecyl)dimethyl(2-hydroxyethyl)-ammonium bromide (in $CDCl_3$)

Compound	Chemical shifts (ppm)												
	H^{A1}	H^{A2}	H^{A3}	H^{B}	H^{C}	H^{D}	H^{E1}	H^{E2}	H^{F}	H^{G}	H^{H}	H^{I}	H^{J}
BUA	5.80	6.40	6.10	4.10	1.70	1.30	1.30	1.60	3.35	-	-	-	-
DOA	-	-	-	-	-	-	-	-	-	2.25	2.45	3.6	3.95
Ethanol surfmer predicted	5.82	6.40	6.16	4.15	1.60	1.28	1.52	1.74	3.13	3.38	3.77	4.16	4.83
Ethanol surfmer experimental	5.80 (d)	6.40 (d)	6.10 (dd)	4.10 (m)	1.70 (m)	1.30 (m)	1.70 (m)	1.75 (m)	3.50 (t)	3.35 (s)	3.75 (q)	4.15 (m)	5.00 (s)

Where: (s), (d), (t), (q) and (m), are splitting patterns (singlet, doublet, triplet, quadruplet and multiplet respectively).
BUA: 11-Bromoundecyl acrylate
DOA: Dimethylethanol amine
Ethanol surfmer: (11-acryloyloxyundecyl)dimethyl(2-hydroxyethyl)ammonium bromide

4.4.1.2 (11-acryloyloxyundecyldimethyl)ethylammonium bromide.

As already outlined in Section 4.4.1.1 above, the major changes in the proton chemical shifts of (11-acryloyloxyundecyldimethyl)ethylammonium bromide (Fig. 4.5 and Table 4.2) below, are associated with the formation of quaternary nitrogen atom [4].

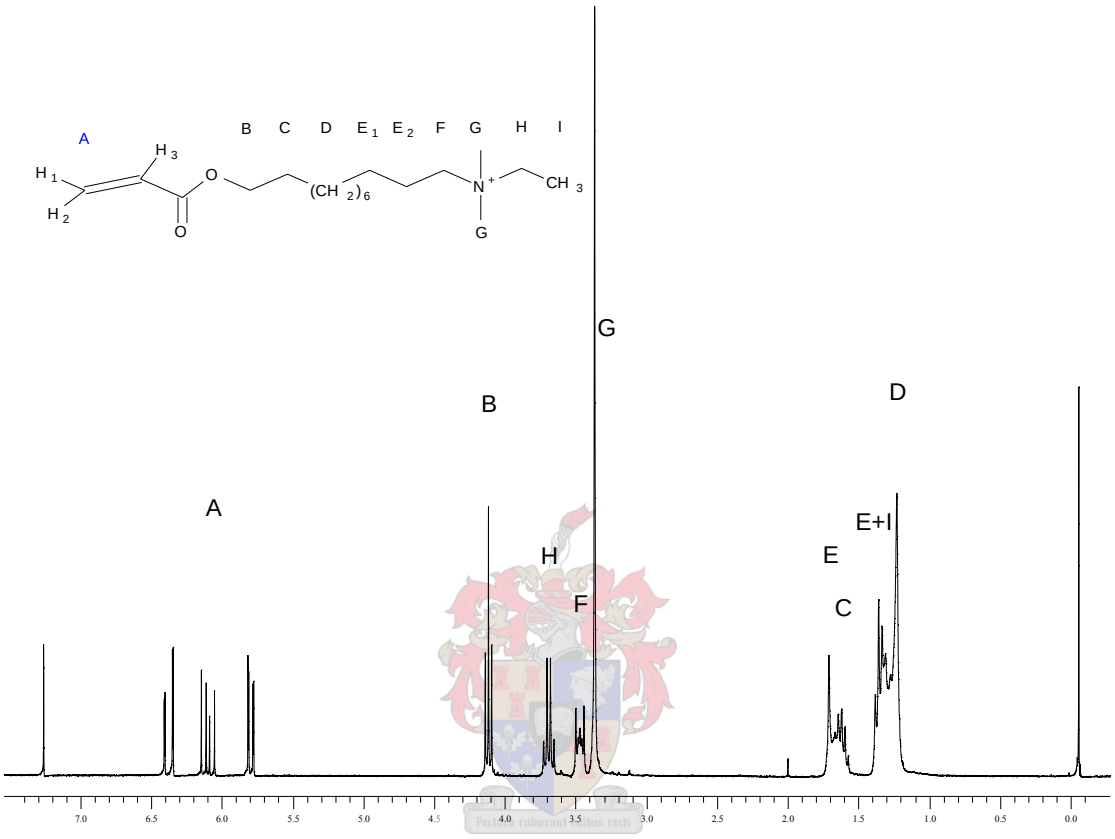

Fig. 4.5 ^{1}H NMR spectrum of (11-acryloyloxyundecyldimethyl)ethylammonium bromide (in $CDCl_3$).

Table 4.2. ^{1}H NMR chemical shift data of (11-acryloyloxyundecyldimethyl)ethylammonium bromide (in $CDCl_3$)

Compound	Chemical shifts (ppm)											
	H^{A1}	H^{A2}	H^{A3}	H^{B}	H^{C}	H^{D}	H^{E1}	H^{E2}	H^{F}	H^{G}	H^{H}	H^{I}
BUA	5.80	6.40	6.10	4.10	1.70	1.30	1.30	1.60	3.35	-	-	-
DHA	-	-	-	-	-	-	-	-	-	2.25	2.15	1.00
Ethyl surfmer predicted	5.82	6.40	6.16	4.15	1.60	1.28	1.38	1.71	3.15	3.24	3.68	1.43
Ethyl surfmer Experimental	5.80 (d)	6.40 (d)	6.10 (dd)	4.10 (t)	1.65 (m)	1.30 (m)	1.35 (m)	1.70 (m)	3.45 (t)	3.35 (s)	3.70 (q)	1.35 (m)

Where: (s), (d), (t), (q) and (m) are splitting patterns (singlet, doublet, triplet, quadruplet and multiplet respectively).
BUA: 11-Bromoundecyl acrylate
DHA: Dimethylethyl amine
Ethyl surfmer: (11-acryloyloxy)undecyldimethylethylammonium bromide

The differences in the polarities of the surfmer head groups are clearly seen from the chemical shifts in the ^{1}H NMR spectra. The protons H^{F}, H^{G}, H^{H} and H^{I} are more downfield in the Ethanol surfmer with respect to those in the Ethyl surfmer.

The synthesis of exfoliated nanocomposites is favored by the use of polar functional groups i.e. surfactants, polymers or monomers [5-7]. In this study, the polar functional groups could only be obtained from the surfactants since polystyrene (i.e the base polymer) is not polar. Here we wanted to use two surfmers, one being polar and one polar but also possessing hydrogen bonding capability. For the added hydrogen bonding functionality we tried to use dihydroxyethyl amine and trihydroxyethyl amine. Unfortunately the final products could not be dissolved in common deuterated ^{1}H NMR solvents ($CDCl_3$, D_20, DMSO, etc). This was attributed to a high probability of a number of side reactions that can occur during the synthesis. These reactions could include.

a) Transesterification by the 2-hydroxyethyl substituent groups on the amine which leads to the formation of 11-bromoundecan-1-ol and another product. The transesterification products can then react further. This is shown Fig. 4.6. below.

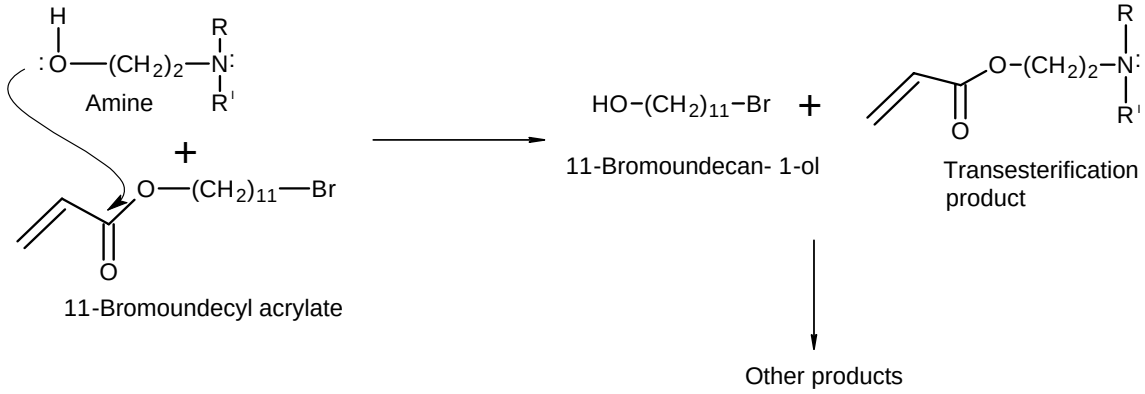

Fig. 4.6 Transesterification reaction of 11-bromoundecyl acrylate by the substituents on the amine. R = $–CH_2CH_2OH$ and R^I = –H for the dihydroxyethyl amine. R and R^I are $–CH_2CH_2OH$ for the trihydroxyethyl amine.

b) Dihydroxyethyl amine is a secondary amine, meaning that instead of reacting with 11-bromoundecan-1-ol to form a surfmer only, it could further react by donating its proton to a basic species [8-10]. In this case a second molecule of dihydroxyethyl amine or the hydroxyl groups on the hydroxyethyl substituents, giving rise to a new ternary nitrogen that can further react to produce a double tailed surfmer, transesterification products etc. Part of the proposed reaction pathwaw is outlined in Fig. 4.7 below.

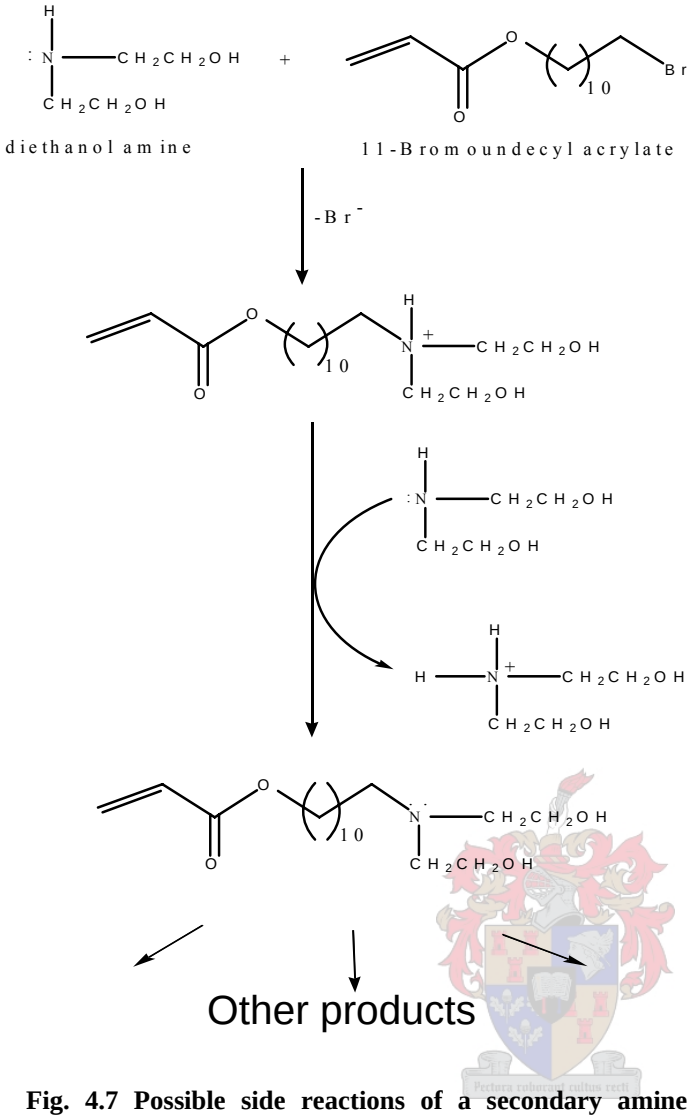

Fig. 4.7 Possible side reactions of a secondary amine during the synthesis of quaternary ammonium compounds.

4.4.2 Fourier transform infra-red spectroscopy.

From the IR spectra of the surfmers (Appendix 1: Fig. 1 and Fig. 2) the following assignments of peaks were made (see Table 4.3).

Infrared spectroscopy was used as a tool for identifying and confirming functional groups proposed from theory and ^{1}H NMR. All the functional groups expected were found to be present, further confirming the successful synthesis of the surfmers [11].

Table 4.3. IR band assignment for Ethanol surfmer and Ethyl surfmer

	Ethanol surfmer		Ethyl surfmer	
Assigned groups	Wavelength (cm^{-1})	Signal intensity	Wavelength (cm^{-1})	Signal intensity
$-CH_2-$	690, 723.5, 811	w	690, 722.4, 809	w
>C-O-	1191	s	1187	s
$-CH_3$	1407	m	1404	m
$-CH_2-$	1475	m	1475	m
>C-C<	983	m	983, 1052	m
>C-N<	1292	m	1292	m
>C=C<	1636	m	1632	m
>C=O	1721	s	1725	s
$-CH_2$	2853, 2920	s	2845, 2920	s
=C-H	3018	m	3003	m
O-H	3490	s, broad	-	-

Where: s = strong intensity, m = moderately intense peak and w = weak intensity.

4.4.3 Electrospray mass spectrometry.

Electrospray is a mild method of ionization for mass spectrometry. The spectra obtained normally contain only the molecular ions, with little or no fragmentation. The analysis can either be done in the positive or negative mode. In the negative mode an acidic proton is removed from the species under analysis and it thus becomes negatively charged for analysis by mass spectrometry. On the other hand, if analysis is done in the positive mode a proton is added to Schiff base type groups to make them positively charged for analysis by mass spectroscopy. Here analysis was carried out in the positive mode since the surfmers were already positively charged. This means that

the most intense peak or peak with 100% abundance (the base peak) should be due to the surfmers without the mass of the bromide counter ion. The ESMS spectra for the surfmers are given in Fig. 4.8 [(A) and (B)] below.

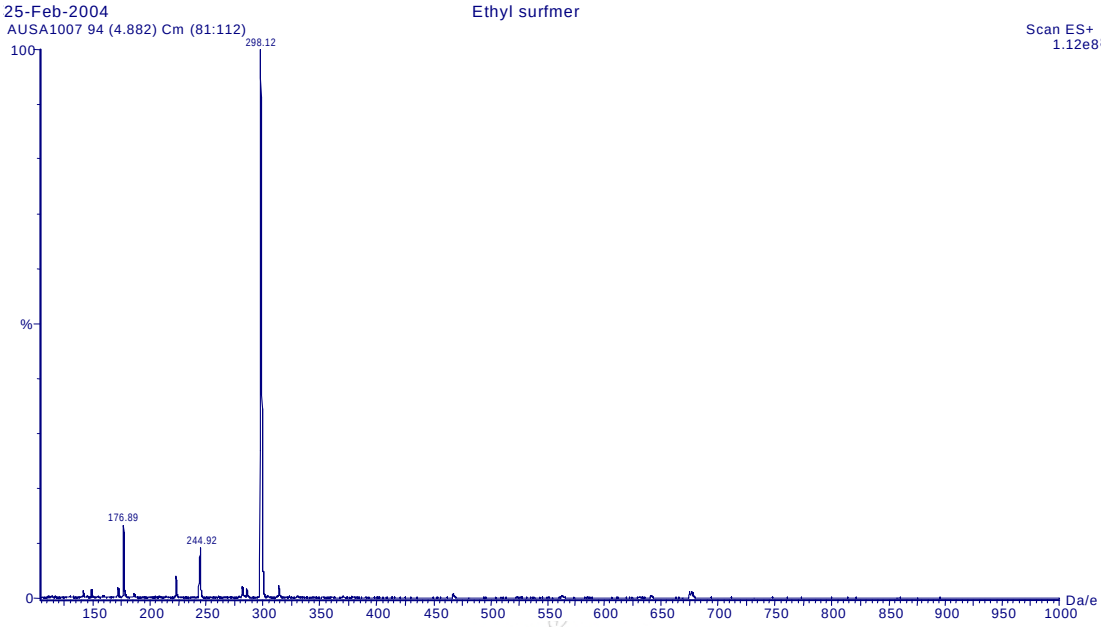

Fig. 4.8 (A) ESMS spectrum of Ethyl surfmer.

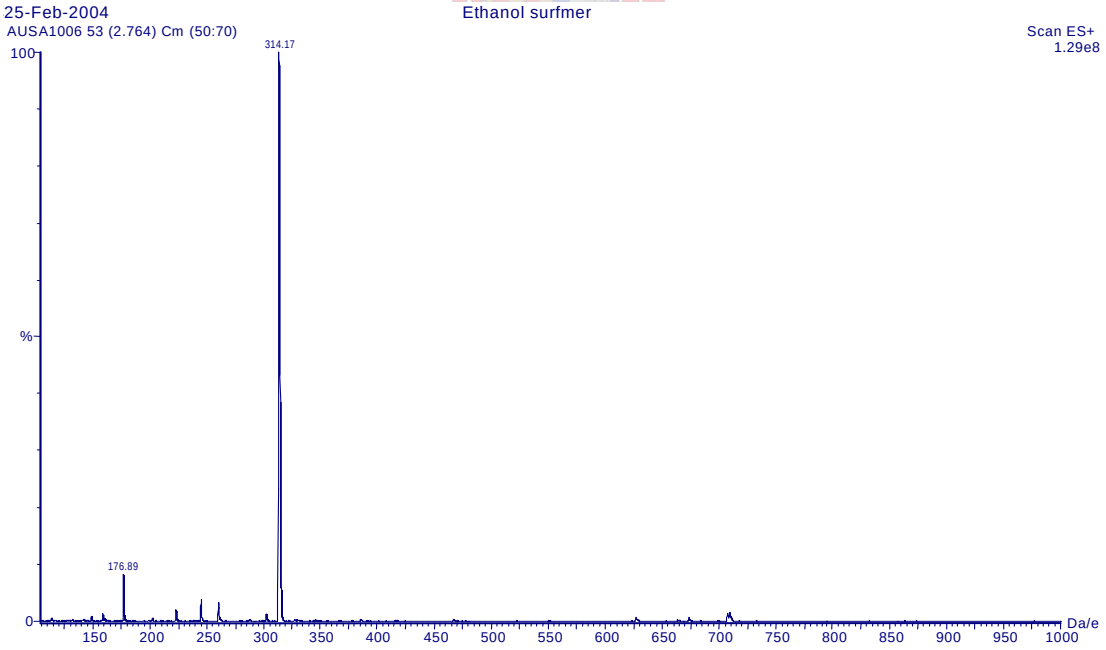

Fig. 4.8 (B) ESMS spectrum of Ethanol surfmer.

The theoretical m/z values were calculated using the atomic masses from the periodic table, thus the slight difference between the theoretical and the experimental values could be due to variation in isotopes (see Table 4.4 below). The weak peaks at 176.89 and 244.92 in the spectar could not be assigned to any ions but are probably due to some impurities.

Table 4.4. ESMS peak assignments for the surfmers Ethanol surfmer and Ethyl surfmer

Surfmer	Theoretical m/z of base peak	Experimental m/z of base peak
Ethanol surfmer	314.48	314.17
Ethyl surfmer	298.48	298.12

4.4.4 Thermal analysis of surfmers.

4.4.4.1 Thermogravimetric analysis.

TGA measures the weight loss of a material due to the formation of organic volatile material arising from the thermal degradation of species as a function of a temperature programme. The thermal stability of a compound depends on its chemical structure, intra- and intermolecular forces. The only difference in the chemical structure of the two surfmers Ethanol and Ethyl is the nature of the head group. The former is thermally more stable than the later. For comparison, thermal stability of cetyltrimethylammonium bromide (CTAB), a classical surfactant, was also analyzed. CTAB only shows decomposition and has a lower final degradation temperature relative to the surfmers. This is shown in the onset and maximum degradation temperatures from Fig. 4.9 and Table 4.5 below.

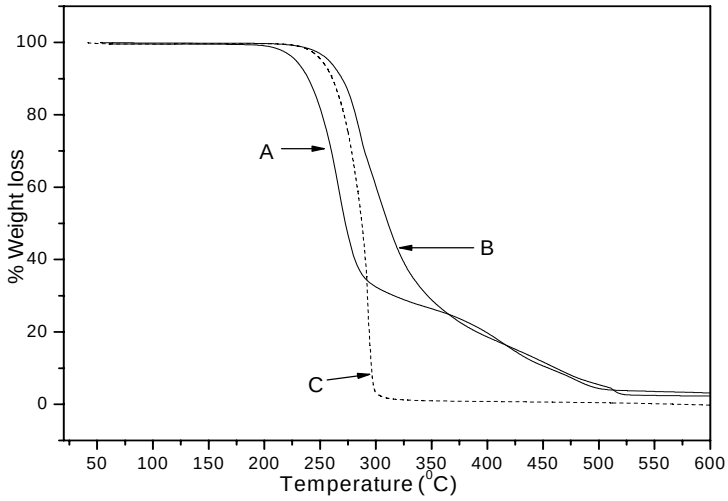

Fig. 4.9 TGA thermograms: Ethyl surfmer (A) Ethanol surfmer (B) and CTAB (C).

Table 4.5 Thermal stability of surfmers

Surfmer	$T_{1\ ONSET}/^0C$	$T_{2\ ONSET}/^0C$	$T_{MAX}/^0C$
Ethyl (A)	240	290	508
Ethanol (B)	270	-	522
CTAB (C)	261	-	303

Where: $T_{1\ ONSET}/^0C$, $T_{2\ ONSET}/^0C$, $T_{MAX}/^0C$ are the first onset degradation temperatures taken at 10% degradation [12], the metastable onset of degradation and final degradation temperatures respectively.

The surfmers follow a two-step degradation pathway (see Fig. 4.9). In TGA the first degradation is always due to the weakest groups in the compound. In the surfmers the weakest link from bond energy considerations is the >C-N< bonds. Thus the first degradation step could be the degradation of the head group [13]. This is very possible given that nitrogen containing compounds become unstable above 200 ^{0}C because they degrade, giving off ammonia. The second slow step, which is very visible with Ethyl surfmer, starts at about 290 ^{0}C. This step is probably due to the degradation of the tail that contains high-energy bonds i.e. >C-C< and >C=O.

4.4.4.2 Differential scanning calorimetry.

DSC measures the temperatures and heat flows associated with transitions in materials as a function of time and temperature. These measurements provide the quantitative and

qualitative information about chemical and physical changes that involve endothermic (heat absorbed) and exothermic (heat evolved) transitions.

The first heating DSC curve of Ethyl surfmer showed only one major endothermic peak. This peak is due to the melting of the surfmer crystals and thus gives the melting point (see Fig. 4.10). On the contrary, Ethanol surfmer showed two melting peaks, i.e. a small peak and a major melting peak, this could be attributed to the presence of different crystalline forms in the surfmer. The summarized DSC results are shown in Table 4.6 below.

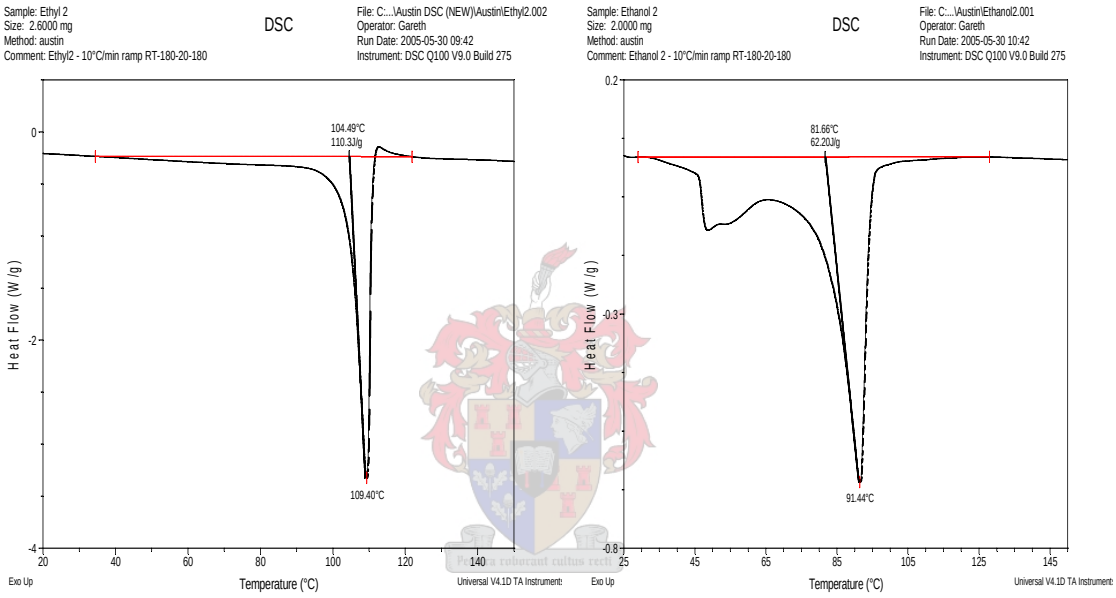

(A) (B)

Fig. 4.10 The first heating DSC thermograms for Ethyl surfmer (A) and Ethanol surfmer (B).

Table 4.6 Melting temperatures of surfmers from DSC

Surfmer	$T_{MELTING}/^0C$	$\triangle H/(J/g)$
Ethanol	81.7	62.2
Ethyl	104.5	110.3

Where: $T_{MELTING}/^0C$ and $\triangle H/(J/g)$ are the melting transition temperature and enthalpy of melting respectively.

The melting points of crystalline compounds are depended on several factors, such as intermolecular forces, purity, strength of the electrostatic attraction between opposite

charges that make the crystals, etc. The difference in the melting points and enthalpy of melting of the surfmers arises mainly from the head group in this case. From Table 4.6 it is evident that the Ethyl surfmer has a higher melting temperature and a higher enthalpy of melting than the Ethanol surfmer. At this point a sound explanation for these findings cannot be given but it is suggested that it could be due to strong interaction in crystals of Ethyl surfmer or some other thermodynamic aspects.

The cooling DSC curve for the Ethyl surfmer showed one exothermic peak i.e crystallization peak and the second heating curve showed one endothermic peak i.e. the melting peak (see Fig. 4.11 A). On the contrary, Ethanol surfmer's cooling curve showed multiple peaks (three peaks) this could be attributed to the presence of different crystalline forms (see Fig. 4.11 B). The second heating curve for Ethanol surfmer also showed the presence of different crystalline forms as seen by the double melting peak (see Fig. 4.11 B).

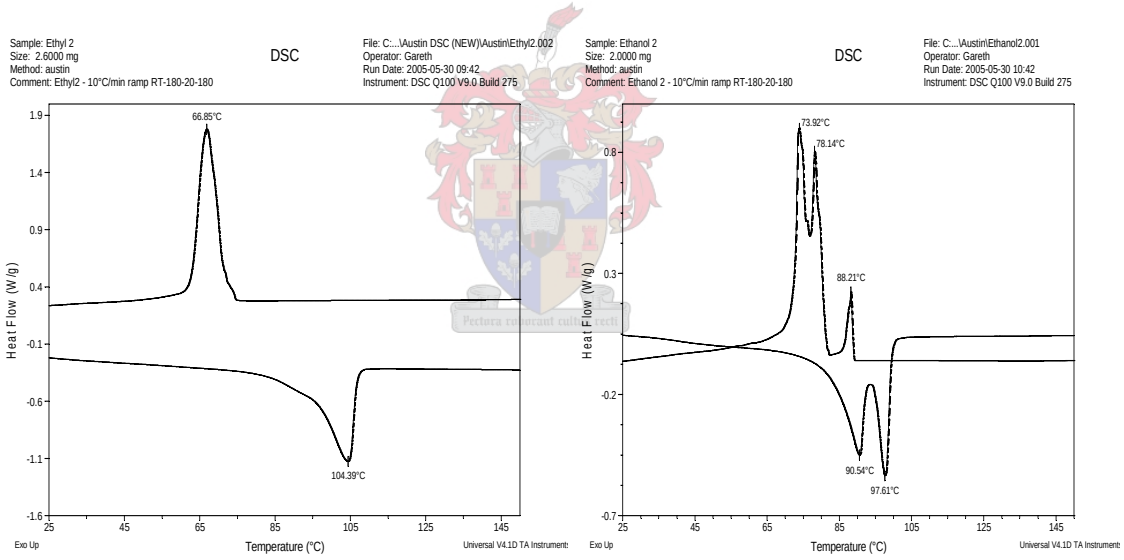

(A) (B)

Fig. 4.11 The cooling (positive Heat Flow) and the second heating (negative Heat Flow) DSC thermogram for Ethyl surfmer (A) and Ethanol surfmer (B).

It was not possible to observe the Ethanol surfmer's different transitions using polarized optical microscope and thus determine whether the 88.2 ^{0}C transition in the cooling curve is related to the formation of a thermotropic liquid crystalline mesophases. Thus more research is required here.

4.4.5 CMC determination by conductivity measurements.

The variation of the conductivity with the surfmer concentration in water is shown in Fig. 4.12 below.

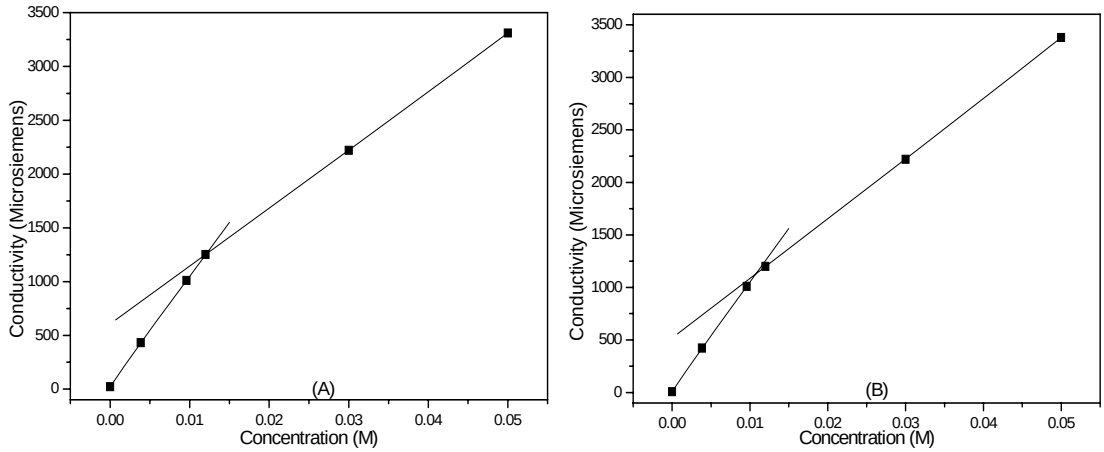

Fig. 4.12 Variation of conductivity with surfmer concentration for the Ethanol surfmer (A) and the Ethyl surfmer (B).

The CMC values as determined by conductivity were 0.0105 M and 0.0116 M for the Ethyl and the Ethanol surfmers, respectively. Ethanol surfmer's head group is more polar than that of the Ethyl surfmer, hence its high CMC value relative to that of the latter. This is in agreement with the results of Joynes and Sherrington [14], who showed that increasing the hydrophilicity of the head group results in an increase in interactions with water through hydrogen bonding, hence disfavoring micelle formation. The CMC values reported here for the Ethyl and the Ethanol surfmers are comparable to the value reported for a similar surfactant 11-acryloyloxyundecyltrimethylammonium bromide (AUTMAB) of 0.017 M [15]. The difference between these three surfmers resides in the alkyl groups of the ammonium polar head, the hydrophobic tail remaining exactly the same. Ethyl surfmer has a polar head less hydrophilic than AUTMAB due to the ethyl group, resulting in lower CMC value. This is in accordance with the results of other researchers [2,14,16-19], who showed that increasing hydrophobicity results in lower CMC values. The CMC value for Ethanol surfmer was also found to be lower than for the AUTMAB surfmer. This cannot reasonably be attributed to an increase in the hydrophobicity of the polar head in the case of Ethanol surfmer. Indeed, the presence of the hydroxyl group allows the polar head of Ethanol to form hydrogen bonds with water and with other polar heads. The low CMC value found seems to show

that the ability to form hydrogen bonds between polar heads favors self-assembly in micellar structures in the case of Ethanol surfmer.

4.4.6 Polarised optical microscope with a heating stage.

Binary phase diagrams of Ethyl surfmer/water and Ethanol surfmer/water systems were created using polarized optical microscope and the phase transitions were followed using a heating stage. The binary phase diagrams (Fig. 4.14 below) show that both surfmers can form isotropic solutions and lyotropic liquid crystalline (LLC) lamellar phases (typical maltese crosses and oily streaks [20] see Fig. 4.13 below) in water.

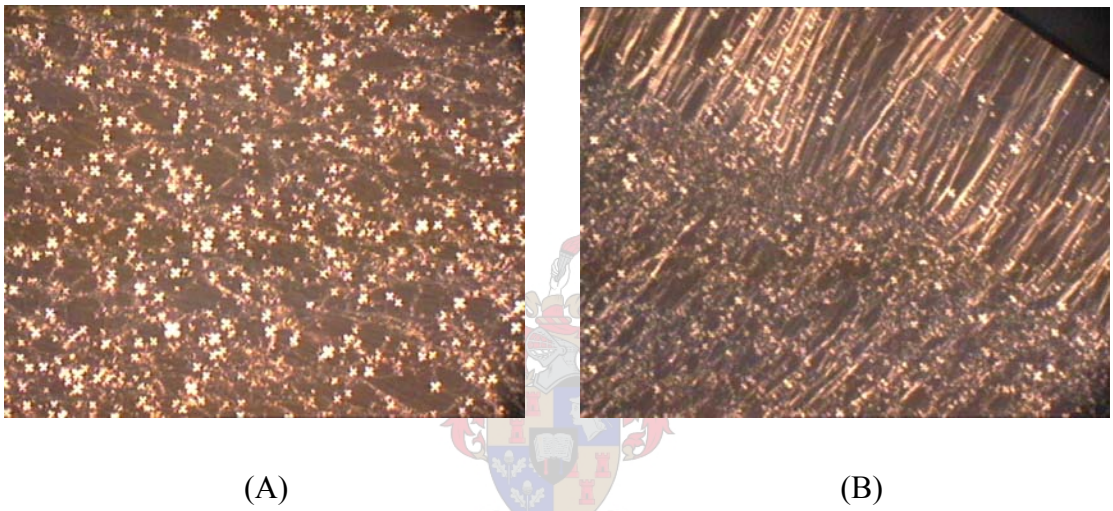

Fig. 4.13 Lamellar liquid crystalline phase of the Ethanol surfmer (A) and the Ethyl surfmer (B), obtained from polarised optical microscope at room temperature (25 ^{0}C) and 80% concentration.

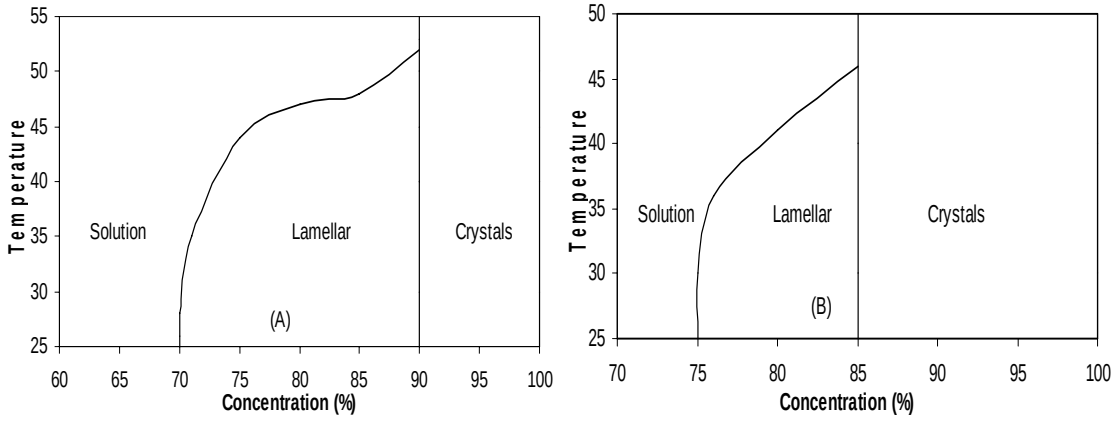

Fig. 4.14 Phase diagrams for (A) Ethanol surfmer and (B) Ethyl surfmer, obtained from polarised optical microscope with a heating stage (25 ^{0}C is room temperature).

The shape of the structures in the LLC phases are dependant on thermodynamic considerations and on surfactant packing parameters [21-22]. The observation that the Ethanol surfmer forms the lamellar liquid crystalline phase from lower surfactant concentration, i.e. 70% surfmer in water, relative to 75% for the Ethyl surfmer, is attributed to the fact that the Ethanol surfmer can form intermolecular hydrogen bonds between its head groups [21-23], whereas no such interactions are present in the latter system. The lamellar liquid crystalline phase region of the Ethanol surfmer is stable up to 52 ^{0}C whereas that of the Ethyl surfmer is stable up to 48 ^{0}C. The difference in the transition temperatures is also attributed to hydrogen bonding present in the Ethanol surfmer. The solution phase (isotropic) contains nonaggregated surfactant molecules and micelles (at concentrations greater than CMC) and the crystal phase contains mainly hydrated crystalline forms of the surfmers.

Both the type of polymerizable group (i.e. olefinic, methacrylic or acrylic) and the position of the polymerizable group (H type, i.e. polymerizable group located in the hydrophilic head group or T type, i.e. polymerizable group located in the hydrophobic tail) have a profound effect on surfactant self assembly. The sodium 10-undecenoate/water system resulted in isotropic, hexagonal and lamellar liquid crystalline phases. The T type polymerizable group in sodium 10-undecenoate (i.e. an allyl group) is hydrophobic, thus it does not interact with water, resulting in the formation of liquid crystals earlier. On the other hand, the H type surfmer dodecyldimethyl-ammoniumethylmethacrylate bromide has been shown to form isotropic, hexagonal, bicontinuous cubic and lamellar liquid crystalline phases [24]. The reason for the difference in the phase behavior of this H type surfmer and our T type surfmers is based on the nature of the methacrylate group relative to the acrylate group, as well as the differences in the position of the polymerizable group. Hartmann *et al*. [17] have showed that by changing the organic polymerizable counterion from an acrylate to a methacrylate resulted in formation of a cubic phase, in addition to the lamellar liquid crystalline phase observed when an acrylate counterion is used. The methyl group on the methacrylate group increases hydrophobicity and bulkiness, resulting in less interaction with water molecules. It has also been shown that the position of the polymerizable group affects the properties of surfmers [25]. The T type surfmer can form a ‘loop’ or ‘wicket like’ structure at the micelle-water interface, and

this may lead to steric hindrance and destabilization of liquid crystals [26-27]. This however does not happen in the H type surfmers.

LLC phases have nontheless found many applications in science, engineering, and device technology. Examples include liquid crystal displays, liquid crystal thermometers, optical imaging, medical applications etc. They can also be used as nanoreactors for nanoparticle synthesis, where advantage is taken of their nanometer size. This application can also be applied to these surfmers, especially where the functional group takes part in the reaction [28-29].

4.4.7 Small angle X-ray scattering.

Both SAXS patterns shown in Fig. 4.15 below contain one major Bragg peak.

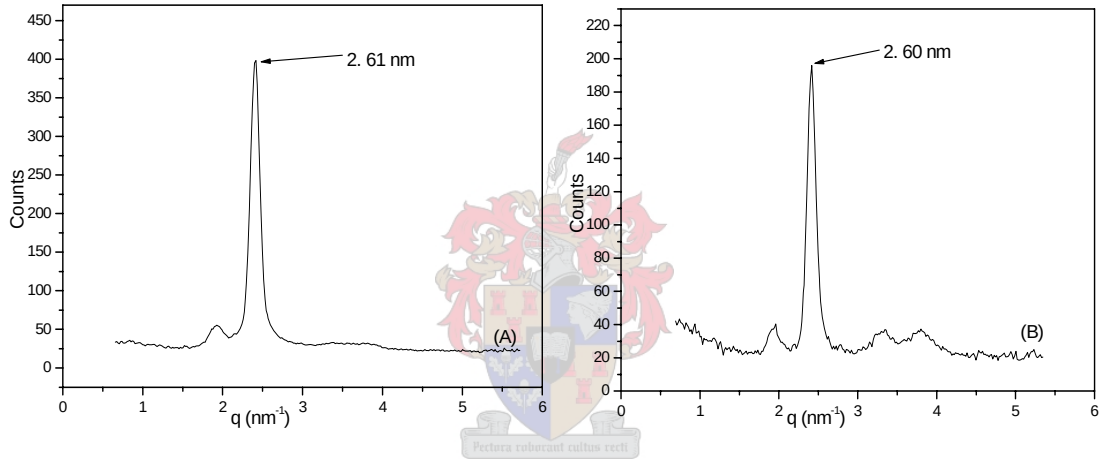

Fig. 4.15 SAXS patterns (taken at room temperature) for Ethyl surfmer (A) and Ethanol surfmer (B) at a surfactant concentration of 80% by mass in water.

The appearance of Bragg peaks indicates long range order [30-31]. The order is due to the organised lamellar liquid crystalline phase as observed by polarized optical microscope.

The lamellar liquid crystalline phase thickness is independent of the head group but rather dependant on the length of the surfactant tail. This is shown by the same d spacing between the repeat units i.e. ~ 2.6 nm in this case. The lamellar liquid crystalline phase thicknesses are comparable to those found for mixtures of single and double chain methacrylate or acrylate based surfmers i.e. 2.8-3.3 nm, by Eastoe *et al*. [31]. Their surfmers had the same chain lengths as the Ethanol and the Ethyl surfmers. However, the origin of the small peaks in the SAXS patterns could not be known. Thus

further analysis using WAXS could provide valuable information about the origin of these peaks.

4.5 Results and discussion of homopolymers of surfmers.

4.5.1 ^{1}H NMR.

^{1}H NMR spectra of polymerized Ethyl surfmer and Ethanol surfmer are shown in Fig. 4.16 and Fig. 4.17, respectively. As can be seen by the disappearance of the ethylenic protons at 5.85 to 6.45 ppm, the surfmers were polymerized. The disappearance and broadening of peaks is characteristic of polymerized systems. This is because of an increase in the relaxation time for protons due to reduced motion of the polymer chains formed [1,31]. After polymerization the solutions remained translucent but there was an increase in the viscosity of the solutions in agreement with literature [31-32]. Acrylate containing monomers are known to polymerize to high degrees of polymerization [32-34]. Samples of the homopolymers were analyzed by ESMS. The characteristic peaks due to surfmers were not detected, confirming polymerization of the surfmers. ESMS can unfortunately not be used for larger molecular masses, hence this technique was not used to determine the molecular masses of the surfmers. There were also problems associated with the m/z charge ratio (i.e. polysurfmers had numerous charges along one chain), again making it impossible to use this technique for molecular mass determination. Further, the molecular masses of the homopolymers could also not be determined by GPC because the homopolymers did not dissolve in tetrahydrofuran (THF), the GPC eluent. Another consideration was that the homopolymers were highly surface active [14], and could thus be adsorbed onto the column [32]. The arthour suggest that more information could be obtained from voscometry measurements.

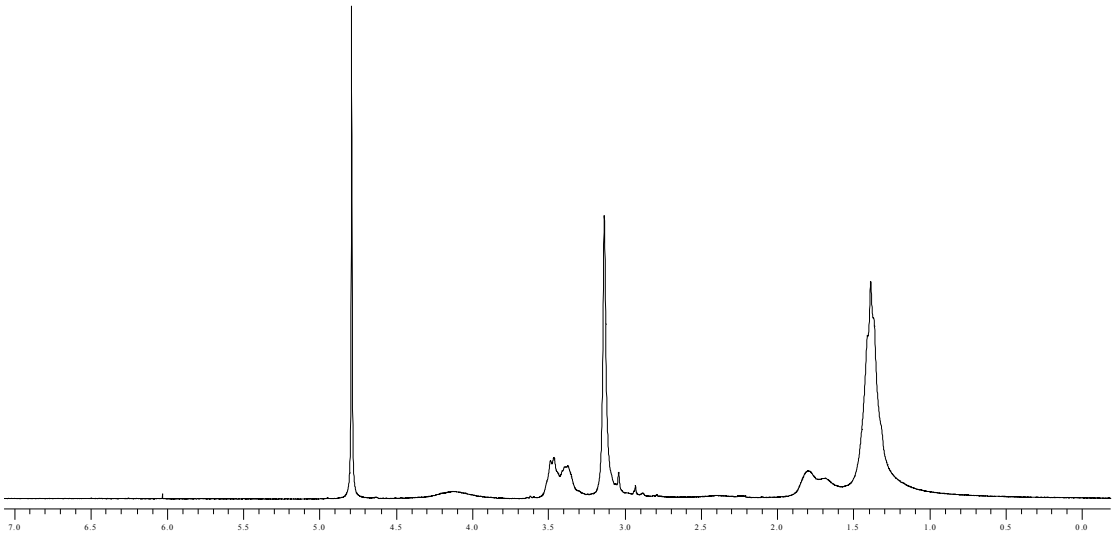

Fig. 4.16 ^{1}H NMR spectrum of polymerised Ethyl surfmer in deuterated water.

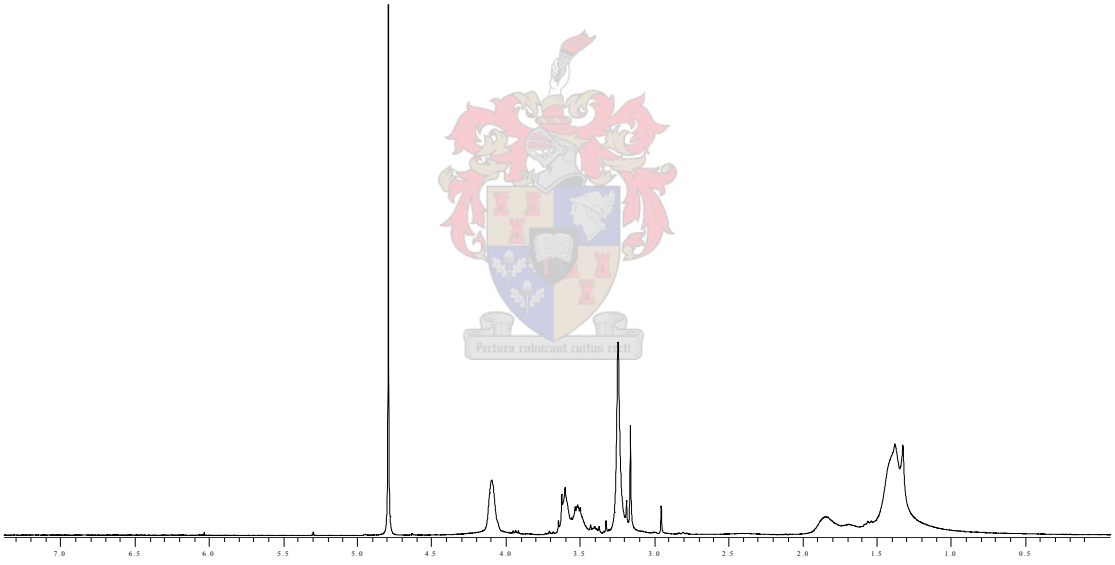

Fig. 4.17 ^{1}H NMR spectrum of polymerised Ethanol surfmer in deuterated water.

4.5.2 Thermal analysis of the homopolymers.

4.5.2.1 Thermogravimetric analysis.

The thermograms of the homopolymers (Fig. 4.18 and Table 4.7) are very similar to those of the surfmers (Section 4.4.4.1), for they follow a two-step degradation pathway, they have the same T_{MAX} and poly(Ethanol surfmer) is thermally more stable than poly(Ethyl surfmer). Thus the degradation pathway for the surfmers and their homopolymers is likely to be the same.

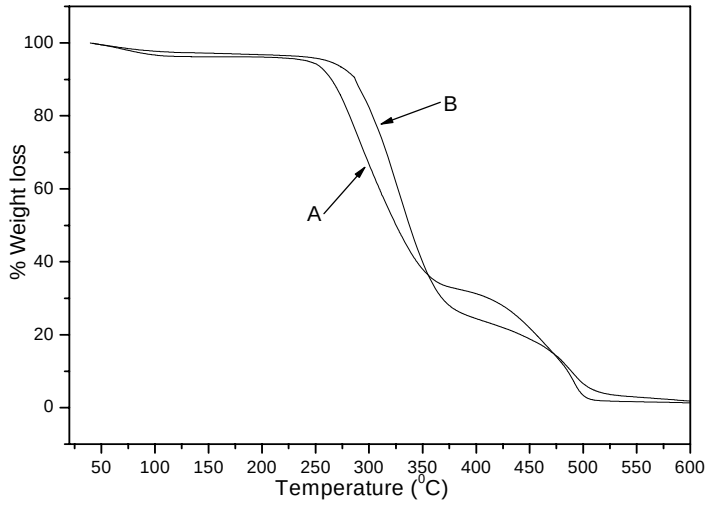

Fig. 4.18 TGA thermograms of polymerized Ethyl surfmer (A) and Ethanol surfmer (B).

Table 4.7 Thermal stability of polymerized surfmers

Surfmer	$T_{1\ ONSET}/^0C$	$T_{2\ ONSET}/^0C$	$T_{MAX}/^0C$
Poly(Ethanol)	287	361	522
Poly(Ethyl)	265	376	508

Where: $T_{1\ ONSET}/^0C$, $T_{2\ ONSET}/^0C$, $T_{MAX}/^0C$ are the first onset degradation temperatures taken at 10% degradation [12], the metastable onset degradation and final degradation temperature respectively.

4.5.2.2 Differential scanning calorimetry analysis of the polysurfmers.

The first heating scans for the polysurfmers showed that they were polycrystalline due to multiple endothermic peaks at temperatures above the endothermic transition temperature of the surfmers. When the second heating cycles were carried out on the polysurfmers, the same phenomenon was observed (see Fig. 4.19 below). The polysurfmers can also show thermotropic liquid crystalline properties but since there are many peaks it is very difficult to arrive at that deduction. A possible reason is the mobility restriction imposed by the chain and the fact that placement in the chain will have mixed chirality (mostly syndiotactic) and therefore both intra and interchain crystallites conform.

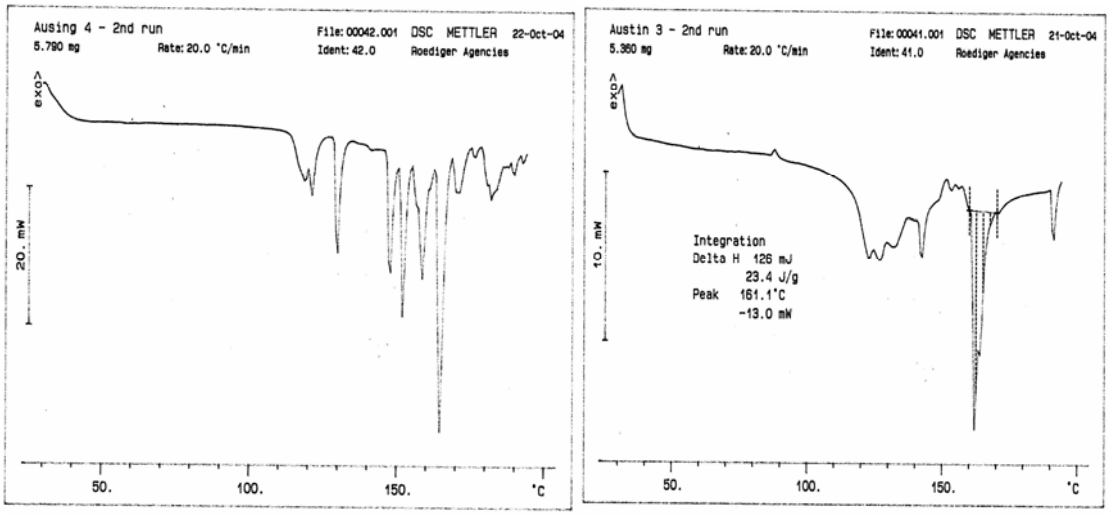

(A) (B)

Fig. 4.19 Second heating DSC thermograms of poly(Ethanol surfmer) (A) and poly(Ethyl surfmer) (B).

References.

1. D. Joynes, D. C. Sherrington; Polymer, 37 (1996) 1453-1462.

2. M. J. Unzue, H. A. S. Schoonbrood, J. M. Asua, A. M. Goni, D. C. Sherrington, K. Stahler, K. Goebel, K. Tauer, M. Sjoberg, K. Holmberg; J. App. Polym. Sci., 66 (1997) 1803-1820.

3. www.sigma-aldrich.com; 11-bromoundecan-1-ol data sheet, Accessed (February, 2004).

4. X. Fu, S. Qutubiddin; Polymer, 42 (2001) 807-813.

5. M. Okamoto, S. Morita, H. Y. Kim, T. Kotaka, H. Tateyama; Polymer, 42 (2001) 1201-1206.

6. R. A. Vaia, E. P. Giannelis; Macromolecules, 30 (1997) 8000-8009.

7. M. Kawasumi, N. Hasegawa, M. Kato, A. Usuki, A. Akada; Macromolecules, 30 (1997) 6333-6338.

8. A. Streitwieser, C. H. Heathcock, E. M. Kosower; Introduction to Organic Chemistry, Macmillan Publishing Company, New York. 4th Edition (1992) 741.

9. R. J. Bezzant; Basic Organic Chemistry, McGraw-Hill Publishing Company Limited, London. (1967) 183-184.

10. S. H. Pine, J. B. Hendrickson, D. J. Cram, G. S. Hammond; Organic Chemistry, McGraw-Hill Book Company, London. 4th Edition (1980) 419.

11. J. D. Roberts, M. C. Caserio; Basic principles of organic chemistry, W. A. Benjamin Inc., New York (1964) 29-34.

12. G. Chigwanda, C. A. Wilkie; Polymer Degradation and Stability, 80 (2003) 551-557.

13. L. Biasci, M. Aglietto, G. Ruggeri, F. Ciardelli; Polymer, 35 (1994) 3296-3304.

14. D. Joynes, D. C. Sherrington; Polymer, 38 (1997) 1427-1438.

15. M. Dreja, W. Pyckhout-Hintzen, B. Tieke; Macromolecules, 31 (1998) 272-280.

16. S. Abele, A. Zicmanis, C. Graillat, C. Monnet, A. Guyot; Langmuir, 15 (1999) 1033-1044.

17. P. C. Hartmann, P. Dieudonne, and R. D. Sanderson; Colloids and Interface Science, 284 (2005)289-297.

18. M. Jansson, A. Jonsson, P. Li, P. Stilbs; Colloids and Surfaces, 59 (1991) 387-397.

19. G. Sugihara, Y. Arakawa, K. Tanaka, S. Lee, Y. Moroi; Journal of Colloid and Interface Science, 170 (1995) 399-406.

20. F. B. Rosevear; The Journal of the American Oil Chemists Society, 31 (1954) 628-639.

21. F. Testard, T. Zemb; C. R. Geoscience, 334 (2002) 649-663.

22. S. Svenson; Journal of Dispersion Science and Technology, 25 (2004) 101-118.

23. B. J. Boyd, C. J. Drummond, I. Krodkiewska, F. Grieser; Langmuir, 16 (2000) 7359-7367.

24. C. L. Lester, C. Guymon; Polymer, 43 (2002) 3707-3715.

25. M. Summers, J. Eastoe; Advances in Colloid and Interface Science, 100-102 (2003) 137-152.

26. S. M. Hamid, D. C. Sherrington; Polymer, 28 (1987) 325.

27. F. M. Menger, S. Wrenn, J. Phys. Chem., 78 (1974) 1387.

28. S. Puvvada, S. Baral, M. G. Chow, B. S. Qadri, R. B. Ratna; J. Am. Chem. Soc., 116 (1994) 2135-2136.

29. L. Qi, Y. Gao, J. Ma; J. Colloids. Surf. A., 157 (1999) 285-294.

30. K. M. McGrath; Colloid and Polymer Science, 274 (1996) 499-512.

31. M. Summers, J. Eastoe, R. M. Richardson; Langmuir 19 (2003) 6357-6362.

32. D. Cochin, F. Candau, R. Zana; Macromolecules, 26 (1993) 5755-5764.

33. K. Ito, K. Tanaka, H. Tanaka, G. Imai, S. Kawaguchi, S. Itsuno; Macromolecules, 24 (1991) 2348.

34. K. Nagai, Y. Ohishi; J. Polym.Sci., Polym. Chem., 25 (1987) 1.

Chapter 5 Polystyrene-clay nanocomposites.

5.1 Introduction.

This Section focuses on the modification of clay using the synthesized surfmers (prepared as described in Chapter 4) and the subsequent synthesis of polystyrene-clay nanocomposites. For comparison, polystyrene-clay nanocomposites were also synthesized using cetyltrimethyl-ammonium bromide (CTAB), a classical surfactant. CTAB has a carbon chain length comparable to the synthesized surfmers. It is known that classical surfactants e.g. CTAB, yield predominantly intercalated nanocomposites [1], whereas exfoliated nanocomposites are mainly obtained using surfmers [1]. Thus, the synthesis and analysis of polymer-clay nanocomposites prepared using surfmers and classical surfactant modified clays are ideal for relating the level of clay dispersion to the resultant thermal and mechanical properties of polystyrene-clay nanocomposites. The nanocomposites were characterised by FT-IR, SAXS, TEM, TGA, DMA and GPC.

5.2 Experimental procedures.

The materials and the strategies used in the synthesis of the polystyrene-clay nanocomposites are now described.

5.2.1 Materials.

Sodium montmorillonite clay (i.e. MMT clay containing primarily Na^+ ions in the interlayer space) was obtained from Southern Clay Products, Inc (U.S.A). It is a fine powder with an average particle size of less than 13 μm^3 by volume in the dry state, and a cation exchange capacity of 92.6 meq/100 g clay. Stabilised styrene monomer was obtained from Aldrich. The stabilizers were removed from the monomer (styrene) by washing three times with 3% KOH solution and then purifiying by distillation under reduced pressure at 30 ^{0}C. AIBN was obtained from Aldrich and was purified by re-crystallization from hot methanol. CTAB was obtained from Aldrich and used without further purification. The surfmers were synthesized as described in Chapter 4, Sections 4.2.2 - 4.2.4.

5.2.2 Bulk polymerization of styrene.

Freshly distilled styrene (5 g, 0.048 mol) and AIBN (0.025 g) were placed into a Schlenk tube. The Schlenk tube was then immersed in liquid nitrogen and the contents frozen. Vacuum was applied to the frozen mixture for 5 mins, to remove any oxygen from the Schlenk tube. The frozen mixture was then brought to ambient temperature. This procedure was repeated twice. The Schlenk tube was then placed in an oil bath and the polymerization carried out at 60 ^{0}C for 72 h. The solid polystyrene was then dissolved in chloroform and precipitated in excess methanol to yield a white powder of monomer-free polystyrene.

5.2.3 Ion exchange of Na^+-MMT by surfmers and CTAB.

Ion exchange of Na^+-MMT with Ethanol surfmer.

Na^+-MMT (3 g, 2.780 meq) was dispersed in 250 ml deionised water under vigorous stirring (700 rpm). Ethanol surfmer (1.426 g, 3.615 mmol) in 100 ml of deionised water was slowly added to the dispersion, under continued vigorous stirring. The resultant dispersion was stirred for a further 6 h. After 6 h the dispersion was filtered under reduced pressure and the ion exchanged cake was thoroughly washed with deionized water. Samples of the filtrate were taken at regular intervals and tested with a solution of 0.1M $AgNO_3$ for the presence of released bromide counterions. The washing was discontinued only after the filtrate did not give a positive test to $AgNO_3$. The washed cake was then dried in a vacuum oven at 40 ^{0}C overnight. Thereafter the dry cake was ground in a mortar and pestle, followed by sieving through a 63-μm mesh to yield very fine, dry, organically modified clay, which was subsequently used for the synthesis of nanocomposites.

The ion exchange of Na^+-MMT by Ethyl surfmer and by CTAB was performed under similar conditions. The ratio of CEC of clay to surfactant was kept constant at 1:1.3.

5.2.4 Synthesis of polystyrene-clay nanocomposites by bulk polymerization.

The synthesis of polystyrene-clay nanocomposite using (11-acryloyloxyundecyl) dimethylethylammonium exchanged MMT (Ethyl-MMT) was done as follows: Ethyl-MMT (0.250 g) and AIBN initiator (0.024 g) were added to a

Schlenk tube containing freshly distilled styrene monomer (4.750 g, 0.046 mol). The Schlenk tube was then immersed in liquid nitrogen and the contents frozen. Vacuum suction was then applied to the frozen mixture for 5 min to remove any oxygen from the tube. The frozen mixture was allowed to return to ambient temperature. The process was repeated twice (freeze and thaw). Thereafter the mixture was stirred and sonicated for 4 h. The Schlenk tube was placed in an oil bath and the polymerization was carried out at 60 ^{0}C for 72 h. The solid bulk polymer was dissolved in chloroform to form a suspension, followed by precipitation in excess methanol. After filtration and vacuum drying at ambient temperature, an off-white powder of polystyrene-clay nanocomposite was obtained.

All the polystyrene-MMT nanocomposites prepared by bulk polymerization were prepared according to a similar procedure. For each organoclay a series of nanocomposites of increasing clay loading were prepared in order to study the influence of clay loading on the properties of the nanocomposites. The nanocomposites prepared by this procedure were for surfmer-modified clay, CTAB-modified clay and physical mixtures of surfmer-modified clay and CTAB-modified clay in known ratios.

5.2.5 Synthesis of polystyrene-clay nanocomposites by solution polymerization.

Synthesis of polystyrene-clay nanocomposite using (11-acryloyloxyundecyl) dimethyl(2-hydroxyethyl)ammonium exchanged clay (Ethanol-MMT).

Ethanol-MMT (0.25 g) and AIBN initiator (0.05 g) were added to a Schlenk tube containing 30 ml of toluene and freshly distilled styrene monomer (4.75 g, 0.046 mol). The Schlenk tube was then immersed in liquid nitrogen and the contents frozen. Vacuum suction was then applied to the frozen mixture for 5 mins to remove any oxygen from the tube. The frozen mixture was brought to ambient temperature (thaw). This procedure was repeated twice. Thereafter the mixture was stirred and sonicated for 4 h. After this the Schlenk tube was placed in an oil bath and polymerization was carried out at 80 ^{0}C for 24 h. The product was then precipitated in excess methanol,

filtered and vacuum dried at ambient temperature to yield a white powder of polystyrene-clay nanocomposite.

All the polystyrene-MMT nanocomposites prepared by solution polymerization were prepared following a similar procedure. For each organoclay, a series of nanocomposites of increasing clay loading were prepared, allowing the author to study the influence of clay loading on the properties of the nanocomposites. Solution polymerization was carried out for surfmer-modified clays only.

5.3 Analytical methods.

5.3.1 Small angle x-ray scattering.

Refer to Section 4.3.8 in Chapter 4.

5.3.2 Transmission electron microscopy.

TEM was used to directly visualize the morphology of the clay particles in polystyrene-clay nanocomposites at the nanometer level. Bright field TEM images were recorded on a JEM 200CX (JEOL Tokyo, Japan) TEM at an accelerating voltage of 120 kV. Prior to analysis samples of polystyrene-clay nanocomposites were stained with OsO_4, then embedded in epoxy resin and cured for 24 h at 60 ^{0}C. The embedded samples were then ultra microtomed with a diamond knife on a Reichert Ultracut S ultra microtome at room temperature. This resulted in sections with a nominal thickness of ~ 100 nm. The sections were transferred from water at room temperature to 300-mesh copper grids, which were then transferred to the TEM apparatus.

5.3.3 Atomic force microscopy.

AFM was used for the visual determination of surface morphology of the nanocomposites. A Veeco Topometrix Explorer AFM instrument was used for the analyses. Samples were analyzed in the contact mode.

5.3.4 FT-IR spectroscopy.

Refer to Section 4.3.2 in Chapter 4.

5.3.5 Thermogravimetric analysis.

Refer to Section 4.3.2 in Chapter 4.

5.3.6 Dynamic mechanical analysis.

The mechanical properties of the prepared nanocomposites were determined using a Perkin Elmer DMA 7e instrument. Prior to analysis samples were pressed into thin discs using a hydraulic pump. Samples were brought to -20 ^{0}C and held there for a minute before being heated at a heating rate of 5 ^{0}C/min to 200 ^{0}C. Analysis was done using a 1 mm probe.

5.3.7 Gel permeation chromatography.

GPC was used for the determination of the molecular masses of the nanocomposites. GPC was performed using a Waters 600E system controller equipped with a Waters 610 Fluid Unit pump, a Waters 410 Differential Refractometer as detector, and a column set of PLgel 5 mm guard 50 x 7.5 mm and PLgel 5 mm mixed-C 300 x 7.5 mm (Polymer Laboratories). Measurements were done at 30 ºC, with a flow rate of 1 ml/min, using THF as eluent. Molecular masses were determined relative to narrow polystyrene standards (EasiVial PS from Polymer Laboratories). Prior to analysis samples were vigorously stirred in THF for a week (so as to have all the soluble component into solution). The samples were then filtered through a 0.45-µm filter membrane, thus only the THF soluble components were analysed.

5.4 Results and discussion.

5.4.1 Functionalization of Na^+-MMT by surfactants.

5.4.1.1 Functionalization of Na^+-MMT at room temperature.

The structure of Na^+-MMT comprises layers made up of one octahedral alumina sheet sandwiched between two tetrahedral silica sheets. About one in six of the aluminum ions in the octahedral layers of Na^+-MMT is isomorphously substituted in the sheet structure by magnesium or other divalent ions; this results in negative charges that are in turn counter-balanced by Na^+ cations residing in the interlayer space [2]. The Na^+ ions in the gallery space can be ion exchanged by an organic cation (surfactant) to yield surfactant-modified clay.

Two polymerizable surfactants (surfmers) [Ethyl and Ethanol] and a non-polymerizable surfactant CTAB were used to ion exchange the Na^+ ions in Na^+-MMT. TGA was then used to determine the total amount of surfactant that ion exchanged the Na^+ ions in clay (extent of ion exchange) [1,3-5].

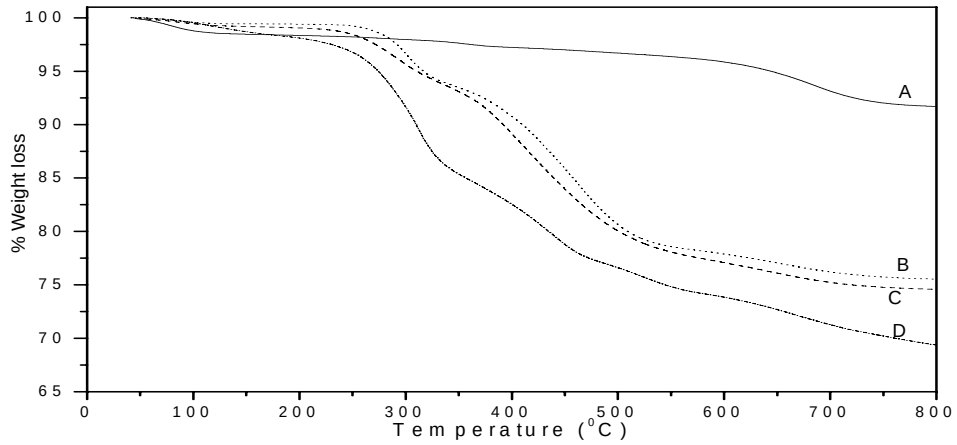

Fig. 5.1 TGA thermograms for (A) Na^+-MMT, (B) Ethyl-MMT, (C) Ethanol-MMT and (D) CTAB-MMT.

The weight loss of Na^+-MMT in Fig. 5.1 (A) is due to the loss of adsorbed water [3]. The amount of the weight lost of 8.3%, is very close to the literature value of 7% [6]. The weight lost by surfactant-modified clays (B-D) is due to the decomposition of the surfactant plus due to adsorbed water in clay. Thus TGA offers a very quick and inexpensive way of mostly qualitative, but somewhat quantitative, determination of the extent of the ion exchange reaction.

Table 5.1 Extent of ion exchange of the modified clays

Compound	**% Weight loss at 800^0C**	**% Mass of surfactant in clay**	**% Ion exchange**
Na^+-MMT	8.30	n/a	n/a
Ethyl-MMT	24.5	16.2	69.5
Ethanol-MMT	25.4	17.1	69.9
CTAB-MMT	30.6	22.3	93.6

The percentages of ion exchange of clays in Table 5.1 are based on the following three assumptions:

- The volatile material inside the clay, save for hydrated sodium ions, does not come out of the clay layers during the ion exchange reaction.

- The number of moles of sodium ions that move out of the clay galleries is equal to the number of moles of surfactant that go into the clay galleries.

- The surface ion exchange does not change (increase or decrease) the water content in clay significantly i.e. the hydrated water in the clay does not take part in the ion exchange reaction [7].

It can be seen that CTAB is ion exchanged more so than the Ethanol and Ethyl surfmers. This may be explained on the basis of steric repulsions inside the interlayer space caused by the size of the head group of the quaternary ammonium ions [3]. CTAB has a smaller head group than Ethanol and Ethyl surfmers, and hence less steric repulsions, resulting in its ability to ion exchange to a larger extent. This hypothesis is however not in agreement with the deductions made by Bongiovanni *et al*. [8], who proposed that ion exchange onto homoionic MMT was independent of the hydrophilic head group of the surfactant.

5.4.1.2 Functionalization of Na^+-MMT by surfmers at 50 ^{0}C.

Keeping all the other parameters constant besides temperature, the ion exchange reactions using surfmers (i.e. Ethanol and Ethyl) were then carried out at 50 ^{0}C. These experiments were carried out in a bid to optimize the ion exchange reaction so that the interlayer space was as hydrophobic as possible, as this would lead to a better compatibility with styrene. The results of the ion exchange reactions of Na^+-MMT using Ethyl and Ethanol surfmers at 50 ^{o}C are shown in Table 5.2 below.

Table 5.2 Extent of ion exchange of the modified clays at 50 ^{0}C

Compound	**% Weight loss at 800^{0}C**	**% Mass of surfactant in clay**	**% Ion exchange**
Na^+-MMT	8.3	n/a	n/a
Ethyl-MMT	25.1	16.8	72.4
Ethanol-MMT	25.3	17.0	69.5

The extent of the ion exchange results at 50 ^{0}C are the same as at room temperature (see Table 5.1), within experimental error.

5.4.1.3 Functionalization of Na^+-MMT by surfmers at very high shear.

It was then decided to carry out the ion exchange at high shear (i.e. high speed stirring of 3250 rpm) using a mechanical stirrer. Again the total amount of surfmer ion exchanged was the same.

This implied that extent of ion exchange is neither affected by stirring rate nor by temperature. These findings suggest that some exchange sites are not accessible to the surfmers [3], given in all cases the extent of ion exchange was not 100% and that the amount of surfmer used was in excess (1.3 : 1) with regards to the CEC. This study would gain from an alternative analysis of the degree of exchange, by mass for instance.

5.4.2 Study of the rate of ion exchange by ultraviolet spectroscopy.

After having observed that the extent of ion exchange was not affected by shear rate and temperature, the rate of ion exchange was determined using UV; the surfmers contained a UV active acrylate group. Samples were withdrawn from the ion exchange reaction vessel at regular intervals. The samples were then centrifuged and filtered through a 0.45-μm filter membrane to remove the clay and ion exchanged surfmer. The resultant solutions were then diluted before UV analysis.

No conclusive results were obtained, possibly because of the following two reasons: (a) The analysis wavelength (i.e. 195 nm) was very close to the minimum detection limit of the machine (i.e. 190 nm), meaning that the sensitivity of the machine was very low, making it difficult to detect small variations. (b) 10% of the clay particles had a volume of less than 2 μm^3 in the dry state [6], although this volume increases when the particles are in solution. It is possible that the filter membrane did not trap some of the particles, which then absorbed UV, making the quantification measurements difficult.

5.4.3 FT-IR analysis of the functionalized clays.

The FT-IR spectrum of Na^+-MMT clay (Appendix 2: Fig. 1) shows absorption peaks at 3438, 3625 and 1632 cm^{-1} (see Table 5.3 below). These peaks were assigned to OH stretching (hydration) and hydrated water deformation bonds [7]. The intense peak at

1045 cm^{-1} is due to the stretching of the Si-O bonds, whereas the peaks at 468 and 524 cm^{-1} are due to the bending of the Si-O bonds, and the peak at 625 cm^{-1} is due to the stretching of the Al-O bonds [7,9-13].

The appearance of new peaks in the FT-IR spectra of the modified clays (Appendix 2: Fig. 2 to Fig. 4) is a clear indication that the ion exchange reaction had indeed taken place (see Table 5.3). The spectrum of CTAB surfactant is shown in Appendix 2: Fig. 5. The absorption peak of the carbonyl group in surfmer-modified clays shifted to a lower wavenumber i.e. 1714 cm^{-1}, relative to 1721 and 1725 cm^{-1} in Ethanol and Ethyl surfmers respectively. This is an indication that the acryloyl group is hydrogen bonded to the hydroxyl groups on the surface of the clay [7]. However, the wavelength of absorption due to the hydroxyl groups on clay did not change after the ion exchange process, further confirming the earlier assumption i.e. the water in clay does not change significantly during the ion exchange process. The other peaks that were expected to be seen in the spectra of the modified clays were not observed because the strongly absorbing clay masked them.

Table 5.3 FT-IR results of Na^+-MMT, Ethanol-MMT, Ethyl-MMT and CTAB-MMT

	Na^+-MMT	**Ethanol-MMT**	**Ethyl-MMT**	**CTAB-MMT**
Assigned groups	Wavelength (cm^{-1})	Wavelength (cm^{-1})	Wavelength (cm^{-1})	Wavelength (cm^{-1})
Al-O	625	627	627	620
Si-O	524, 468, 1045	524, 466, 1049	524, 466, 1049	520, 470, 1049
$-CH_3$		1411	1408	
$-CH_2-$		1471	1468	1467, 1493
>C=C<		1632	1636	
>C=O		1714	1714	
-C-H		2845, 2929	2853, 2928	2853, 2928
O-H	1632, 3438, 3625	1632, 3430, 3633	3430, 3633	1647, 3438, 3625

5.4.4 Analysis of the basal spacing of the modified clays by SAXS.

SAXS measurements were used to follow the changes in the interlayer spacing caused by the ion exchange process. The d spacing (interlayer distance) was calculated using the formula: $d = 2\pi/q$ (where q is the wave vector; its value corresponds to the associated Bragg peak position). The interlayer distance for the Na^+-MMT clay (Fig. 5.2 A), 1.1 nm is comparable to values reported in literature for Na^+-MMT clay [1,6,10-12,14]. The SAXS patterns for the modified clays, (Fig. 5.2 B (i) and B (ii) below) show an increase in interlayer distance relative to unmodified clay. The increase in interlayer distances further proved the success of the ion exchange reaction.

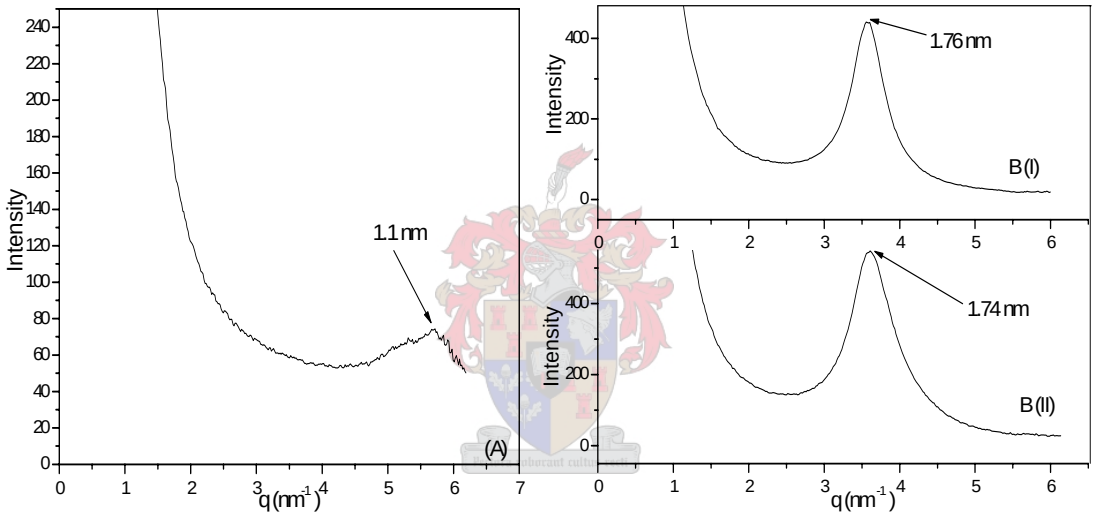

Fig. 5.2 SAXS patterns of (A) Na^+-MMT, B (i) Ethanol-MMT and B (ii) Ethyl-MMT.

Thus SAXS patterns also confirmed that ion exchange had occurred (as had TGA and FT-IR results). The interlayer distances of the two surfmer modified clays were similar (i.e. 1.76 nm for Ethanol-MMT and 1.74 nm for Ethyl-MMT). It was initially expected that the Ethanol surfmer would have a larger interlayer distance than the Ethyl surfmer. This is because the Ethanol surfmer can interact more with the clay surface through hydrogen bonding between the acrylate groups and the 2-hydroxy-ethyl groups with the hydroxyl groups on the clay surface, hence a larger d spacing [15]. This should differ from the Ethyl surfmer, which (besides the quaternary group) only interacts by hydrogen bonding to clay through the acrylate groups [7]. The results obtained were however the opposite, this shows that the interlayer distance is mainly governed by the length of the alkyl chain of the modifying surfactants [11] and

the clay charge density [2]. Here, the length of the alkyl chain of the modifying surfactants and the clay charge density are the same, hence the same interlayer distance (see Fig. 5.2 B).

On the other hand, the interlayer distance of CTAB-MMT clay (Appendix 2: Fig. 6) was found to be 1.86 nm, which shows fair agreement with literature (i.e. 2.0 nm) [10]. The d spacing for CTAB-MMT clay is greater than the d spacings for the surfmer-modified clays because the former has a relatively longer chain length (16-carbon backbone) relative to the 14-carbon backbone of surfmers.

5.4.5 Polystyrene-clay nanocomposites/polymerization in bulk.

5.4.5.1 Synthesis of polystyrene.

For comparison of the changes in thermal and mechanical properties of polystyrene due to the presence of clay filler, a polystyrene standard was prepared under conditions similar to those employed for the preparation of nanocomposites (see Section 5.2.4). The ^{1}H NMR spectrum of polystyrene is shown in Fig. 5.3 below. There are no ethylenic protons at ~ 5.25, 5.75 and 6.75 ppm. There is a broadening of peaks and the appearance of new peaks at ~ 1.2 to 2.0 ppm. These shifts are characteristic of polymerized polystyrene systems. The broadening is due to an increase in the relaxation time for protons due to inhibited movement of the polymer chains formed [16-17]. The sharp peak at ~ 1.6 ppm is due to traces of water in the deuterated solvent (in this case chloroform).

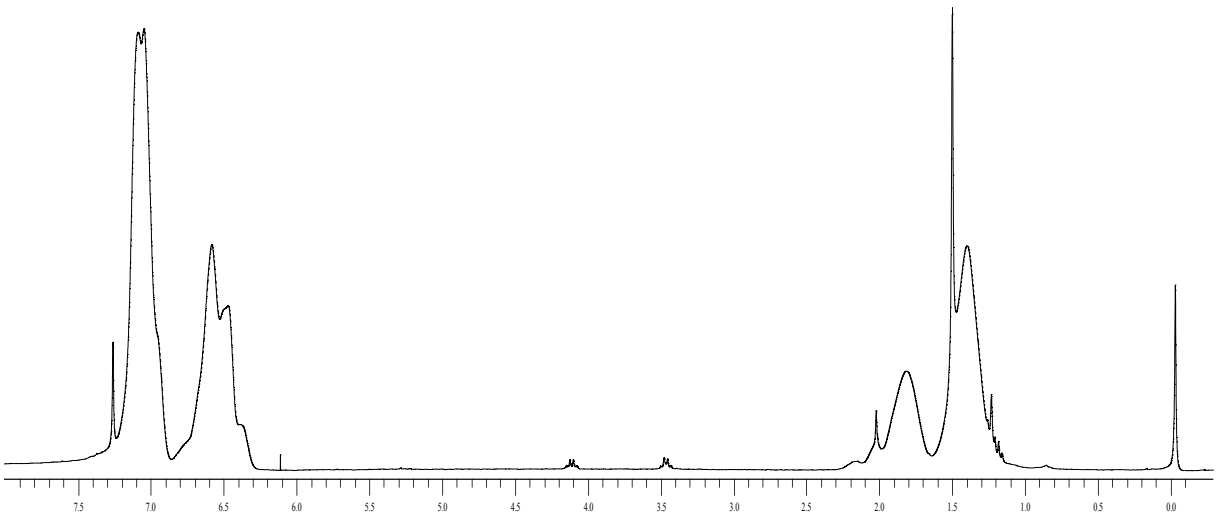

Fig. 5.3 ^{1}H NMR spectrum of polystyrene (in $CDCl_3$).

5.4.5.2 FT-IR analysis of polystyrene-clay nanocomposites.

The FT-IR analysis of polymers is theoretically very complex [18]. In the case of polystyrene-clay nanocomposites the complexity is exacerbated by the presence of the clay particles and surfactant molecules in polystyrene. The main absorption bands could nonetheless be seen in the spectra of the polymer-clay nanocomposites (see Table 5.4 below). The spectra are shown in Appendix 2: Fig. 7 to Fig. 10.

Table 5.4. FT-IR results of polystyrene-clay nanocomposites

	Polystyrene	**Polystyrene-(Ethanol-MMT) nanocomposite**	**Polystyrene-(Ethyl-MMT) nanocomposite**	**Polystyrene-(CTAB-MMT) nanocomposite**
Assigned groups	Wavelength (cm^{-1})	Wavelength (cm^{-1})	Wavelength (cm^{-1})	Wavelength (cm^{-1})
Al-O		627	627	620
Si-O		524, 466, 1048	524, 466, 1047	528, 462, 1049
$-CH_2-$	1449, 1493	1449, 1493	1449, 1493	1459, 1493
>C-C<	696, 756, 1026	694, 754, 1030	694, 757, 1030	692, 757, 1031
>C=C<	1646-1942	1637-1941	1639-1948	1647-1943
-C-H	2853, 2913	2853, 2913	2845, 2920	2853, 2917
Ar-H	3018, 3054, 3089	3025, 3058, 3085	3025, 3054, 3081	3030, 3065, 3083

Where Ar-H is for the aromatic carbon-hydrogen bond and C=C is for the aromatic double bonds.

Compared to the spectrum of polystyrene (Appendix 2: Fig. 7) the absorptions (i.e. overtones) due to the benzene ring (i.e. ~ 1630-1950 cm^{-1}) are visible in the spectra of the nanocomposites. This is also true for the absorptions in the region ~ 3018-3090 cm^{-1}, which are characteristic of hydrogen atoms attached to an aromatic carbon atoms [19]. The peaks at ~ 524, 466 and 1048 cm^{-1} were assigned to the Si-O bonds, and the peak at ~ 627 cm^{-1} to the Al-O bonds, as outlined in Section 5.4.3. At this point, the evidence gathered proved that the composites contained all the species that were expected to be present.

5.4.5.3 Analysis of polymer-clay nanocomposites using SAXS.

SAXS has not been widely used for the analysis of polymer-clay nanocomposites. This is probably due to the scarcity of SAXS facilities as opposed to the widely used WAXD. SAXS was nonetheless used here for the determination of the morphology of clay particles in the nanocomposites. Below are the SAXS patterns of the polystyrene-clay nanocomposites.

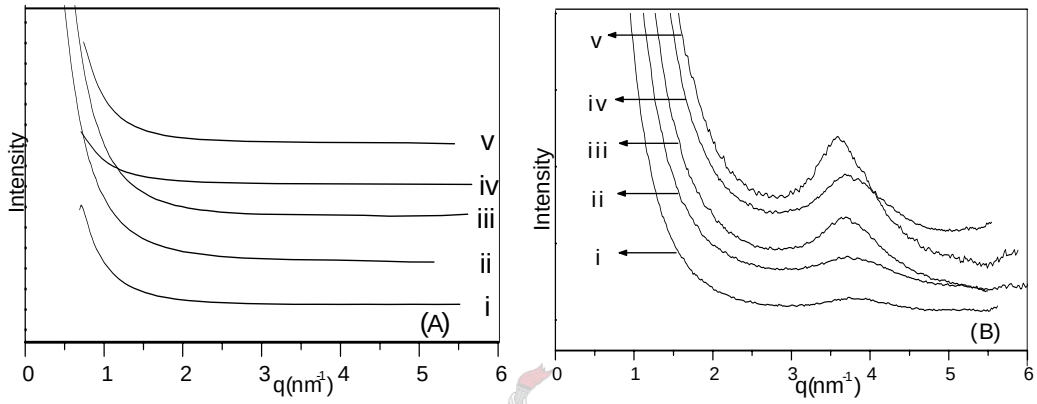

Fig. 5.4 SAXS patterns of (A) polystyrene-(Ethyl-MMT) nanocomposites and (B) polystyrene-(Ethanol-MMT) nanocomposites. Fig. 5.4 (A) i-v, represents polystyrene-(Ethyl-MMT) nanocomposites containing: 2.1, 3.7, 5.7, 7.7 and 18.5% clay respectively. Fig. 5.4 (B) i-v, represents polystyrene-(Ethanol-MMT) nanocomposites containing: 1.5, 5.3, 7.1, 18.5 and 21.3% clay respectively.

The SAXS patterns in Fig. 5.4 (A) did not show any visible peaks for the polystyrene-(Ethyl-MMT) nanocomposite (i.e. i-v), indicating total exfoliation. Exfoliated structure was obtainained at, as high as 18.5% clay content. This agrees well with the results of Choi *et al*., who obtained exfoliation at 20% clay loading [7]. This is very remarkable, as it is widely believed that exfoliation is obtained only at low clay levels (i.e less than 10%) [1]. The patterns in Fig. 5.4 (B) show a visible broadening of the peaks (i.e. i-v), with respect to the peak due to Ethanol-MMT (Fig. 5.2 B (i)). The broadening of the peaks can be attributed to either: partial exfoliation or an insufficient sensitivity of the apparatus as the clay level decreases [20]. At this point partial exfoliation seems to be highly likely in this case, but TEM analysis was used to confirm this.

It was initially thought that since the Ethanol surfmer is more polar than the Ethyl surfmer it would result in exfoliated nanocomposites [21-22]. At this point the reason for this unexpected behaviour might be obtained from looking at thermodynamic

effects. Here it is necessary to look at the interactions between the clay and polymer, clay and surfactant, and polymer and surfactant. An optimum balance of all these interactions generally leads to an exfoliated nanocomposite [4]. It appears that Ethyl surfmer has a balance of all these interactions, for it is hydrophilic (i.e. ammonium head group) and the acrylate group is polar. These functionalities allow it to interact with clay through electrostatic interactions and hydrogen bonding, respectively. The surfmer is also hydrophobic (i.e. the alkyl chain), thus enabling it to interact with polystyrene.

On the contrary, the Ethanol surfmer has all the characteristics mentioned for Ethyl surfmer. In addition, it has a 2-hydroxyethyl substituent that is polar, which implies more interaction with clay and less interactions with hydrophobic polystyrene. This leads to an imbalance of interactions, with the Ethanol surfmer ending up acting like glue, in preventing the clay layers from separating completely [2]. Other researchers also agree that an optimum number of polar interactions are required for one to obtain an exfoliated nanocomposite [5,23]. This means that in addition to the localised copolymerization of styrene and the surfmer inside the clay galleries we also need a certain number of polar groups on the surfactant. At this point the available literature is still very unclear regarding the importance of random copolymerization inside clay galleries. A general view is that copolymerization provides the driving force for exfoliation [2]. Zhang *et al*. [11] proposed that a double bond causes the propagating chain to anchor onto the surface of the clay and the polymerization of styrene in between clay requires a large space. The copolymerization of styrene and the surfmer results in the extensive movement of clay platelets, yielding the exfoliated structure. On the contrary, no extensive movement of the clay platelets takes place for classical surfactant modified clays, thus intercalated nanocomposites result.

The SAXS patterns for CTAB (Appendix 2: Fig. 11) shows that intercalated nanocomposites were obtained, in agreement with existing literature [1,24-25]. CTAB does not have the optimum interactions with clay and does not have a polymerizable group hence does not copolymerize with styrene. This further confirms the importance of both a polymerizable group and optimum number of polar groups on the surfactant.

The process of exfoliation could have started during sonication. A sonicator produces ultrasonic waves that are strong enough to break the clay agglomerates into fine dispersible particles. The sonication was carried out with all the ingredients present (i.e modified clay, styrene and initiator), hence the ultrasonic waves could also break up some of the initiator molecules, and initiate polymerization [26-27]. In this work, the initiator was added to the mixture before sonication so as to ensure that some initiator penetrates inside the clay galleries, hence initiation inside the clay galleries. It took up to 90 min to disperse the surfmer-modified clays in styrene monomer. Two hypotheses can be proposed:

(i) During sonication some polystyrene chains were formed. These chains moved into the clay galleries, making it more hydrophobic, facilitating more monomer to move into the clay galleries, hence dispersing the modified clay after such a long time. The proposed polymerization and dispersion were seen by the increase in viscosity as sonication progressed.

(ii) The long time necessary to disperse surfmer based organoclays in styrene was due to styrene wetting the clay surfaces [2]. The wetting of clay was proposed to be the first step to exfoliation from a thermodynamic point of view [2] and thus could be the rate determining step, hence the slowest.

Regarding these hypotheses, sonication was also carried out without the initiator and the increase in viscosity was again observed, but without quantification. Qutubuddin and Fu [1] also observed an increase in viscosity when they dispersed organically modified-MMT clay in styrene.

Thus, an increase in viscosity could largely be due to the dispersion of organoclay in monomer and only partly due to polymerization. Modified clays are used as rheology modifiers and, if properly dispersed, they cause an increase in viscosity of a dispersion [1]. As opposed to the surfmer-modified clays, the CTAB-modified clay was easier to disperse in styrene, for high viscosity dispersions were obtained within about 15 min of sonication. This could be linked to the high extent of ion exchange of CTAB surfactant (see Section 5.4.1.1).

To confirm the type of nanocomposites proposed from results of SAXS measurements, TEM analysis was used as a complimentary technique.

5.4.5.4 Analysis of polystyrene-clay nanocomposites using TEM.

TEM is an excellent qualitative technique for the characterization of the extent of dispersion of clay in polymer-clay nanocomposites [20].

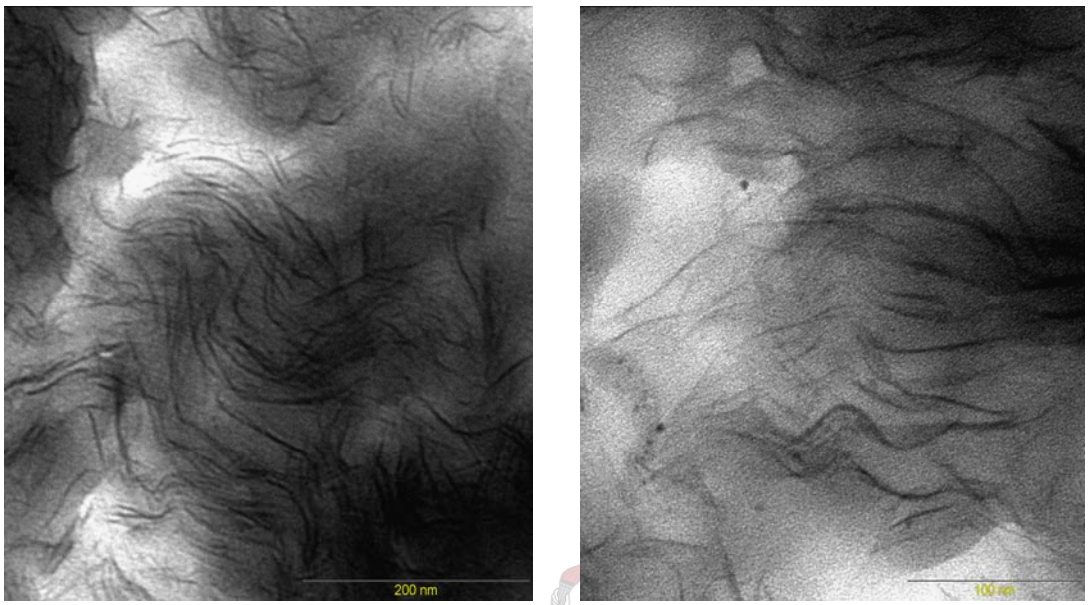

Fig. 5.5 TEM images of exfoliated polystyrene-(Ethyl-MMT) nanocomposite containing 5.7% clay (scale 200 nm and 100 nm).

The images of the polystyrene-(Ethyl-MMT) nanocomposite (scale 200 nm and 100 nm) clearly show high degree of disorder in the morphology of the clay layers. The dark lines in the figure corresponds to the silicate nanolayers. The clay platelets have separated from each other completely. Thus, TEM analysis confirmed the fully exfoliated structure of this nanocomposite as determined by SAXS. SAXS patterns did not show any diffraction peaks, implying an exfoliated structure (Section 5.4.4).

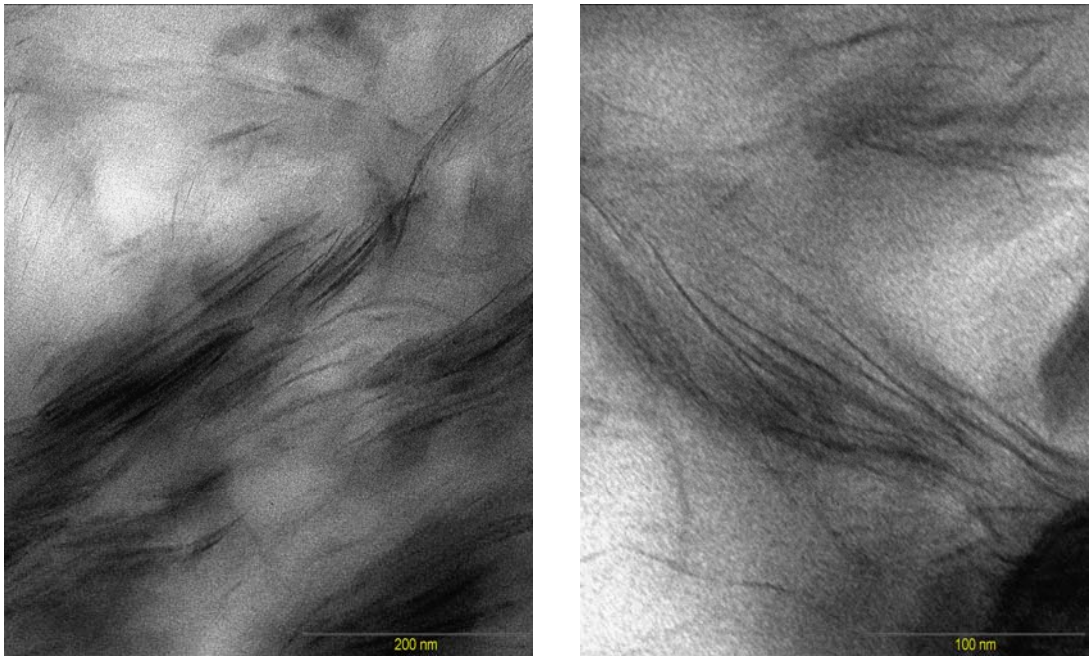

Fig. 5.6 TEM images of partially exfoliated polystyrene-(Ethanol-MMT) nanocomposite containing 5.3% clay.

The TEM images of the polystyrene-(Ethanol-MMT) nanocomposite (scale 200nm and 100nm) shows a partially exfoliated structure (exfoliated/intercalated) nanocomposite. This is in agreement with the results of SAXS analysis, which showed extensive broadening of peaks implying an exfoliated/intercalated structure (Section 5.4.4).

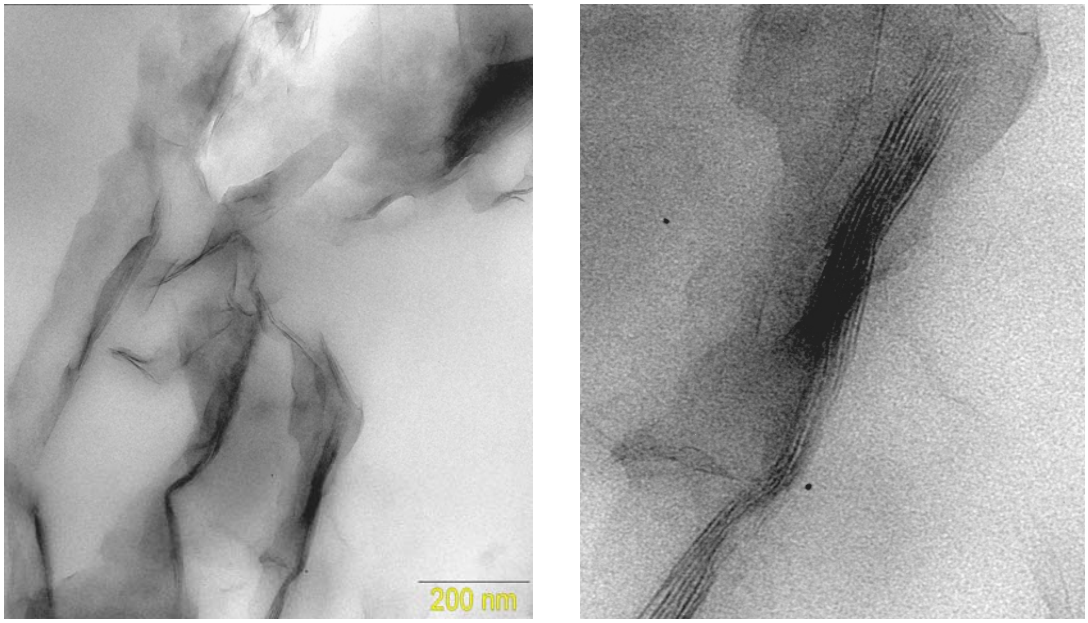

(A) **(B)**

Fig. 5.7 (A) TEM image of intercalated polystyrene-(CTAB-MMT) nanocomposite containing 6.0% clay, (B) a magnified section of (A).

TEM images of polystyrene-(CTAB-MMT) nanocomposite with 6% clay are shown in Fig. 5.7. As expected, the TEM image of polystyrene-(CTAB-MMT) nanocomposite clearly showed no visible exfoliation, but the presence of an intercalated structure. This agrees well with existing literature [1]. (B) is a magnified section of (A), clearly showing the intercalated structure.

5.4.5.5 Analysis of polystyrene-clay nanocomposites using AFM.

AFM is a surface technique and thus provides topological information on the nanocomposite surface. Unlike TEM, which does not see the polymer matrix, AFM can see both the matrix and the dispersed phase (analyte). Provided the analyte is at the surface of the matrix, and the analyte is relatively smaller than the probe tip, AFM will provide information on the morphology of the analyte relative to the matrix. AFM analysis was done in the contact mode. We initially wanted to have phase images, obtainable by carrying out the analysis in the non-contact mode. However, we could not have any results from the analysis because the samples were rough and during analysis there was some sort of interference which resulted in noise and no image.

In contact mode steric repulsions between the electron cloud on the probe tip and the electron cloud in the analyte results in an image that corresponds to the analyte

structure. Unfortunately it was not possible to see the clay nanoparticles (see Fig. 5.8 below). This is mainly because the majority of clay particles are embedded inside the polystyrene matrix and hence cannot be seen [21].

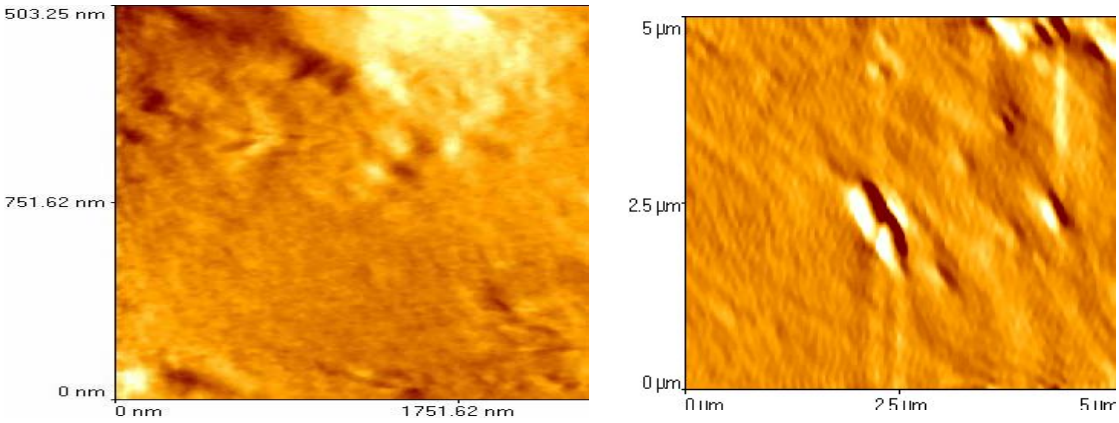

(A) (B)

Fig. 5.8 AFM images of (A) polystyrene-(Ethyl-MMT) nanocomposite containing 5.7% clay and (B) polystyrene-(Ethanol-MMT) nanocomposite containing 5.3% clay.

5.4.5.6 Analysis of polystyrene-clay nanocomposites using GPC.

The polymers prepared in this study generally had very high molecular masses. This is typical of free radical bulk polymerization and is attributed to two factors (i) high viscosity and (ii) temperature of polymerization.

(i) Termination in free radical polymerization is diffusion controlled. Diffusion is very limited at high viscosity. In bulk polymerization the viscosity increases significantly as polymerization progresses. Thus, the propagating species will be moving very slowly (i.e. limited diffusion). This implies that the probability of two propagating species to come together and terminate is very small. On the other hand the monomer i.e. styrene is very small and thus diffuses easily in the viscous system and adds (polymerizes) to a growing chain, resulting in products of high molecular masses.

(ii) The low temperature of polymerization (i.e. 60 ^{0}C) implies that the number of radicals in the system is low. A low number of propagating radicals implies a low probability of two radicals coming together to terminate, hence resulting in high molecular masses.

The average molecular masses of the nanocomposites were higher than that of polystyrene prepared according to Section 5.4.5.1, as shown in Table 5.5 below. This can be explained by two factors, (a) before polymerization sonication resulted in high viscosity dispersions, which further exacerbates effect (i) above and (b) the structure of the clay. Clay platelets are impervious, thus a radical growing inside the clay gallery cannot be terminated by another radical outside that gallery. This analysis however disagrees with Qutubuddin and Fu [1], who prepared nanocomposites by bulk polymerization and observed a decrease in molecular masses as clay loading increased. They attributed this to to the high viscosity of organophilic MMT-styrene dispersion that affects the diffusion of initiator molecules and chain propagation during polymerization. The author disagrees with their deductions, see explanation above (i.e. a and b).

Table 5.5 Variation of molecular masses and polydispersity index (PDI) with clay loading of the polystyrene-clay nanocomposites

Sample	**Clay content (%)**	**M_n x 10^3 (g/mol)**	**M_W x 10^3 (g/mol)**	**PDI (M_W/M_n)**
Polystyrene	-	170	510	3.1
Polystyrene-(Ethanol-MMT) Nanocomposite	1.5	230	740	3.2
	5.3	240	690	2.8
	7.1	200	860	4.2
	18.5	170	440	2.6
	21.3	400	1 190	3.0
Polystyrene-(Ethyl-MMT) Nanocomposite	2.1	190	690	3.7
	3.7	190	580	3.1
	5.7	210	630	2.9
	7.7	140	840	5.9
	18.5	240	1 120	4.7
Polystyrene-(CTAB-MMT) Nanocomposite	0.8	120	480	4.0
	1.2	80	540	6.8
	3.5	80	540	6.8
	6.0	80	540	6.4

5.4.5.7 Thermal analysis of polystyrene-clay nanocomposites.

The thermal stability of the synthesized polystyrene-clay nanocomposites is shown in Fig. 5.9 below.

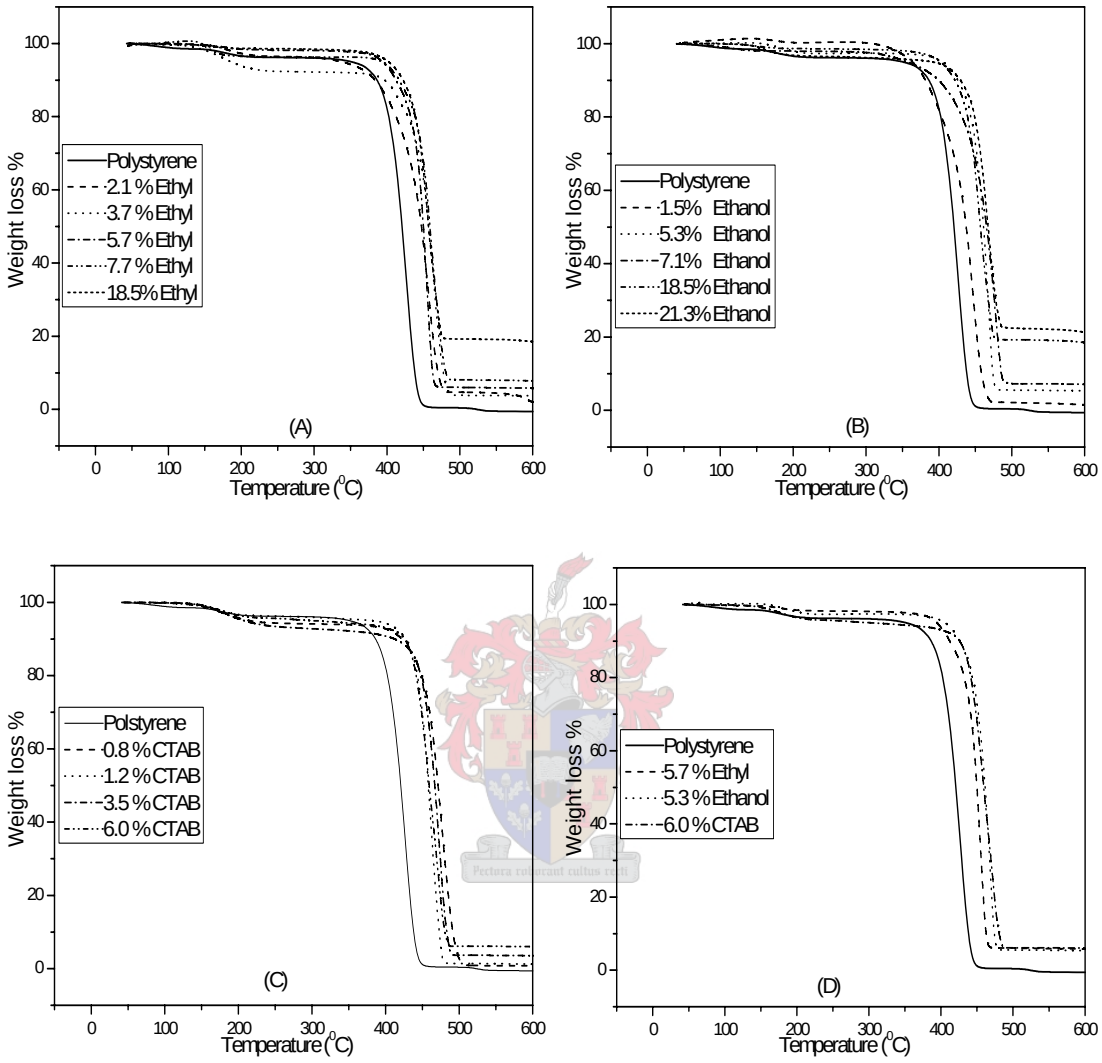

Fig. 5.9 (A-D) Thermal stability of polystyrene-clay nanocomposites as a function of clay loading. The inserts show the amount of clay in the thermograms as a percentage and the surfactant used to make the organoclay. (A) is for polystyrene-(Ethyl-MMT) nanocomposites, (B) is for polystyrene-(Ethanol-MMT) nanocomposites, (C) is for polystyrene-(CTAB-MMT) nanocomposites and (D) is a comparison of thermal stability of the three different nanocomposites at similar clay loadings. In all cases, the thermogram of polystyrene is included as a reference.

All nanocomposites synthesized were more thermally stable relative to the virgin polystyrene. The improvement in thermal stability of the nanocomposites is due to the formation of clay char that acts as a mass transport barrier and an insulator between the polymer and the superficial zone where combustion of the polymer takes place [28]. The thermal stability can also be attributed to the restricted thermal motion of

the polystyrene in the gallery [29]. The enhancement in thermal stability is almost independent of the amount of clay. At very low clay loadings for the surfmer modified clay nanocomposites it is observed that the enhancement is low, but increases sharply and then very slightly as clay loading increases. CTAB modified clay nanocomposites only required very low clay content for maximum thermal stability. This behavior has also been observed by Doh and Cho [30] who observed that maximum thermal stability of intercalated polystyrene-clay nanocomposites was attained when only 0.3 wt % of clay was used.

A comparison of thermal stability of the three different nanocomposites at a similar clay loadings is given in Table 5.6 below.

Table 5.6 TGA data for polystyrene nanocomposites with similar clay loadings (see Fig. 5.9 D)

Sample	**$T_{10\%}$**	**$T_{50\%}$**	**% clay i.e. % char $_{600}{}^{0}C$**
Polystyrene	386	420	0
Polystyrene-(Ethanol-MMT) Nanocomposite	426	461	5.3
Polystyrene-(Ethyl-MMT) Nanocomposite	412	450	5.7
Polystyrene-(CTAB-MMT) Nanocomposite	427	460	6.0

Where: $T_{10\%}$, $T_{50\%}$ and % clay in nanocomposites i.e. % Char $_{600}{}^{o}C$ represents the onset of decomposition taken at 10% decomposition, temperature at 50% decomposition, and the % remains (char) at 600 ^{0}C respectively [31].

Table 5.6 and Fig. 5.9 (D) shows that there is at least about 30 ^{0}C stability in the nanocomposites relative to polystyrene. On the other hand, the thermal stabilities of these three nanocomposites are quite similar regardless of the extent of clay dispersion. However, polystyrene-(CTAB-MMT) nanocomposite is more thermally stable, followed by polystyrene-(Ethanol-MMT) nanocomposite and lastly polystyrene-(Ethyl-MMT) nanocomposite. The author was expecting that the thermal stability of the exfoliated polystyrene-(Ethyl-MMT) nanocomposite would be more stable than the other two. The author proposes that it is necessary to have several close packed layers (stacked layers) of clay in order to provide a suitable barrier between burning zone and the underlying flammable material that is being gassified. This proposal would mean that the intercalated structures would be more stable, as is observed in this case. This agrees with results of Giannelis who discovered that at the same clay loading of 10%, intercalated polyimide nanocomposite was more thermally

stable relative to the exfoliated polyimide nanocomposite [32]. This correlates with the findings of Gilman *et al*., who observed that in certain systems an exfoliated structure does not necessarily bring about the most improvement in nanocomposite properties e.g. flammability [33].

5.4.5.8 Analysis of polymer-clay nanocomposites using DMA.

In general, at low clay levels, all the synthesized nanocomposites showed an inferior storage modulus relative to that of the virgin polystyrene. This effect is more pronounced for the surfmer-modified clays regardless of the extent of clay dispersion, as shown in Table 5.7 below.

Table 5.7 DMA data for polystyrene-clay nanocomposites at varying clay loadings

Sample	**% clay**	**G^I x 10^8 (Pa)**	**G^{II} x 10^8 (Pa)**	**T_g (^{0}C)**
Polystyrene	-	8.5	0.22	108
Polystyrene-(Ethanol-MMT) Nanocomposite	1.5	4.5	0.20	117
	5.3	10.5	0.25	121
	7.1	11.5	0.25	121
	18.5	11.8	0.25	121
Polystyrene-(Ethyl-MMT) Nanocomposite	2.1	7.05	0.16	112
	3.7	7.15	0.16	118
	5.7	13.2	0.35	121
	18.5	13.1	0.27	122
Polystyrene-(CTAB-MMT) Nanocomposite	0.8	4.5	0.18	115
	1.2	7.9	0.13	113
	3.5	11.0	0.25	117
	6.0	11.7	0.39	117

Where G^{II} and G^I are loss modulus and storage modulus.

This effect was however, reversed as clay loading increased. The storage modulus increased with an increase in clay content, in agreement with literature [1,5,13,34-35]. The enhancement in storage modulus is caused by the high aspect ratio of the dispersed clay and the interaction of the copolymer chains and clay layers, resulting in the suppression of the mobility of the copolymer segments near the interface [36]. The

extent of clay dispersion is seen in the values of storage modulus, where the exfoliated polystyrene-(Ethyl-MMT) nanocomposites show a relatively higher modulus compared to those of the partially exfoliated polystyrene-(Ethanol-MMT) nanocomposites and the intercalated polystyrene-(CTAB-MMT) nanocomposites.

Fig. 5.10 (A and B) below shows the plotted variation of tan δ and storage modulus vs. temperature of surfmer based nanocomposites at 18.5% clay loading each.

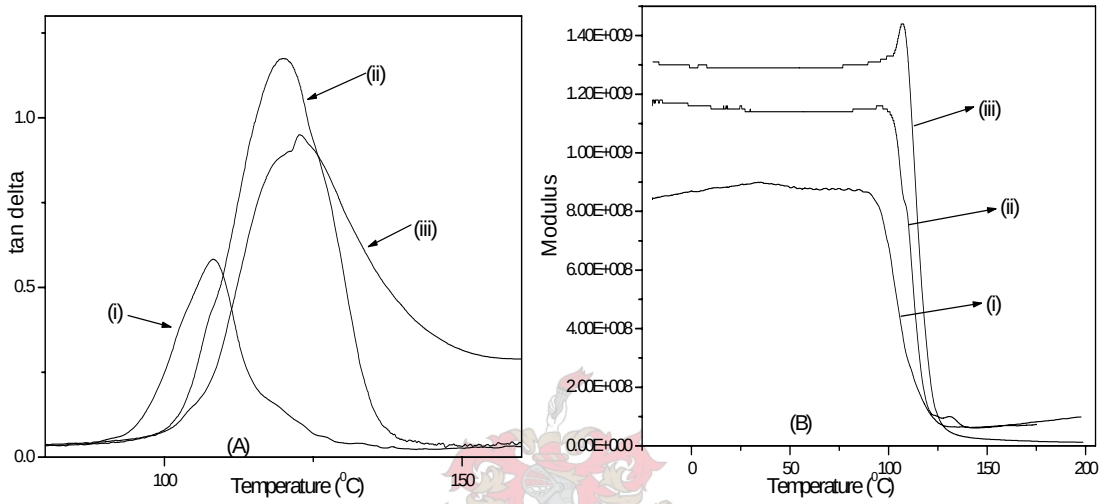

Fig. 5.10 Variation of (A) tan δ and (B) storage modulus against temperature. In both (A) and (B), (i) is polystyrene (ii) is polystyrene-(Ethanol-MMT) nanocomposite and (iii) is polystyrene-(Ethyl-MMT) nanocomposite.

The small hump in the storage modulus spectrum of polystyrene-(Ethyl-MMT) nanocomposite at about 115 ^{0}C, Fig. 5.10 (B), is due to enthalpy of relaxation of the chains.

As shown in Fig. 5.10 (A), the tan δ peaks for the nanocomposites have shifted to higher temperatures with respect to virgin polystyrene, in agreement with literature [37]. This is also coupled to broadening of the peaks, which is generally attributed to the restricted mobility of the chains brought about by the clay filler [37-38]. The broadening of the peak was more pronounced in the exfoliated nanocomposite where the highly dispersed clay inhibits mobility to a greater extent relative to the partially exfoliated polystyrene-(Ethanol-MMT) nanocomposite. This can also be said for all the prepared nanocomposites in Table 5.6. The glass transition T_g of the nanocomposites taken from the tan δ peaks was at a higher temperature than that of polystyrene and increased slightly with an increase in clay content. The reason for this is the clay layers act as cross-linkers, thus restricting polymer motion [27,39]. This

agrees with the findings of Tyan *et al*. [35], who also observed a slight shift in tan δ peaks for intercalated polystyrene-clay nanocomposites, but is in stark disagreement with Qutubuddin and Fu [1], who observed a decrease in the T_g temperature with an increase in clay loading. Qutubuddin and Fu attributed this to reasons outlined in Section 5.4.5.6. However, the athour disagrees with them using arguments cited in that Section.

5.4.6 Preparation of polystyrene-clay nanocomposites from blends of modified clays by bulk polymerization.

In many applications of polymers, blends are very common for they sometimes give better properties than can be achieved by copolymerization. In the preparation of polymer-clay nanocomposites normally one type of a modified clay is used. As already outlined, exfoliated nanocomposites are normally achieved by the use of surfmer modified clays. The major drawback in the use of surfmers is that they are expensive to make, thus making exfoliated nanocomposites very costly [40]. To circumvent this drawback there are two alternatives, (i) during modification of clay one uses a solution containing a mixture of classical surfactant and surfmer to modify clay and (ii) uses blends of classical surfactant modified clay and surfmer modified clay. Option (i) has already been investigated [14]. To our knowledge there is no literature available on the use of modified clay blends to prepare polymer-clay nanocomposites. Thus, this Section focuses on the use of clay blends to synthesize nanocomposites.

The nanocomposites were prepared from blends of (i) Ethyl-MMT clay and CTAB-MMT clay (Ethyl-MMT-CTAB-MMT) and (ii) Ethanol-MMT clay and CTAB-modified clay (Ethanol-MMT-CTAB-MMT).

The clays were thoroughly mixed in known ratios (percentage by mass of surfmer-modified clay to classical surfactant-modified clay); in all cases, the total amount of clay was kept constant at 5%. Quantities of styrene monomer and AIBN were kept constant as well. The author's main aim was to determine whether exfoliated polystyrene-clay nanocomposites could be obtained when modified clay blends were used. The degree of dispersion of clay would then be related to the thermal properties of the prepared nanocomposites.

5.4.6.1 Analysis of polystyrene-clay nanocomposites obtained using modified clay blends, by SAXS measurements.

The SAXS patterns for the mixed clays showed some very interesting results. The polystyrene-(Ethanol-MMT-CTAB-MMT) nanocomposite system had a partially exfoliated structure. This was deduced from the broadening of the peaks, Fig. 5.11 (A). The polystyrene-(Ethyl-MMT-CTAB-MMT) nanocomposite system resulted in a partially exfoliated structure for 25/75 ratio, Fig. 5.11 (B). This was indicated by a very broad shoulder that started at approximately 1.45 nm. On the other hand, almost total exfoliation was obtained for 50/50 and 75/25 ratios.

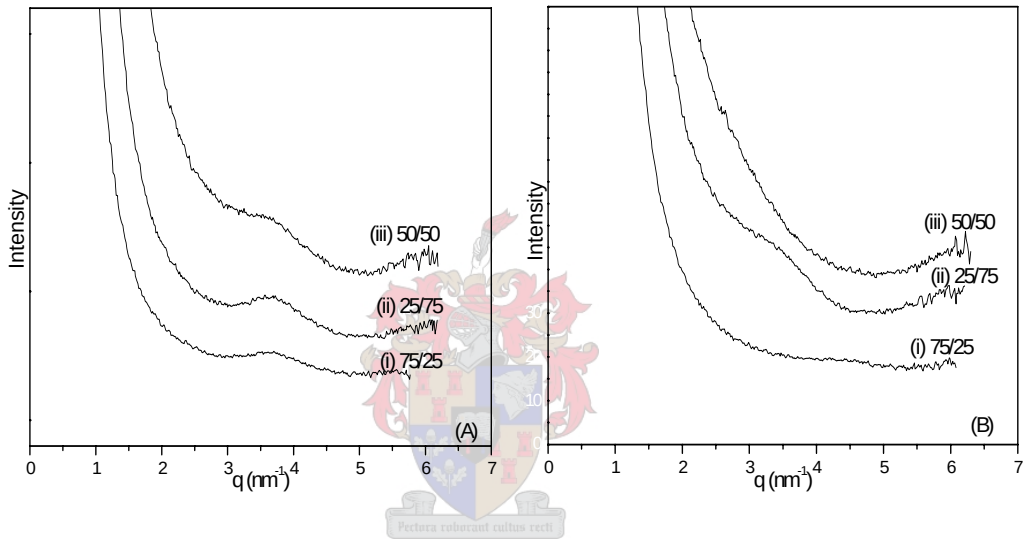

Fig. 5.11 SAXS patterns of polystyrene-clay nanocomposites obtained using blends of modified clays. Where (A) is polystyrene-(Ethanol-MMT-CTAB-MMT) nanocomposites and the ratios of Ethanol-MMT to CTAB-MMT clay are given for each SAXS pattern and (B) is polystyrene-(Ethyl-MMT-CTAB-MMT) nanocomposites and the ratios of Ethyl-MMT to CTAB-MMT clay are given for each SAXS pattern.

Thus, it is possible to use blends of classical modified clays and surfmer-modified clays to obtain exfoliated nanocomposites. A small but significant amount of the surfmer may have partitioned between the two clays by moving through the monomer medium. This would explain the data in Fig. 5.11 (B).

5.4.6.2 GPC analysis for polystyrene-clay nanocomposites obtained using modified clay blends.

The prepared nanocomposites resulted in high molecular masses (see Table 5.8 below), which has already been attributed to the nature of bulk polymerization and the structure of clay (see Section 5.4.5.6).

Table 5.8 Variation of clay loading with molecular masses of the mixed clay polystyrene-clay nanocomposites

Sample	Ratio of modified clays	$M_n \times 10^3$ (g/mol)	$M_W \times 10^3$ (g/mol)	PDI (M_W/M_n)
Polystyrene	-	170	510	3.1
Polystyrene-(Ethanol-MMT-CTAB-MMT) Nanocomposites	100/0	230	690	2.8
	75/25	60	290	5.3
	50/50	40	230	5.6
	25/75	60	300	5.1
	0/100	80	540	6.8
Polystyrene-(Ethyl-MMT-CTAB-MMT) Nanocomposites	100/0	210	630	2.9
	75/25	40	230	5.8
	50/50	80	400	5.2
	25/75	60	450	7.9
	0/100	80	540	6.8

5.4.6.3 Thermal analysis (TGA) of polystyrene-clay nano-composites obtained using modified clay blends.

The thermal stabilities of the nanocomposites synthesized from blends of modified clays are very similar to those synthesized using one modified clay. There is no significant change in stability, as the ratio of modified clays changes. This is most pronounced for the partially exfoliated polystyrene-(Ethanol-MMT-CTAB-MMT) nanocomposites, see Fig. 5.12 (A). As observed in Section 5.4.5.7, the thermal stability of the nanocomposites could be related to the level of clay dispersion, where the intercalated structures are more thermally stable relative to the exfoliated structures. On the other hand, a slight shift of thermal stability was observed as we moved from (exfoliated) 100% polystyrene-(Ethyl-MMT) nanocomposite to (intercalated) 100% polystyrene-(CTAB-MMT) nanocomposite in the polystyrene-(Ethyl-MMT-CTAB-MMT) nanocomposite system see Fig. 5.12 (B) below. This could be brought about by the differences in the level of clay dispersion as we move from the exfoliated to intercalated structure.

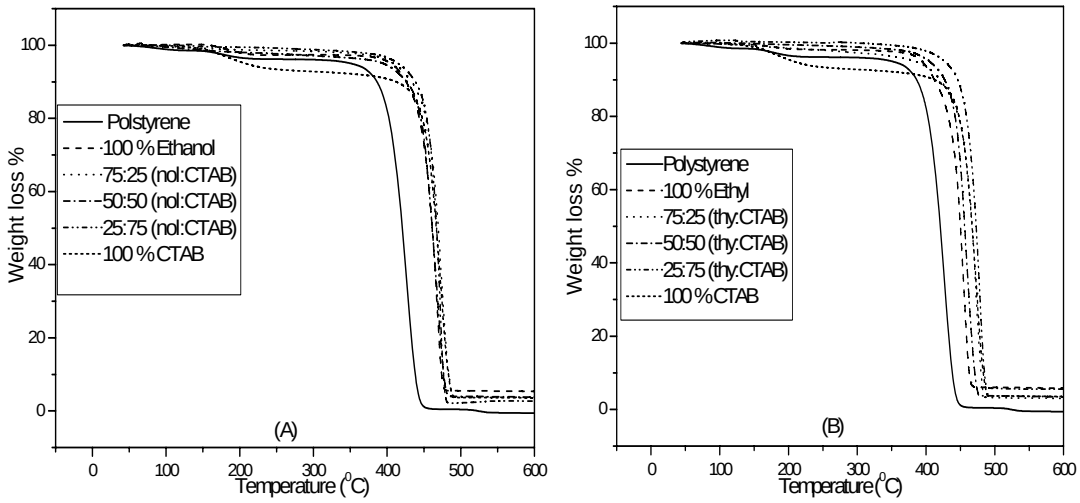

Fig. 5.12 (A-B) shows thermal stability of polystyrene-clay nanocomposites at 5% clay loading. (A) is for the polystyrene-(Ethanol-MMT-CTAB-MMT) nanocomposite (B) is for the polystyrene-(Ethyl-MMT-CTAB-MMT) nanocomposite. In both cases the thermogram of polystyrene is included as a reference. The ratios of the surfmer to classical surfactants are shown.

5.4.7 Preparation of polystyrene-clay nanocomposites by solution polymerization.

For comparison of the bulk polymerized systems the polystyrene-clay nanocomposites were synthesized by solution polymerization using surfmer modified clays. It was however very difficult to keep the dispersion in solution because the clay is not soluble in the solvent, thus in principle it was more like a suspension polymerization. This resulted in the particles coming out of solution as the polymerization reaction progressed. Nanocomposites with varying clay loadings were prepared. A polystyrene standard was also synthesized using a similar method.

5.4.7.1 SAXS analysis of polystyrene-clay nanocomposites synthesized by solution polymerization.

As expected, the polymerization only resulted in intercalated polystyrene-clay nanocomposites (see Fig. 5.13 below). This is mainly attributed to the fact that there was competition between the monomer and the solvent (toluene) for intercalation into the clay galleries [41]. This is an unfavorable situation from a thermodynamic point of view.

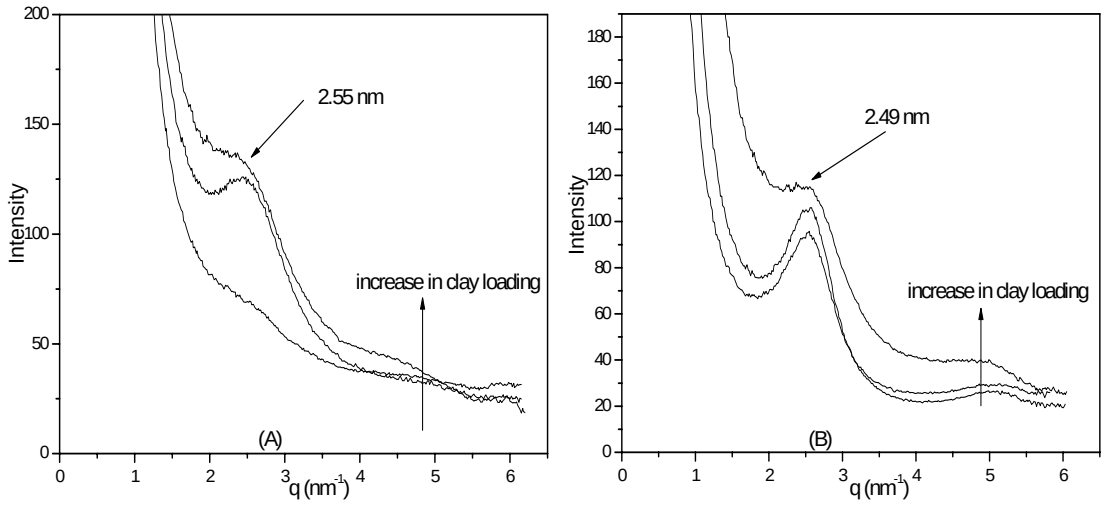

Fig. 5.13 SAXS patterns of (A) polystyrene-(Ethanol-MMT) nanocomposites containing 2, 11 and 17% clay and (B) polystyrene-(Ethyl-MMT) nanocomposites containing 1.5, 9.7 and 14% clay. The arrows in the diagram show the directions of clay increase.

From Fig. 5.13 above the average interlayer distance for polystyrene-(Ethanol-MMT) nanocomposites is 2.55 nm and that for polystyrene-(Ethyl-MMT) nanocomposites is 2.49 nm. These interlayer distances are greater than those found by Akelah and Moet [42], of between 1.72 and 2.45 nm (for polystyrene-clay nanocomposites obtained in solution using a polymerizable surfactant modified clay). The idea that polystyrene-(Ethanol-MMT) nanocomposites resulted in a larger d spacing in solution polymerization than polystyrene-(Ethyl-MMT) nanocomposites is very interesting. However, at this point, the author has no sound explanation for this behavior; any true explanation is probably linked to thermodynamic and kinetic considerations. Thus, more thorough research in this area is recommended. However, the author believes that the styrene monomer will partition between the medium and the interlayer galleries so that when the surfmers polymerize some styrene would copolymerize, also some surfmer should have partitioned into the solvent/monomer medium.

5.4.7.2 GPC of polystyrene-clay nanocomposites synthesized by solution polymerization.

The low molecular masses obtained (Table 5.9) were due to the nature of solution polymerization. The viscosity of the polymerization media did not increase significantly due to the presence of solvent, thus the growing chains had high diffusion rates, hence easy termination. The temperature of polymerization of 80 ^{0}C resulted in more radicals being formed, hence there was a high chance of termination.

However, the process resulted in a narrower polydispersity index relative to bulk polymerized systems.

Table 5.9 Variation of molecular masses with clay loading of the polystyrene-clay nano-composites prepared in solution

Sample	Clay content%	$M_n \times 10^3$ (g/mol)	$M_W \times 10^3$ (g/mol)	PDI i.e. (M_W/M_n)
Polystyrene		10.2	19.0	1.9
Polystyrene-(Ethanol-MMT) Nanocomposite	2	7.9	14.6	1.9
	11	6.4	14.6	2.3
	17	7.1	15.9	2.2
Polystyrene-(Ethyl-MMT) Nanocomposite	1.5	8.1	15.2	1.9
	9.7	8.3	15.4	1.9
	14	7.8	14.6	1.9

5.4.7.3 Thermal analysis of polystyrene-clay nanocomposites prepared in solution.

The nanocomposites (see Fig. 5.14 below) showed a slight increase in thermal stability as clay loading increased and were more stable than the virgin polystyrene as before. As in bulk systems, polystyrene-(Ethanol-MMT) nanocomposites were more stable than polystyrene-(Ethyl-MMT) nanocomposites at similar clay loadings. The onset of degradation of nanocomposites prepared in solution was less than that observed for those prepared in bulk. However, the temperature at 50% decomposition was similar in the two systems, depicting a similar decomposition pathway. The difference in the onset of decomposition can be explained on the basis of the difference in the molecular masses of the products resulting from the two methods [43]. The high molecular masses of the nanocomposites synthesized by bulk polymerization resulted in a higher onset of decomposition temperatures.

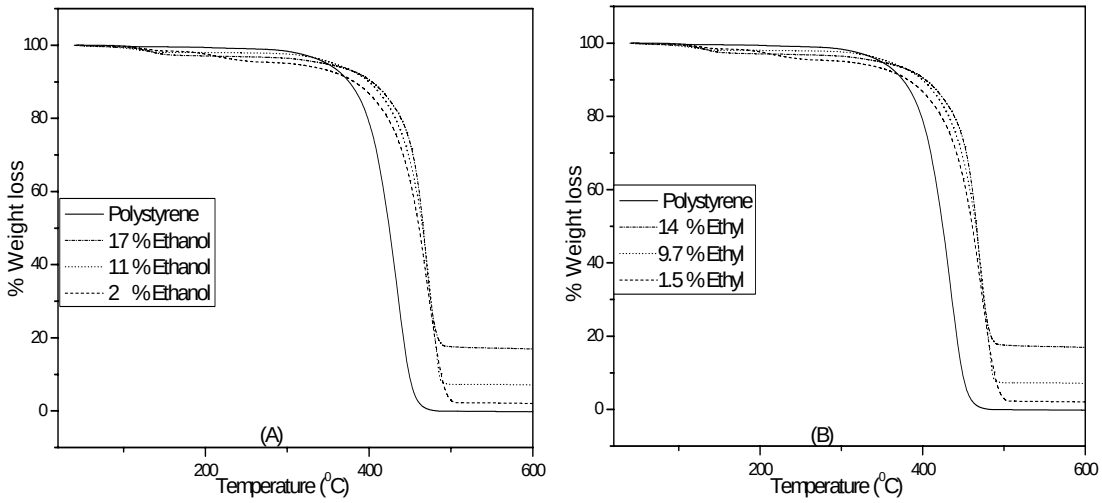

Fig. 5.14 (A-B) Thermal stability of polystyrene-clay nanocomposites as a function of clay loading. (A) is for polystyrene-(Ethanol-MMT) nanocomposite and (B) is for polystyrene-(Ethyl-MMT) nanocomposites. In both cases the thermogram of polystyrene is included as a reference.

References.

1. S. Qutubuddin, X. Fu; Polymer, 42 (2001) 807-813.

2. M. Rosorff; Nano Surface Chemistry. Marcel Dekker Inc. New York-Basel (2002) 653-673.

3. L. Biasci, M. Aglietto, G. Ruggeri, F. Ciardelli; Polymer, 35 (1994) 3296-3304.

4. T. D. Fornes, D. L. Hunter, D. R. Paul; Macromolecules, 37(2004) 1793-1798.

5. M. Kawasumi, N. Hasegawa, M. Kato, A. Usuki, A. Okada; Macromolecules, 30 (1997) 6333-6338.

6. www.nanoclay.com; Southern Clay Products Inc., Cloisite^{R} Na^{+} data sheet, Accessed (April, 2004).

7. Y. S. Choi, H. T. Ham, I. J. Chung; Chem. Mater., 16 (2004) 2522-2529.

8. R. Bongiovanni, M. Chiarle, J. Pelizzetti; J. Dispersion. Sci. Tech., 14 (1993) 255-268.

9. D. Yei, S. Kuo, Y. Su, F. Chang; Polymer, 45 (2004) 2633-2640.

10. M. Wang, F. Zhao, Z. Guo, S. Dong; Electrochimica Acta, (2004) 1-8.

11. W. A. Zhang, D. Z. Chen, H. Y. Xu, X. F. Shen, Y. E. Fang; European Polymer Journal, 39 (2003) 2323-2328.

12. S. Sadhu, A. K. Bhowmick; J. Appl. Polym. Sci., 92 (2004) 698-709.

13. M. Xu, Y. S. Choi, Y. K. Kim, K. H. Wang, I. J. Chung; Polymer, 44 (2003) 6387-6395.

14. C. Tseng, J. Wu, H. Lee, F. Chang; J. App. Polym. Sci., 85 (2002) 1370-1377.

15. R. A. Vaia, E. P. Giannelis; Macromolecules, 30 (1997) 8000-8009.

16. M. Summers, J. Eastoe, R. M. Richardson; Langmuir, 19 (2003) 6357-6362.

17. D. Joynes, D. C. Sherrington; Polymer, 37 (1996) 1453-1462.

18. R. J. Young; Introduction to Polymers, Chapman and Hall Ltd, London, (1981) 138-140.

19. J. D. Roberts, M. C. Caserio; Basic Principles of Organic Chemistry, W. A. Benjamin Inc., New York (1964) 29-34.

20. A. B. Morgan, J. W. Gilman; J. App. Polym. Sci., 87 (2003) 1329-1338.

21. M. Okamoto; Encyclopedia of Nanoscience and Nanotechnology. American Scientific Publishers, California, 8 (2004) 791-843.

22. C. I Park, O. O. Park, J.G. Lim, H. J. Kim; Polymer, 42 (2001) 7465-7475.

23. M. Okamoto, S. Morita, H. Y. Kim, T. Kotaka, H. Tateyama; Polymer, 42 (2001) 1201-1206.

24. C. Tseng, J. Wu, H. Lee, F. Chang; Polymer, 42 (2001) 10063-10070.

25. D. B. Zax, D. K. Santos, H. Hegemann, E. P. Giannelis, E. Manias; J. Chem. Phys., 112 (2000) 2945-2951.

26. J. G. Ryu, S. W. Park, H. Kim, J. W. Lee; Material Science and Engineering, C 24 (2004) 285-288.

27. S. Ganguli, D. Dean, K. Jordan, G. Price, R. Vaia; Polymer, 44 (2003) 6901-6911.

28. J. Wang, J. Du, J. Zhu, C.A Wilkie; Polymer Degradation and Stability, 77 (2002) 249-252.

29. A. Bluimstein; J. Polym. Sci. A., 3 (1965) 2665-2673.

30. J. H. Doh, I. Cho; Polym. Bull., 41 (1998) 511.

31. G. Chigwanda, C. A. Wilkie; Polymer Degradation and Stability, 80 (2003) 551-557.

32. E. Giannelis; Advanced Materials, 8 (1996) 29-31.

33. J. W. Gilman, T. Kashiwagi, A. B. Morgan, R. H. Harris, L. D. Brassell, M. R. VanLandingham, C. L. Jackson; NISTIR 6531, (2000) 1-55

34. W. Zhang, D. Chen, Q. Zhao, Y. Fang; Polymer, 44 (2003) 7953-7961.

35. H. Tyan, K. Wei, T. Hsieh; J. Polym. Sci.: Part. B: Polym. Phys., 38 (2000) 2873-2878.

36. J. Luo, I. M. Daniel; Composite Science and Technology, 63 (2003) 1607-1616.

37. M. W. Noh, D. C. Lee; Polym. Bull., 42 (1999) 619-626.

38. Y. Yu, J. Yeh, S. Liou, Y. Chang, Acta Materialia, 52 (2004) 475-486.

39. A. Akade, A. Usuki; Materials Science and Engineering, C 3 (1995) 109-115.

40. D. R. Robello, N. Yamaguchi, T. Blanton, C. Barnes; J. Am. Chem. Soc., 126 (2004) 8118-8119.

41. R. A. Vaia, E. P. Giannelis; Macromolecules, 30 (1997) 7990-7999.

42. A. Akelah, A. Moet; J Mater Sci, 31 (1996) 3589-3596.

43. J. Bicerano; Prediction of polymer properties. Marcel Dekker Inc., New York, (1993) 335.

Chapter 6: Conclusions and recommendations.

6.1 Conclusions.

The acrylate-based cationic surfmers: (11-acryloyloxyundecyl)dimethyl(2-hydroxyethyl)ammonium bromide (abbreviated as Ethanol surfmer) and (11-acryloyloxyundecyl)dimethylethylammonium bromide (abbreviated as Ethyl surfmer) were successfully synthesized and characterised. CMC values depended on the polarity of their head groups, as measured by conductivity. The surfmers displayed lyotropic liquid crystalline behaviour above 70 wt % concentration by weight in water. Surfmers were thermally stable up to 240 ^{0}C, as depicted by TGA analysis. They readily polymerized to yield polysurfmers.

The synthesized Ethanol and Ethyl surfmers, and the commercial surfactant cetyltrimethylammonium bromide (CTAB), were successfully used to modify (ion exchange) sodium montmorillonite (Na^{+}-MMT), resulting in modified clays. The modified clays were characterized by TGA, FT-IR and SAXS. The TGA results showed that the total amount of surfactant ion exchanged (i.e. the extent of ion exchange) was higher for CTAB than for the surfmers. Shear rate and temperature did not affect the extent of the ion exchange process for surfmers. FT-IR confirmed the presence of surfactants inside the interlayer space of the modified clays. SAXS showed an increase in the interlayer distance of the modified clays relative to pristine clay. CTAB-MMT clay had a larger interlayer space relative to those of the surfmers, due to the dependence of the interlayer distance on the surfactant chain length for the same clay charge density.A higher extent of ion exchange and a larger interlayer distance resulted in a higher rate of dispersion of the modified clay in styrene. Thus CTAB-MMT clays were easy to disperse in styrene, relative to the surfmer modified clay.

Polymerization of styrene in the presence of the dispersed clays resulted in the formation of polystyrene-clay nanocomposites. Bulk polymerization resulted in the formation of three types of nanocomposite structures: intercalated nanocomposites for CTAB-MMT clay, partially exfoliated nanocomposites for Ethanol-MMT clay and exfoliated nanocomposites for Ethyl-MMT clay. The nanocomposite structures were confirmed by SAXS and TEM. Nanocomposites synthesized using mixtures of

Ethanol-MMT clay and CTAB-MMT clay resulted in partially exfoliated structures. SAXS measurements of nanocomposites synthesized using mixtures of Ethyl-MMT clay and CTAB modified clay showed partially exfoliated structures for the 25:75 ratio of Ethyl-MMT clay to CTAB-MMT clay and almost total exfoliated structures for the ratios 50:50 and higher. Solution polymerization of the surfmer based modified clays in toluene resulted in intercalated structures. A good balance of a number of interactions influences the resulting nanocomposite structure, e.g polymer versus clay, clay versus surfactant, surfactant versus polymer and solvent interactions. A balance of all these interactions results in an exfoliated structure, as was observed when Ethyl-MMT clay was used for the preparation of polystyrene-clay nanocomposites.

The thermal stability of polystyrene was significantly enhanced by the introduction of clay filler. It was found that the thermal stability was dependent on the extent of clay dispersion and independent of the clay content. CTAB and Ethanol based nanocomposites were slightly more stable than Ethyl based nanocomposites. It is proposed that this behavior can be attributed to the extent of clay dispersion, where the intercalated nanocomposites give better thermal stability. The thermal stability of nanocomposites obtained from mixtures of modified clays and those prepared in solution were also observed to follow the same pattern.

The mechanical properties, as determined by DMA, revealed that there was inferior storage modulus at low clay content for all nanocomposites regardless of extent of clay dispersion relative to polystyrene. However, as the clay loading increased this was reversed and reinforcement was obtained. The extent of clay dispersion manifested itself in the value of the storage modulus, where the exfoliated nanocomposites had superior values relative to the partially exfoliated and the intercalated nanocomposites. The T_g values from tan δ curves were higher for all nanocomposites relative to polystyrene, regardless of clay content. The T_g shifted slightly to higher temperatures as the clay content increased. Clay hindered polymer motion as observed by the broadening of the tan δ peaks. The broadening was more pronounced for exfoliated nanocomposites relative to the other two nanocomposite structures.

The molecular masses of the bulk polymerized systems were very high, in the 10^5 g/mol range, and the nanocomposites had relatively higher molecular masses than polystyrene. Solution polymerization, resulted in low molecular masses, the molecular masses were in the range 10^3 g/mol.

6.2 Recommendations for future work.

The following areas require further research:

- Further characterization and application of surfmers and their homopolymers in e.g. emulsion polymerization, (applications of the lyotropic liquid crystalline properties).

- Determination of the rate of ion exchange of Na^+-MMT by the synthesized surfmers. Clays are commercial products and thus optimization of every process will help in maximization of profit margins.

- Further characterization of the prepared nanocomposites for impact, tensile strength, barrier properties etc. This could help in the determination of an appropriate niche application for the prepared nanocomposites.

- Thermodynamic and kinetic considerations of the interactions that lead to the exfoliated structure. This would explain why Ethyl surfmer resulted in exfoliated nanocomposites whereas Ethanol surfmer resulted in partially exfoliated nanocomposites in bulk yet the surfmers are very similar in structure. On the other hand, the question why the same surfactants result in only intercalated nanocomposites with different interlayer distance in solution will also be answered. The study will also help in explaining why it is necessary to have a polymerizable group on the surfactant used in the modification of clay. Information on the optimum number of polar groups on the monomer or surfactants will also be obtained from the study.

- Reverse ion exchange of the prepared nanocomposites to obtain the degree of polymerization of the chains attached to clay and those not attached. This could give an insight on the kinetics of free radical polymerization inside and outside clay galleries during nanocomposite formation.

- Use the modified clays for other monomers, given the structure of the modifying surfmer relative to the monomer used of paramount importance. Then compare the results to those of polystyrene.

Appendix 1. FT-IR spectra of surfmers.

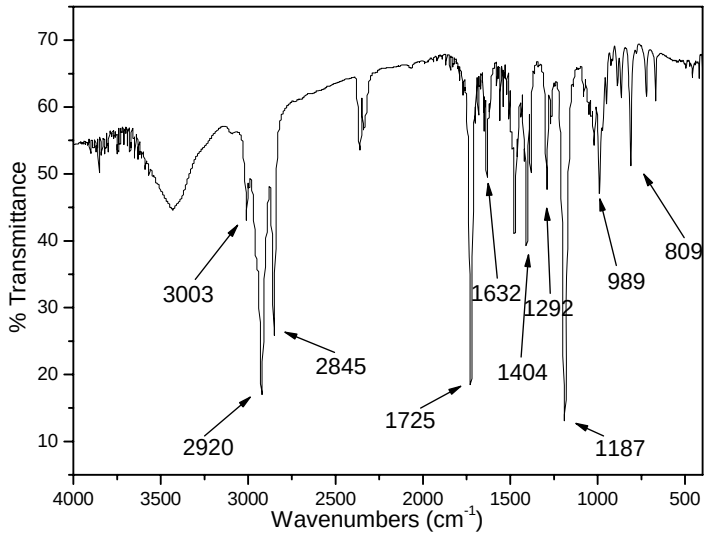

Fig. 1 FT-IR spectrum of (11-acryloyloxyundecyl)dimethylethylammonium bromide, (Ethyl) surfmer.

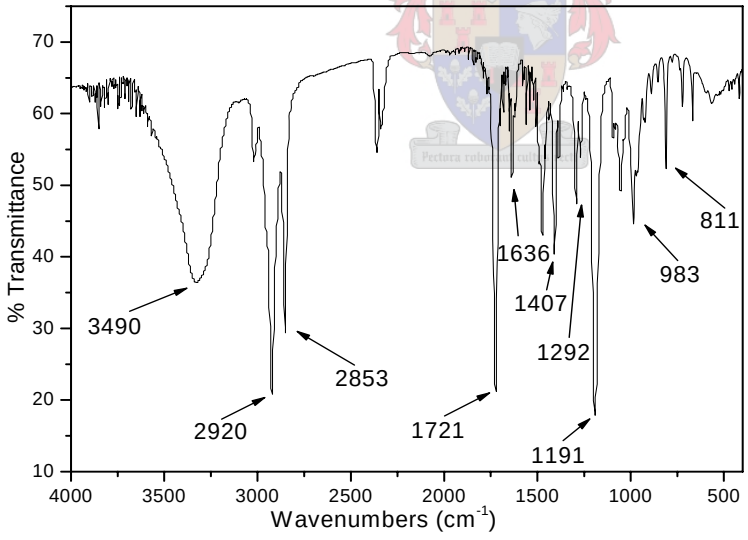

Fig. 2 FT-IR spectrum of (11-acryloyloxyundecyl)dimethyl(2-hydroxyethyl)-ammonium bromide, (Ethanol) surfmer.

Appendix 2. Characterization of nanocomposites.

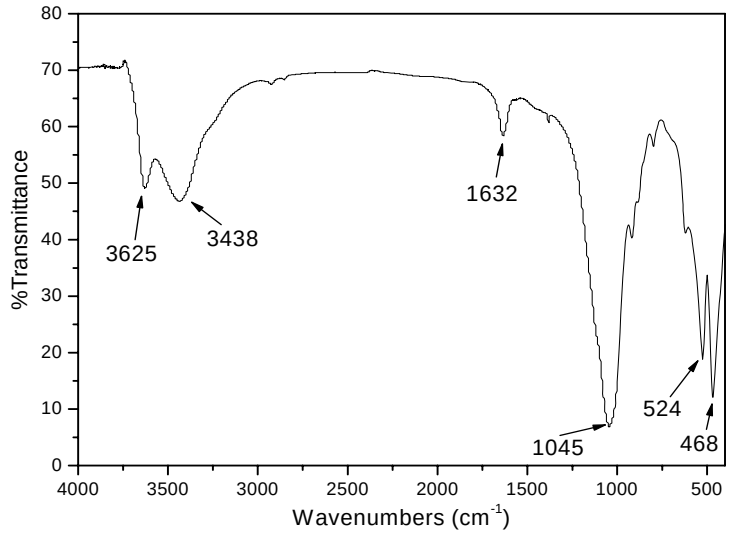

Fig. 1 FT-IR spectrum of sodium montmorillonite (Na^+-MMT) i.e. pristine clay.

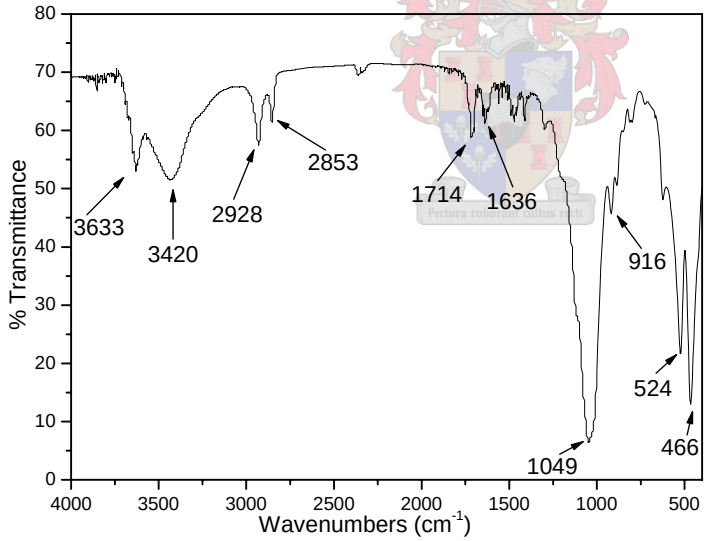

Fig. 2 FT-IR spectrum of Ethyl surfmer modified clay (Ethyl-MMT).

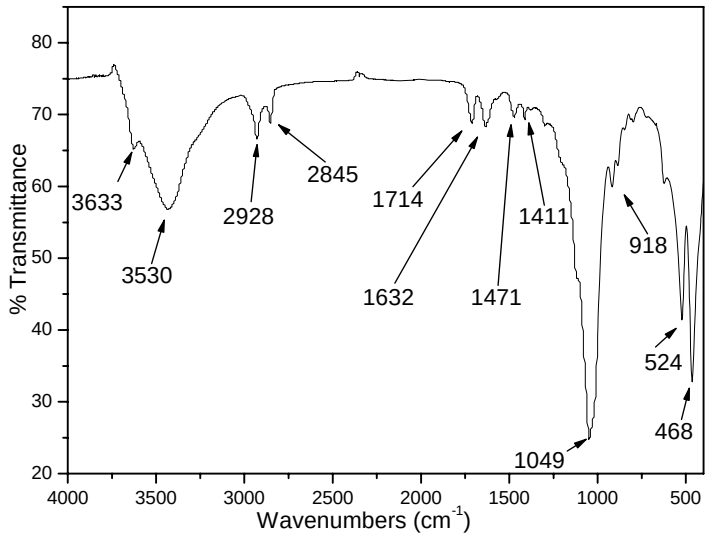

Fig. 3 FT-IR spectrum of Ethanol surfmer modified clay (Ethanol-MMT).

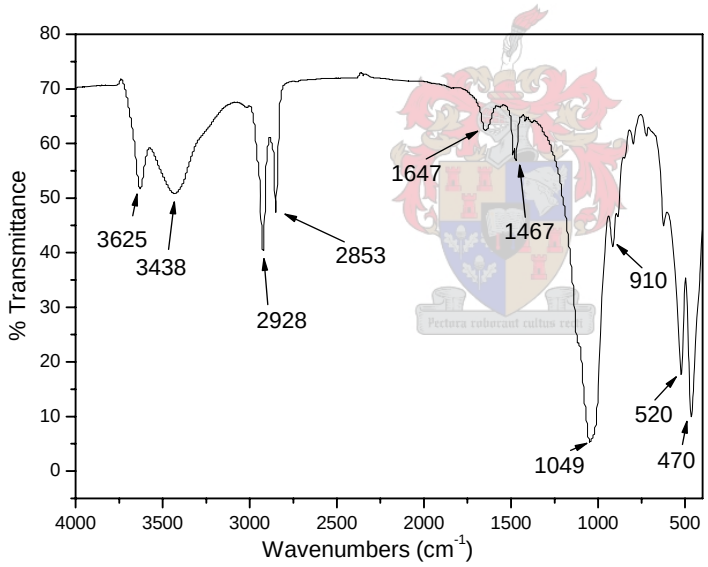

Fig. 4 FT-IR spectrum of CTAB modified clay (CTAB-MMT).

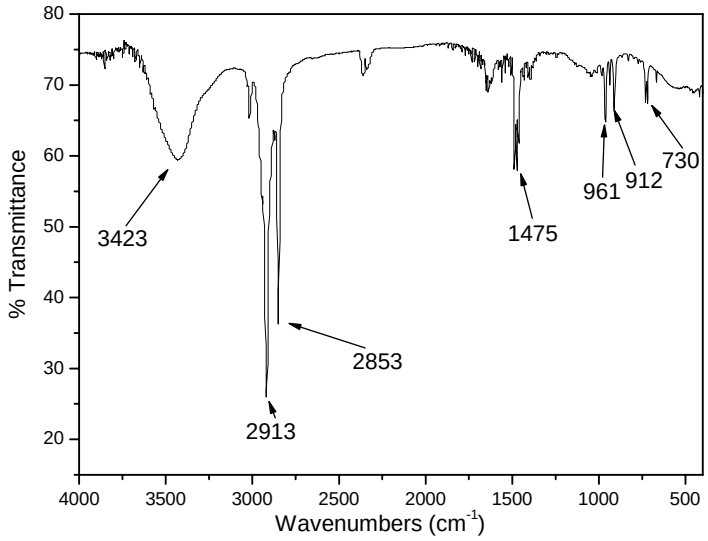

Fig. 5 FT-IR spectrum of cetyltrimethylammonium bromide (CTAB) surfactant.

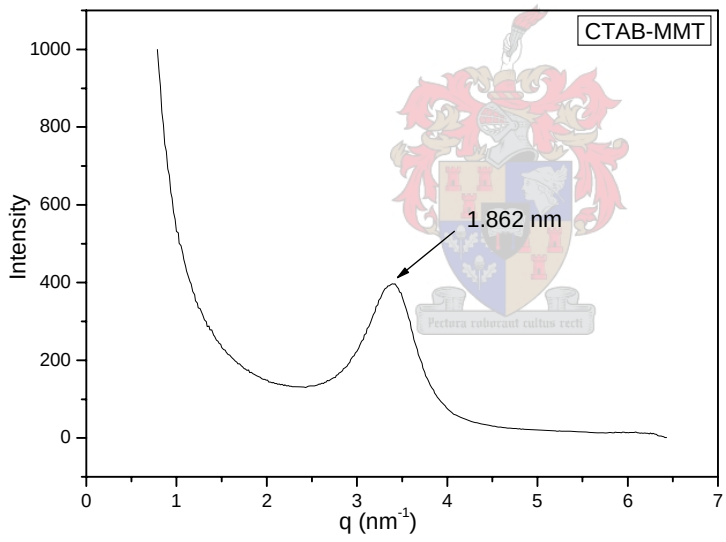

Fig. 6 SAXS pattern of CTAB modified clay (CTAB-MMT).

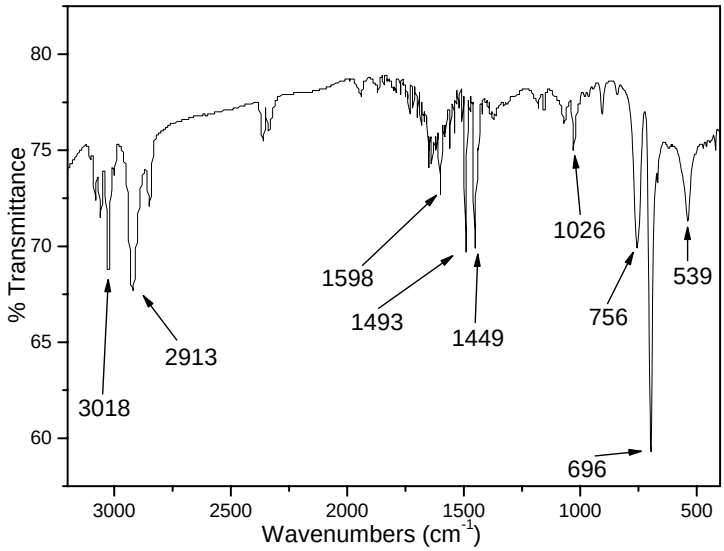

Fig. 7 FT-IR spectrum of polystyrene.

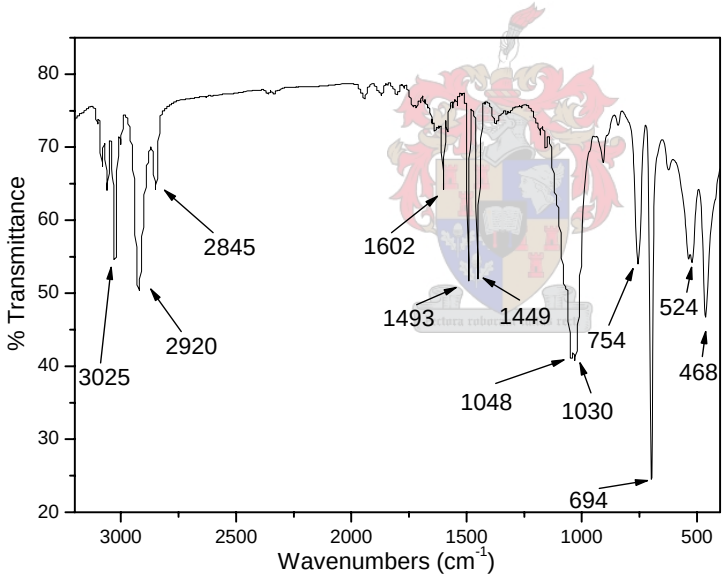

Fig. 8 FT-IR spectrum of polystyrene-(Ethyl-MMT) nanocomposite with 5.7% clay content.

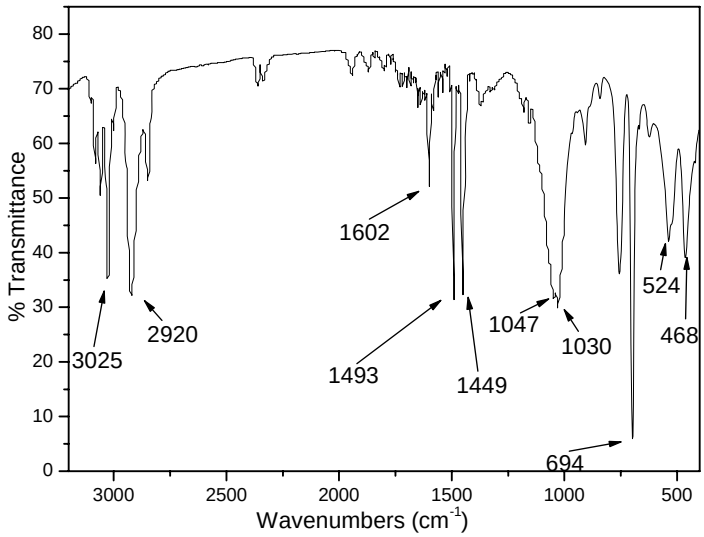

Fig. 9 FT-IR spectrum of polystyrene-(Ethanol-MMT) nanocomposite with 5.3% clay content.

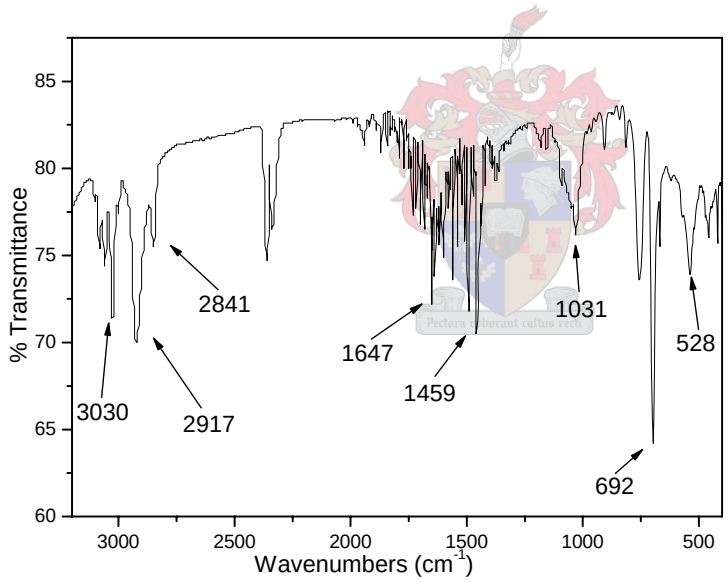

Fig. 10 FT-IR spectrum of polystyrene-(CTAB-MMT) nanocomposite with 6% clay content.

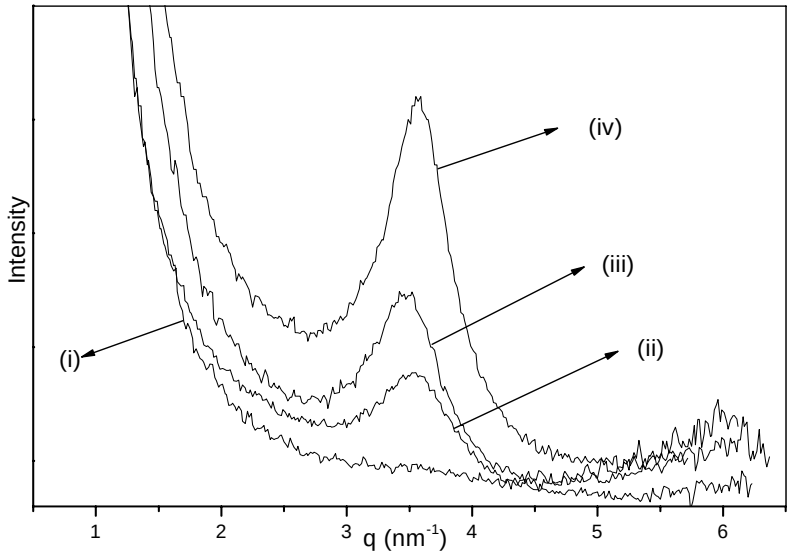

Fig. 11 SAXS patterns of polystyrene-(CTAB-MMT) nanocomposites; where (i)-(iv) are the nanocomposites containing 0.8, 1.2, 3.5 and 6.0% clay.